IMPROVING STRATEGIES ON TORIC INTRAOCULAR LENS POWER CALCULATION

TIAGO LUÍS DO CARMO BRAVO FERREIRA

Tese para obtenção do grau de Doutor em Medicina

na Especialidade de Oftalmologia

na NOVA Medical School | Faculdade de Ciências Médicas

julho, 2018

IMPROVING STRATEGIES ON TORIC INTRAOCULAR LENS POWER CALCULATION

Tiago Luís do Carmo Bravo Ferreira

Orientadores: João Goyri O'Neill, Professor Catedrático

Paulo Ribeiro, Professor Auxiliar; Filomena Ribeiro, Professora Convidada

Tese para obtenção do grau de Doutor em Medicina

na Especialidade de Oftalmologia

Acknowledgments

My first acknowledgments words go to the patients who kindly participated in this research, contributing towards the pursuit for a perfect vision.

Firstly, and more prominently, I thank to my Supervisors:

To Professor Filomena Ribeiro, for the daily guidance in clinical practice, but also for her suggestions and ideas, that taught me to question more deeply.

To Professor Paulo Ribeiro, for his invaluable support during this thesis and especially for his expertise in mathematical calculation. Completing this work would not have been possible without him.

To Professor João Goyri O'Neill, for being my mentor and the driving force behind this thesis and for his continuous guidance since day one of my residence. Also, in the name of all his students, for being an inspiration throughout life.

To my friends, for the privilege of having always their full support. I would especially like to acknowledge Gonçalo Simões and Maria Celeste Morim, for their contagious enthusiasm, motivation and friendship.

A remakable word of gratefulness to my colleagues in the Ophthalmology Department of Hospital da Luz. I especially acknowledge Fernanda Vaz and Eduardo Marques (who I will always remember) for their continuous mentoring throughout my career and for being my friends.

Finally, special thanks are owed to my parents for life and for the values they conveyed me, including the sense of mission and rigor. They are the reason I became who I am: a dedicated and happy doctor.

Índice

Acknowledgments ..... **i**

Thesis publications ..... **v**

Prizes awarded ..... **ix**

List of abbreviations ..... **xi**

Abstract ..... **xix**

Chapter 1: General introduction 23

1.1 Introduction 24

1.2 Thesis outline 25

Chapter 2: Theoretical background 27

2.1 Optic system and corneal structure 29

2.2 Optical aberrations of the eye 33

2.3 Importance of the posterior corneal surface 40

2.4 Methods for correcting astigmatism 45

2.5 Analysis of astigmatic data 50

2.6 Preoperative evaluation for toric intraocular lens implantation 61

2.7 Toric IOL power calculation 75

2.8 Surgically induced astigmatism 78

2.9 Preoperative marking of the IOL axis of alignment 80

2.10 Intraoperative technique 82

2.11 Postoperative astigmatism evaluation and measures to optimize outcomes 83

Chapter 3: Objectives 85

3.1 General objective 87

3.2 Specific objectives 87

Chapter 4: Prevalence of astigmatism in the Portuguese population 89

4.1 Introduction and objectives 91

4.2 Material and methods 92

4.3 Results 93

4.4 Discussion 101

4.5 Conclusions 108

Chapter 5: Improving the evaluation of astigmatism 109

5.1 Comparison between four measurement techniques to assess astigmatism on pseudophakic eyes 112

5.2 Comparability and repeatability of different methods of keratometric assessment 123

5.3 Summary of conclusions of the two studies evaluating color-LED topography 131

Chapter 6: Overcoming the current limitations on toric intraocular lens calculation 133

6.1 Comparison of astigmatic prediction error of new calculation methods for toric intraocular lenses 137

6.2 Comparison of methodologies using estimated or measured values of total corneal astigmatism for toric intraocular lens power calculation 152

6.3 Summary of conclusions from both studies 164

Chapter 7: Enhancing knowledge on surgically induced astigmatism 165

7.1 Introduction and objectives 167

7.2 Materials and methods 168

Preoperative Assessment 168

Surgical Technique 168

Postoperative Assessment 170

7.3 Results 172

7.4 Discussion 182

Chapter 8: General discussion 189

Chapter 9: Conclusions 199

Chapter 10: Future directions for research 203

List of Figures 207

List of Tables 211

References 213

Thesis publications

This work originated the following publications:

Ferreira TB, Hoffer KJ, Ribeiro P, Ribeiro FJ, O'Neill JG. Ocular Biometric Measurements in Cataract Surgery Candidates in Portugal. PLOS ONE 12(10):e0184837

Ferreira TB, Ribeiro FJ. A novel color-LED corneal topographer to assess astigmatism in pseudophakic eyes. Clinical Ophthalmology. 2016 Aug: 10:1521-29

Ferreira TB, Ribeiro FJ. Comparability and repeatability of different methods of corneal astigmatism assessment. Clinical Ophthalmology 2018;12:29-34

Ferreira TB, Ribeiro P, Ribeiro FJ, O'Neill JG. Comparison of the astigmatic prediction errors associated with new calculation methods for toric intraocular lenses. J Cataract Refract Surg 2017; 43:340-347

Ferreira TB, Ribeiro P, Ribeiro FJ, O'Neill JG. Comparison of Methodologies Using Estimated or Measured Values of Total Corneal Astigmatism for Toric Intraocular Lens Power Calculation. J Refract Surg. 2017;33(12):794-800

Ferreira TB, Ribeiro FJ, Pinheiro J, Ribeiro FJ, O'Neill JG. Comparison of Surgically Induced Astigmatism and Morphologic Features Resulting From Femtosecond Laser and Manual Clear Corneal Incisions for Cataract Surgery. J Refract Surgery, 2018; 34(5):322-329

Ferreira TB, Ribeiro P, Ribeiro FJ, O'Neill JG. Distribuição e determinantes de parâmetros biométricos oculares em candidatos a cirurgia de catarata em Portugal. Oftalmologia 2017;41(4):17-26. (This publication is an introduction to Ferreira TB, Hoffer KJ, Ribeiro P, Ribeiro FJ, O'Neill JG. Ocular Biometric Measurements in Cataract Surgery Candidates in Portugal. PLOS ONE 12(10):e0184837, evaluating data from a smaller cohort)

Ferreira TB, Ribeiro P, Ribeiro FJ, O'Neill JG. Comparação do erro de predição do astigmatismo residual entre dois calculadores de uma lente intraocular tórica.

Oftalmologia 2017;41(4):55-62. (This publication is an introduction to Ferreira TB, Ribeiro FJ. Comparability and repeatability of different methods of corneal astigmatism assessment. Clinical Ophthalmology 2018;12:29-34, comparing two toric intraocular

lens (IOL) calculators to demonstrate the advantage of adding three factors: the effective lens position, spherical equivalent IOL power and total corneal power to toric IOL calculators).

The work was presented in scientific meetings as:

Oral communications:

In international congresses:

Ferreira TB, Ribeiro P, Ribeiro FJ, O'Neill JG. Comparison between four measurement techniques to assess astigmatism in pseudophakic eyes. ASCRS/ASOA Annual Symposium and Congress, New Orleans, USA, 2016

Ferreira TB, Ribeiro P, Ribeiro FJ, O'Neill JG. Toric IOLs: managing conflict corneal measurements and calculators. XXXV Congress of the ESCRS, Lisbon, Portugal, 2017

Ferreira TB, Ribeiro FJ, Ribeiro FJ, O'Neill JG. Comparison of methodologies for considering posterior corneal astigmatism in toric intraocular lens power calculation. XXXV Congress of the ESCRS, Lisbon, Portugal, 2017

Ferreira TB, Ribeiro FJ. Comparison of the astigmatic prediction error of a new toric intraocular lens calculator with other calculation methodologies. ESCRS Winter, Belgrade, Serbia, 2018

Ferreira TB. Symposium Correction of Astigmatism in Cataract Surgery. Correction of astigmatism in cataract surgery Posterior corneal astigmatism: estimate or measure? ESCRS Winter, Belgrade, Serbia, 2018

Ferreira TB, Ribeiro FJ, Pinheiro J, Ribeiro FJ, O'Neill JG. Comparison of Surgically Induced Astigmatism and Morphologic Features Resulting From Femtosecond Laser and Manual Clear Corneal Incisions for Cataract Surgery. ASCRS/ASOA Annual Symposium and Congress, Washington DC, 2018

Ferreira TB, Ribeiro FJ. Comparison of the astigmatic prediction error of a new toric intraocular lens calculator with other calculation methodologies. ASCRS/ASOA Annual

Symposium and Congress, Washington DC, USA, 2018 – **Winner of the Best Paper of the Session (Cataract)**

In national congresses:

Ferreira TB. Curso Otimização dos resultados na cirurgia de catarata - calculadores e nomogramas. 59º Congresso Português de Oftalmologia, Coimbra, 2016

Ferreira TB, Ribeiro P, Ribeiro FJ, O'Neill JG. Comparação do erro de predição do astigmatismo residual entre dois calculadores de uma lente intraocular tórica. 59º Congresso Português de Oftalmologia, Coimbra, 2016

Ferreira TB, Ribeiro P, Ribeiro FJ, O'Neill JG. Distribuição e determinantes de parâmetros biométricos de candidatos a cirurgia de catarata em Portugal. 59º Congresso Português de Oftalmologia, Coimbra, 2016

Ferreira TB, Ribeiro P, Ribeiro FJ, O'Neill JG. Comparison of the astigmatic prediction errors associated with new calculation methods for toric intraocular lenses. Jornadas de Investigação - Colóquios de Oftalmologia. Cascais, 2017

Ferreira TB, Ribeiro P, Ribeiro FJ, O'Neill JG. Ocular Biometric Measurements in Cataract Surgery Candidates in Portugal. Jornadas de Investigação - Colóquios de Oftalmologia. Cascais, 2017

Ferreira TB. Deduzir ou medir o astigmatismo total. Congresso da CIRP, Santa Eulália, Portugal, 2017

Ferreira TB. A novel color-LED corneal topographer to assess astigmatism in pseudophakic eyes. Congresso da CIRP, Santa Eulália, Portugal, 2017

Ferreira TB, Ribeiro FJ, Pinheiro J, Ribeiro P, O'Neill JG. Comparação do astigmatismo induzido cirurgicamente e características morfológicas de incisões por laser de femtosegundo e manuais na cirurgia de catarata. 60º Congresso Português de Oftalmologia, Vilamoura 2017

Ferreira TB, Ribeiro FJ, Ribeiro P, O'Neill JG. Resultados clínicos de uma lente tórica com diferentes estratégias para considerar o astigmatismo corneano total. 60º Congresso Português de Oftalmologia, Vilamoura 2017

Ferreira TB. President of the Symposium "Correção do astigmatismo na cirurgia de catarata". Congresso da CIRP, Santa Eulália, Portugal, 2018.

Ferreira TB. Cálculo da lente tórica – limitações dos calculadores e como ultrapassá-las. Congresso da CIRP, Santa Eulália, Portugal, 2018.

Poster presentations:

In international congresses:

Ferreira TB, Ribeiro P, Ribeiro FJ, O'Neill JG. Comparability and repeatability of different methods of corneal astigmatism assessment. ASCRS/ASOA Annual Symposium and Congress, New Orleans, 2016.

Ferreira TB, Hoffer KJ, Ribeiro P, Ribeiro FJ, O'Neill JG. Ocular Biometric Measurements in Cataract Surgery Candidates in Portugal. XXXV Congress of the ESCRS, Lisbon, Portugal, 2017.

In national congresses:

Ferreira TB, Ribeiro P, Ribeiro FJ, O'Neill JG. Distribution of Corneal Astigmatism in Patients Undergoing Cataract Surgery. Colóquios de Oftalmologia. Cascais, 2016

Prizes awarded

This Thesis won and was supported by a research grant from the Portuguese Ophthalmological Society (Sociedade Portuguesa de Oftalmologia).

The oral communication “Comparison of the astigmatic prediction error of a new toric intraocular lens calculator with other calculation methodologies”, presented at the ASCRS/ASOA Annual Symposium in 2018, won the “Best Paper of the Session (Cataract) award”

The study “Comparison of Methodologies Using Estimated or Measured Values of Total Corneal Astigmatism for Toric Intraocular Lens Power Calculation”, published in the Journal of Refractive Surgery, was awarded the “Best publication of the year” award by the Portuguese Refractive Surgery Society (Grupo de Cirurgia Implanto-Refrativa de Portugal – CIRP).

Note: The results presented herein, in chapters 4 to 7, are formatted according to the style of the journal where the papers were published, with minor modifications.

List of abbreviations

ACA: anterior corneal astigmatism

ACD: anterior chamber depth

AL: axial length

ANOVA: one-way analysis of variance

AO: adaptive optics

APV: astigmatic power vector

AS-OCT: anterior segment optical coherence tomography

ATR: against-the-rule (astigmatism)

BFS: best-fit sphere

CA: coefficient of adjustment

CCI: clear cornea incision

CI: correction index

CCT: central corneal thickness

CD: corneal diameter

CDVA: Corrected Distance Visual Acuity

CNVA: Corrected Near Visual Acuity

D: diopters

DV: difference vector

DVM: direct visual marking

ECM: extra cellular matrix

ELP: effective lens position

FE: flattening effect

FLACS: Femtosecond laser-assisted cataract surgery

HOA(s): higher-order aberration(s)

HSBM: horizontal slit beam marking

i: image size

ICC: intraclass correlation coefficient

ICH E9: International Council for Harmonization Guidelines on Statistical Principals for Clinical Trials

IOL: intraocular lens

IRB: institutional review board (for approval of clinical trials)

IUS: Immersion ultrasound

JCC: Jackson crossed cylinder

K: keratometry

K1: minimum (flat) keratometry

K2: maximum (steep) keratometry

Km: mean keratometry

J_0: vector for horizontal meridian (0°-180°)

J_{45}: vector for oblique meridian (45°-135°)

LASIK: Laser-in-situ-keratomileusis

LED: light-emitting diode

LOA(s): lower-order aberration(s)

LogMAR: Logarithm of the Minimal Angle of Resolution

LT: Lens thickness

MAE: Mean absolute error

ME: magnitude of error

MGD: Meibomian gland disease

MICS: microincision cataract surgery

OB: oblique (astigmatism)

OCT: optical coherence tomography

OLCR: optical low-coherence reflectometry

OVD: ophthalmic viscosurgical device

PCA: posterior corneal astigmatism

PCI: partial coherence interferometry

PRK: photorefractive keratectomy

r: reflective surface

REFc: refraction at the corneal plane

REFv: refraction at the vertex plane

RMS: Root mean square

SD: standard deviation

SD-OCT: spectral-domain OCT

SDVM: subjective direct visual marking

SIA: Surgically induced astigmatism

SIRC: surgically induced refractive change

SVM: summated vector mean (astigmatism)

TCA: total corneal astigmatism

TIA: target induced astigmatism

UDVA: uncorrected distance visual acuity

UNVA: uncorrected near visual acuity

V: vertex distance (mm)

WTR: with-the-rule (astigmatism)

Resumo

A cirurgia de catarata é o procedimento cirúrgico mais frequente em países desenvolvidos. Recentemente, e em paralelo com a maior satisfação dos doentes e uma elevada taxa de sucesso, verificou-se uma transformação da cirurgia de catarata num procedimento refrativo. No entanto, um dos fatores que limita a acuidade visual e independência de óculos após esta cirurgia é o astigmatismo. Cerca de 29% dos doentes submetidos a cirurgia de catarata têm astigmatismo corneano superior a 1.25 dioptrias (D).

O cálculo da potência de lentes intraoculares (LIOs) é baseado em fórmulas derivadas de parâmetros biométricos oculares normativos. Assim, o conhecimento destes parâmetros é de extrema importância. Entre a população portuguesa, não existiam dados publicados relativos aos parâmetros biométricos oculares ou suas associações. Desta forma, descrevemos os parâmetros biométricos oculares e a prevalência de astigmatismo corneano em candidatos a cirurgia de catarata em Portugal. O comprimento axial médio, a profundidade da câmara anterior e a queratometria média encontrados foram mais aproximados dos publicados na população dos Estados Unidos da América do que nas diferentes séries de caucasianas Europeias, sendo que as disparidades observadas podem representar diferenças superiores a 1 D na avaliação do erro refrativo ou na potência da LIO a implantar. O astigmatismo corneano foi também mais elevado do que na maioria das restantes séries publicadas, o que tem óbvias implicações no tipo de LIO a implantar.

Entre as diversas técnicas para a correção do astigmatismo durante a cirurgia de catarata, as LIOs tóricas são a mais eficaz e previsível. No cálculo da potência cilíndrica destas lentes, existem, no entanto, diversas fontes de erro.

No estudo pré-operatório, uma avaliação precisa do astigmatismo a ser corrigido é imperativa. É controverso qual o tomógrafo mais preciso para a medição do astigmatismo corneano total (ACT). Considerando a precisão limitada nesta avaliação, foram recentemente desenvolvidas novas tecnologias, tais como, a topografia de díodos de emissão de luz colorida (LEDs). Esta tecnologia está disponível comercialmente no tomógrafo Cassini (i-Optics, The Hague, Holanda), que utiliza algoritmos de traçado de

raios para medir o ACT. Sendo uma tecnologia recente, a sua precisão e validação clínica devem ser investigadas.

De forma a aprofundar o conhecimento científico sobre este tomógrafo, investigámos qual o método mais preciso de avaliação do astigmatismo corneano, comparando a topografia de LEDs coloridos com dois outros métodos – um tomógrafo de avaliação em fenda e um queratómetro automático. Avaliámos ainda a comparabilidade e repetibilidade destes métodos. O primeiro estudo mostrou que a avaliação do astigmatismo corneano por topografia de LEDs coloridos é a mais precisa entre as tecnologias estudadas. O segundo estudo demonstrou que todas as técnicas apresentam valores de queratometria e eixo de astigmatismo comparáveis entre si. No entanto, a grande dispersão de valores encontrada sugere que elas não devem ser usadas de forma intercambiável.

Para além da precisão limitada na avaliação pré-operatória do astigmatismo, existem outras limitações no cálculo da potência de LIOs tóricas. A primeira é utilização, por grande parte dos calculadores de LIOs tóricas, de um ratio fixo entre a potência cilíndrica nos planos da LIO e da córnea, o que gera hipocorreções em olhos longos e hipercorreções em olhos curtos. Além disso, e apesar da pouca literatura científica alusiva a este tópico, a potência cilíndrica da LIO no plano da córnea depende também da sua potência esférica, devido à diferente vergência dos raios de luz. É ainda imperativo considerar o ACT no cálculo da LIO.

De forma a ultrapassar as limitações enumeradas, foram desenvolvidas novas estratégias de cálculo, incluindo nomogramas e novos calculadores, que tomam em consideração a posição efetiva da lente e/ou o ACT.

Para investigar qual o mais preciso dos novos métodos de cálculo, investigámos o erro de predição no astigmatismo residual de cada um deles em doentes previamente submetidos a cirurgia de catarata com implante de LIO tórica. Comparámos ainda estratégias que estimam o ACT com medições reais do seu valor. O calculador tórico de Barrett e a fórmula Abulafia-Koch foram os métodos com maior previsibilidade. Os resultados do estudo consecutivo demonstraram que, atualmente, a medição direta da superfície posterior da córnea não é mais precisa do que a predição do ACT com modelos

matemáticos. Sugerimos, desta forma, que os resultados clínicos de implante de LIOs tóricas podem ser melhorados recorrendo ao calculador de Barrett ou à fórmula Abulafia-Koch.

A estimativa do astigmatismo induzido cirurgicamente (AIC) é outra fonte de erro a considerar no cálculo de LIOs tóricas. O AIC depende de diversos fatores relacionados com o indivíduo, a incisão cirúrgica e o tipo de cirurgia. Como estes fatores interagem para determinar o AIC não tinha sido estudado anteriormente. De forma a contribuir para um maior conhecimento sobre o AIC, comparámos o seu valor após cirurgia de facoemulsificação com incisões em córnea clara (ICC) realizadas com laser de femtosegundo ou manualmente e investigámos a influência de fatores individuais e características de incisão no AIC. Concluímos que as ICC criadas recorrendo ao laser de femtosegundo resultaram numa arquitetura mais reprodutível em e valores de AIC mais baixos, apesar da diferença nestes não ter sido estatisticamente significativa e se ter verificado uma grande dispersão de valores em ambos os grupos. Assim sendo, para o cálculo da LIO tórica, deverá ser considerado um AIC médio.

Em suma, demonstrámos que a prevalência de astigmatismo corneano na população portuguesa é elevada. Para a avaliação do ACT pré-operatório, a topografia de LEDs coloridos é nova uma tecnologia com elevada precisão. Comprovámos que, entre os novos calculadores de lentes tóricas, os mais precisos são o calculador de Barrett e a fórmula de Abulafia-Koch. Ficou também provado a estimativa do ACT utilizando modelos matemáticos é mais precisa que a sua medição direta com câmaras de Scheimpflug. Apesar da nossa contribuição, com um estudo prospetivo aleatorizado, para o enriquecimento do conhecimento sobre o AIC, a sua previsibilidade na cirurgia de catarata é ainda baixa, quer em cirurgia manual, quer assistida por laser femtosegundo.

Em conclusão, a correta avaliação pré-operatória do ACT, a escolha do calculador de lentes tóricas mais preciso e uma melhor estimativa do AIC melhoram os resultados clínicos da cirurgia de catarata com implante de lentes tóricas. São apontados tópicos futuros de investigação com vista a tornar ainda mais preciso o cálculo destas LIOs.

Abstract

Cataract surgery is the most frequent surgical procedure in developed countries. In recent years, while having increasingly high success and patient satisfaction rates, a steady fusion of cataract and refractive surgery occurred. Nevertheless, one of the factors limiting visual acuity and spectacle independence after cataract surgery is astigmatism. Corneal astigmatism over 1.25 diopters (D) is present in up to 29% of patients submitted to cataract surgery.

Intraocular lens (IOL) power calculation is primarily based on formulas derived from normative ocular biometric parameters. Therefore, knowledge of these parameters is essential. In the Portuguese population, there was no published data on the ocular biometric parameters or their associations, so we described the mean ocular biometric parameters and the prevalence of corneal astigmatism in cataract surgery candidates in Portugal. We found that the mean axial length, anterior chamber depth, and mean keratometry values were closer to those published for the United States population than most series in different European Caucasian populations, with and the disparities representing potential differences of 1 D or more in both refractive error and IOL power evaluation. Corneal astigmatism was higher than that in most published series, which may affect the type of IOL to be implanted.

Among the various techniques for correcting astigmatism during cataract surgery, toric IOLs are the most effective and predictable. When calculating the cylindrical power of these lenses, there are, however, multiple sources of error.

Preoperatively, precise evaluation of the astigmatism to be corrected is mandatory. In such a way, there is an ongoing debate on which instrument is most accurate for evaluating total corneal astigmatism (TCA). Accounting the limited precision, several promising technologies were recently developed, such as color-light emitting diode (LED) topography. This technology is commercially available in the Cassini (i-Optics, The Hague, the Netherlands) topographer, which uses ray tracing algorithms to provide a complete analysis of the cornea. To contribute to the scientific knowledge on this new topographer, we have studied which method evaluates corneal astigmatism with higher

precision by comparing color-LED topography with two other established astigmatism measurement methods (a slit-scanning topographer and an automated keratometer). We investigated the comparability and repeatability of these three methods. In a first study, it was shown that the evaluation of corneal astigmatism by color-LED topography was more precise than the other technologies. A subsequent study demonstrated that all measurement techniques show comparable keratometry and astigmatism axis values. However, the wide data spread found suggests these devices should not be used interchangeably.

Besides the limited precision in the preoperative evaluation of astigmatism, other limitations exist in the power calculation of toric IOLs. One of these limitations is the assumption, by most toric IOL calculators, of a fixed ratio between the cylindrical power at the IOL and corneal planes. This results in undercorrections in long and overcorrections in short eyes. Moreover, although scientific literature is scarce on the subject, the cylindrical power of the IOL at the corneal plane also depends on the IOL's spherical power, due to the different vergence of the light rays. Also, knowledge and consideration of total corneal astigmatism is mandatory for precise toric IOL calculation. To overcome these known limitations, several new calculation strategies were recently developed.

To investigate the most precise of the novel calculation methods, we have calculated the prediction error for each of them in a group of patients submitted to cataract surgery with toric IOL implantation and investigated whether it would be better to directly evaluate total corneal astigmatism or use the current nomograms that estimate its value. Overall, the Barrett toric calculator and the Abulafia-Koch formula yielded the lowest astigmatic prediction errors. Findings from the consecutive study demonstrated that, at present, directly measuring the posterior corneal surface is not superior to predicting its power with theoretical models. We suggest that the clinical results of toric IOL implantation may be improved by using Barrett toric calculator and the Abulafia-Koch.

Another source of error in cataract surgery with toric IOL implantation is arising from the surgically induced astigmatism (SIA), which must considered for toric IOL calculation.

SIA depends on numerous factors related to the individual, the incision, and the type of surgery. How these factors interplay to determine SIA had not been studied. To improve knowledge of SIA, using the same clear cornea incision (CCI) size, we compared its value after phacoemulsification with femtosecond laser and manually-created CCIs and investigated the influence of individual factors and incision characteristics on SIA. It was found that femtosecond laser-created CCIs resulted in more reproducible wound architecture and lower SIA values, although the difference in SIA did not reach statistical significance and the dispersion of SIA magnitudes was high. Association of SIA with specific individual features remains highly variable. Thus, for toric IOL calculation, a mean value should be considered.

In summary, we demonstrated that the prevalence of corneal astigmatism in the Portuguese population is high. To evaluate preoperative total corneal astigmatism, color-LED topography is a precise new technology. We showed the most precise of the recently developed toric IOL calculators are the Barrett toric calculator and the Abulafia-Koch formula. Also, that estimating the total corneal astigmatism with mathematical models revealed to be superior to measuring it directly with Scheimpflug-based tomography. Thus, this should be, at present, the preferred calculation method for toric IOLs. While we contributed to improve knowledge of SIA with a large series in a prospective randomized clinical study, its predictability is still low for both manual and femtosecond laser assisted cataract surgery.

In conclusion, correctly evaluating preoperative total corneal astigmatism, using the most precise toric IOL calculator and precisely predicting SIA will ultimately improve the clinical results of cataract surgery with toric IOLs. Future research topics to further refine calculation of these IOLs are suggested.

Chapter 1: General introduction

1.1 Introduction

Cataract surgery is the most frequent surgical procedure in developed countries.[1] In the past decade, cataract surgery transitioned from a replacement of the opacified crystalline lens to a refractive procedure. Considering this, spherical refractive error became managed with increased precision by optical biometry and new intraocular lens (IOL) power calculation formulas.[2] Moreover, as the refractive outcome became increasingly important, accuracy in preoperative planning for astigmatic correction during the cataract procedure also became critical. A recent study of 282.811 eyes from the European Registry of Quality Outcomes database for cataract and refractive surgery showed that the influence of astigmatism on the precision of spherical equivalent after cataract surgery was considerable, resulted in the recommendation for implanting toric intraocular lenses (IOLs) to improve outcomes.[3]

Astigmatism is a highly prevalent lower-order aberration (LOA) in cataract patients. Its prevalence varies slightly between studies, with reported values of 64.4% of corneal astigmatism between 0.25 diopters (D) and 1.25 D and of 22.2% 1.50 D or higher[4] or 63.96% less than 1.00 D and 27.95% between 1.00 D and 2.00 D.[5] In general, it is estimated that up to 40% of patients undergoing cataract surgery have a corneal astigmatism of 1.00 D or more,[6] and it has been suggested that correction of astigmatism below 0.5 D would have limited visual benefit, whereas correction of astigmatism of more than 0.5 D can improve visual outcomes.[7] Therefore, without surgical correction of this astigmatic component, it is unlikely that spectacle independence will be achieved after surgery.[4] This, in turn, leads to personal, social and economic burdens.[8]

With the importance of achieving emmetropia after surgery, IOL power calculation is a constantly evolving field of research. Currently, for spherical IOL power calculation, the combination of optical biometry with last generation formulas, such as the Barrett Universal II or the Hill-radial basis function formula results in a postoperative refractive result within ±0.50 D of the target in 72 to 80% of the eyes[9,10,11,12], whereas with classical toric IOL calculation only 26 to 35% of the eyes achieve a result within ±0.50 D of the targeted residual astigmatism.[11] In most studies, the mean refractive astigmatism after the implantation of a toric IOL ranges between -0.72 ±0.43 D and -1.03 ± 0.79 D[12,13,14]. These results reflect the need for increased precision in the calculation of the cylindrical

power of these IOLs. This is further supported by the fact that implantation of aspheric, multifocal or toric IOL IOLs designs is ineffective unless minimal residual postoperative astigmatism is achieved.[13]

Despite their efficacy and predictability, toric IOL implantation is a complex process where multiple pre-, intra- and postoperative steps must be optimized in order to minimize errors. The main objective of this research is contributing to further minimize these the possible errors.

1.2 Thesis outline

The next chapter (**Chapter 2**), provides a general introduction covering current knowledge of astigmatism, the importance and methods for its surgical correction, and each of the steps involved in toric IOL implantation.

Chapter 3 details the objectives of this thesis.

The subsequent chapters (**Chapters 4 to 7**) present the studies on which this PhD thesis is based.

Chapters **8 and 9**, discuss findings and enumerate conclusions of the research.

Finally, **Chapter 10** presents future directions for further research on the subject.

Chapter 2: Theoretical background

2.1 Optic system and corneal structure

The optic system of the eye is made up of different components. Light entering the eye is refracted as it passes through the cornea. It then passes through the pupil, being further refracted by the lens. The cornea and lens act together as a compound lens to project an inverted image onto the retina. The cornea, with the anterior chamber and the lens, refracts light, with the cornea accounting for approximately two-thirds of the eye's total optical power. In humans, the refractive power of the cornea is approximately 43 D. The lens can change its shape, with the curvature being controlled by ciliary muscles through the zonules. By changing the curvature of the lens, focusing on objects at different distances is possible. This process is called accommodation. At short focal distances, the ciliary muscle contracts, zonular fibers loosen, and the lens thickens, resulting in an increased curvature and a higher refractive power. Changing focus to an object at a greater distance requires the relaxation of the lens, increasing the focal distance. In young individuals, the refractive power of the lens lies between 19 and 33 diopters.[14]

Despite the importance of the cornea as the most important optical structure of the eye, only in 1944 W. H. Crisp[15] presented the first of Jackson's lectures on this topic, recognizing: his development of the cross cylinder, first described in 1887[16]; the change in corneal refractive power from the center to the periphery[17] (certainly the first description of spherical aberration) and the report that corneal astigmatism is different from the eye's total corneal astigmatism in 75% of cases.[18]

2.1.1 Corneal structure

The cornea is a transparent avascular connective tissue acting as the primary structural barrier of the eye. Together with the tear film, it also provides the anterior refractive surface of the eye. On average, the horizontal diameter of the cornea is 11.5 to 12 mm and about 1 mm larger than the vertical diameter. It has a thickness of about 0.5 mm at the center, gradually increasing towards the periphery. Its shape is prolate – flatter in the periphery and steeper centrally, creating an aspheric optical system. The cornea consists of 6 layers. Three of them, epithelium, stroma and endothelium, are cellular and two of them, Bowman and Descemet membrane, are interface layers.[19]

Furthermore, an additional acellular, strong layer in the pre-Descemet cornea called Dua's layer was recently discovered. Dua's layer separates along the last row of keratocytes in most cases when the big-bubble technique is performed for deep anterior lamellar keratoplasty.[20]

The anterior and posterior curvature of the cornea have, on average, 7.8 mm and 6.5 mm, respectively, and a refractive index of 1.376. The gradual change in tissue thickness is due to an increasing amount of collagen in the peripheral stroma. The central corneal thickness (CCT) ranges from 551 to 565 µm and the peripheral thickness from 612 to 640 µm. Corneal thickness decreases with age. Anterior corneal stroma rigidity appears to be especially important in maintaining the curvature of the cornea, as the anterior curvature resists changes to stromal hydration much more than the posterior stroma.[19]

Both cellular and acellular components are present on the cornea. Cellular components include epithelial cells, keratocytes and endothelial cells, while acellular components are collagen and glycosaminoglycans. Epithelial cells are derived from epidermal ectoderm, while endothelial cells are derived from the neural crest.[21] The corneal epithelium is composed of five to seven cell layers and is about 50 µm thick. The epithelium is uniform, providing a smooth regular surface. It is made up of non-keratinized stratified squamous epithelium. This epithelium is derived from surface ectoderm between 5 and 6 weeks of gestation. The epithelium has a symbiotic relationship with the tear film. The mucin layer of the tear film is in direct contact with the epithelium and produced by conjunctival goblet cells. It interacts closely with the corneal epithelial cells' glycocalix to allow hydrophilic spreading of the tear film with each blink. Corneal epithelial cells have a life span of seven to ten days. The presence of high concentrations of the intracytoplasmic enzyme crystalline, like in lens epithelial cells, may play an important role in maintaining its optical transparency. The epithelium layers consist of three types of cells (superficial cells, wing cells and basal cells).

The most superficial layers consist of two-three flat polygonal cells, with microvilli on the surface increasing the surface area. They have tight junction complexes to prevent tear film fluid from entering the intercellular spaces. Thawing cells are two-three layered and named wing cells because of their shape. Basal cells are a single layer in a cuboid or

columnar form, making up 20 µm in thickness. They have abundant organelles and are mitotically active. Besides stem cells and transient amplifying cells, basal cells are the only corneal epithelial cells capable of mitosis. They are the source of wing and superficial cells. Basal cells are attached to the underlying basement membrane by a hemidesmosomal system. The strong attachment prevents the epithelium from separating from the underlying layers. An abnormality in this attachment may result in corneal erosions or persistent epithelial defects. Tight junctions are present in the lateral walls of apical epithelium cells, providing a permeability barrier at the most superficial level. Adherence junctions are present along the lateral membrane of the apical epithelial cells. They maintain cellular adherence in the region of tight junctions. Gap junctions are permeable channels on the lateral aspects of all epithelial cells, allowing the diffusion of small molecules. The epithelium basement membrane is 40-60 nm thick and composed of Type IV collagen and laminin secreted by the basal cells, forming the lamina lucida and lamina densa. From the basal epithelial cells, anchoring fibrils pass through the basement membrane ending up as anchoring plaques. Anchoring fibrils are made up of type VII collagen and anchoring plaques of type I collagen. If the basement membrane is damaged, fibronectin levels increase and the healing process may be prolonged up to six weeks.[22] In the basement membrane, the palisades of Vogt are undulations providing increased vascularity and surface area for attachment, as well as protection to stem cells. Bowman's membrane is a condensation of collagen and proteoglycans about 12 µm thick. It is situated just anterior to the stroma and it not a true membrane, but rather an acellular condensate of the most anterior portion of the stroma. This smooth layer helps the cornea maintain its shape. When injured, it does not regenerate and scarring may occur. The corneal stroma forms the bulk of the structural framework of the cornea and 80-85% of its thickness. It is transparent, which is a result of the precise organization of its fibers and extracellular matrix (ECM). The collagen within corneal fibrils is predominantly type I, with type VI and type XII collagen also being present.[23] Collagen fibers are arranged in parallel bundles called fibrils. These fibrils are packed in layers or lamellae. The stroma of the human eye contains about two hundred distinct lamellae, with each layer being arranged at right angles relative to fibers in the adjacent lamellae. These structures are of variable dimensions, in humans up to 0.2 mm broad and 2 µm thick. The packing density is higher in the anterior lamellae

than in the posterior stroma. These anterior lamellae are highly interwoven and most appear to enter the Bowman layer.[24] The mid-stromal lamellae are also highly interlaced. The posterior lamellae in the central cornea are more hydrated. Thus, the posterior stroma can swell easily while the more interwoven anterior cannot.[25]

Corneal stroma is made up of keratocytes and ECM. ECM is composed of collagens and glycosaminoglycans (keratin sulfate, chondroitin sulfate and dermatan sulfate). The corneal stroma has keratocytes and about three hundred collagen lamellae which are regularly arranged. Glycosaminoglycanes are predominantly made up of keratin sulfate and, in less quantity, of chondroitin and dermatan sulfate. Keratocytes are the major cell type of stroma, mostly being found in the anterior stroma. They are involved in maintaining the ECM environment. They are able to synthesize collagen and glycosaminoglycans, while also creating matrix metalloproteinases (MMPs), all necessary to maintain stromal homeostasis.

Dua's layer is a well-defined, acellular, strong layer in the pre-Descemet's cornea 6-15 µm thick. It consists of five to eight lamellae of collagen fibers, with no presence of keratocytes.[20]

Descemet membrane is an elastic layer with a thickness of about 7 µm, made up of type IV collagen and laminin. The anterior part of this membrane is secreted before birth and has a distinctive banded appearance, while the part produced after birth has an amorphous ultrastructural texture. The membrane thickens with age and can become up to 10 µm thick.

The endothelium layer is a single layer of 5 µm thickness. Its cells are hexagonal and metabolically active. An endothelial pump regulates the water content. The layer appears as a honeycomb-like mosaic when seen from the posterior side. Adjacent cells share extensive lateral interdigitations and possess gap and tight junctions along the lateral borders. The lateral membrane has a high density of Na^+K^+ ATPase pump sites. The two most important ion transport systems are the membrane-bound Na^+K^+ ATPase and the intracellular carbonic anhydrase pathway. Activity in both systems produces a net flux of ions from the stroma to the aqueous humor. The basal surface of the

endothelium contains numerous hemidesmosomes promoting adhesion to Descemet's membrane.

Immediately anterior to the endothelium is a discontinuous homogenous acellular layer, the Descemet membrane. At birth this membrane is about 3 µm thick, gradually thickening to 10 µm in adults. Descemet's membrane becomes continuous and uniform, fusing peripheral with trabecular beams. The fusion site is called Schwalbe's line. This line is an important gonioscopic landmark, defining the end of Descemet's membrane and the start of the trabecular meshwork.

Endothelial cell density continues to change with aging, declining from the second to eighth decade.[26] Endothelial cells do not regenerate in adults.[27]

The cornea is one of the most densely innervated tissues of the body. Sensation is derived from the nasocilliary branch of the first division of the trigeminal nerve. Thick and straight stromal nerve trunks extend laterally and anteriorly to give rise to plexiform arrangements of progressively thin nerve fibers at several levels within the stroma. The nerve fibers perforate Bowman's layer and eventually form a dense nerve plexus just beneath the basal epithelial cell layer. This is characterized by tortuous, thin beaded nerve fibers interconnected by numerous nerve elements. The cornea also contains autonomic sympathetic nerve fibers.[28]

Although the cornea is avascular, it still relies on components of the blood. It is supplied by very small vessels at the limbus, as well as by terminal branches of the facial and ophthalmic arteries via the aqueous humor and tear film.

2.2 Optical aberrations of the eye

Two main types of optical aberrations, which limit optical quality by causing diffraction and scatter, are present in the human eye: chromatic and monochromatic.[29] Chromatic aberrations (transversal or longitudinal) are due to differences in the refractive indices for different wavelengths of light. The human eye suffers from longitudinal chromatic aberration (average value of 1.82 D).[30] The result of chromatic aberration is the creation of blurred images with color fringes. Monochromatic aberrations arise from the shift between the wavefront (locus of points that are at the same optical distance from their

source point) and a perfect reference sphere, and may be further sub-divided in lower- and higher-order aberrations (LOAs and HOAs, respectively). LOAs include refractive errors (myopia, hyperopia, and regular astigmatism), among other non-visually significant aberrations, and account for approximately 90% of the total wave aberration of the eye.[31,32] HOAs comprise about 10% of the eye's total aberrations, although this division is artificial and both are not mutually independent.[33]

2.2.1 Types of refractive errors

The presence of any refractive error influences the total refractive power of the eye. It prevents the correct focusing of light onto the retina. This can be due to the shape of the eye (a longer or shorter axial length) or to abnormalities in the cornea (steeper or flatter radius) or lens (thickness or changes in shape). The types of refractive errors are myopia, hyperopia, astigmatism, and presbyopia. Myopia results in distant objects being blurry, hyperopia and presbyopia result in close objects being blurry and astigmatism causes objects to appear stretched out or blurry. Other symptoms may include double vision, headaches, and eye strain.

2.2.1.1 Astigmatism

Astigmatism occurs when parallel rays of light entering the eye are not focused at a single point on the retina. Most astigmatism is of corneal origin, but the lens and the retina may also have an effect (the influence of the retina is, generally, minimal). Each surface adds some astigmatism, and the total astigmatism of an optic system is the result of all components. In some cases, one surface may negate the effect of another. In individuals with corneal astigmatism, the cornea is steeper in one meridian than another. While this is mostly due to the anterior corneal surface, the posterior surface has an increasingly recognized role, as detailed in the next chapter.

Astigmatism accounts for about 13% of refractive errors in the human eye. Its prevalence rate is up to 30% or higher, depending on the age or ethnic group. Astigmatism may be due to congenital and acquired reasons, including corneal diseases, trauma, and ocular surgery.[34]

Astigmatism is classified according to its axis, as being with-the-rule (WTR), against-the-rule (ATR) or oblique. By definition, WTR astigmatism is corrected with a plus cylinder lens between 60 and 120 degrees, ATR astigmatism between 150 and 30 degrees, and oblique astigmatism between 31 to 59 or 121 to 149 degrees.

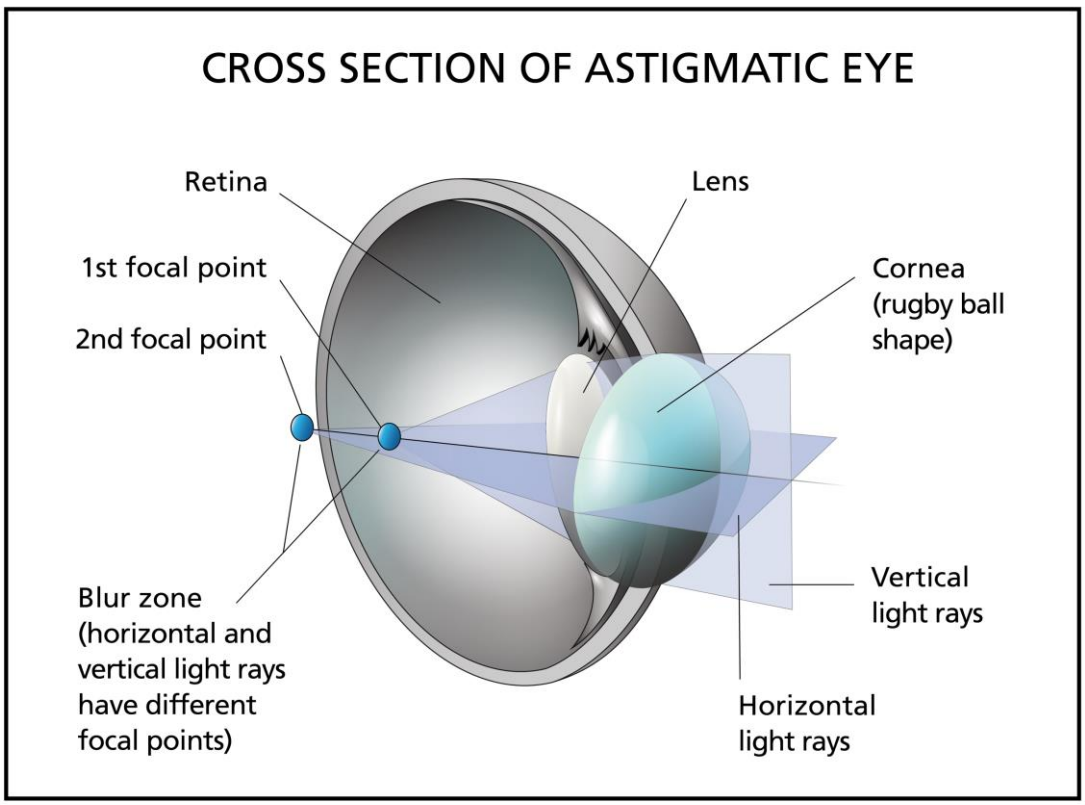

Figure 1 - Graphical representation of an eye with astigmatism.

Corneal astigmatism may be influenced by the tear film, the anterior and posterior curvature of the cornea as well as the aqueous humor. As light does not focus on a single point, retinal images from distant and near objects are blurred and may appear broadened or elongated. The focal distance between the two focal points is called the interval of Sturm (Conoid of Sturm). At the center of the Conoid of Sturm is the circle of least confusion. With the appropriate spherical equivalent in a cylindrical lens, the horizontal and vertical dimensions of the blurred image are similar, with the circle increasing in diameter with increasing amounts of astigmatism. The best visual acuity in an astigmatic eye is achieved when the circle of least confusion is located on the retina.

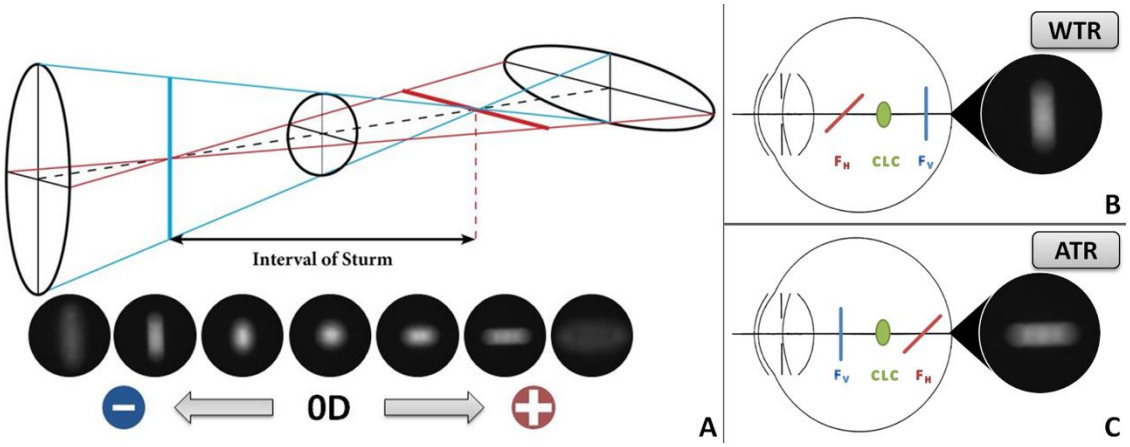

Figure 2 (A) illustrates the interval of Sturm, the circle of least confusion and the retinal images of a circular spot when astigmatism is induced. (B) Illustrates the astigmatic foci in a myopic with-the-rule astigmat. (C) Illustrates the astigmatic foci in a myopic against the rule astigmat.

FV = vertical focus; CLC = circle of least confusion; FH = horizontal focus.

Reprinted with License from Association for Research in Vision and Ophthalmology (ARVO) and Copyright Clearance Center.

While the cornea is the main astigmatic source of the human eye, the lens also contributes to the eye's total astigmatism. A study showed that high astigmats have significantly lower lenticular horizontal and higher lenticular oblique astigmatism than low astigmats. The lenticular component of astigmatism usually reduces the astigmatic effect of the anterior corneal surface.[35] Changes influencing the crystalline lens, such as genetic defects, trauma or subluxation can also induce variations in the optical properties of the lens. Cataract development has also been reported to induce lenticular astigmatism in some cases.[36] In a pseudophakic eye, IOL tilt and/or decentration induce both myopia and astigmatism (oblique).[37]

Astigmatism of retinal original is low. It has been attributed to directional variability in photoreceptor arrangement[38] or, more recently, to a tilted retinal orientation, which might result of unequal lengthening of the sclera in different meridians during axial growth.[39]

Irregular astigmatism is any refractive astigmatism that cannot be corrected by a spherocylindrical lens. It occurs when the two principal meridians of the cornea are not

perpendicular to one another. While all eyes have a small amount of irregular astigmatism, it only is clinically significant in eyes with grossly irregular corneas, such as cases of corneal scars or corneal ectasia.[34]

2.2.1.1.1 Influence of astigmatism on visual acuity

Adaptive optics (AO) is playing an increasing role as an enabling technology in visual science. By allowing scientists to precisely control the visual stimulus, to image the retina at a higher resolution, it has the potential to become a mainstay of the scientific armamentarium. Because there are no common commercial platforms for using AO, individual scientists have used a variety of approaches to generate their own unique systems.[40]

AO has been used to study the role of native astigmatism and ocular aberrations on best focus setting and its shift upon induction of astigmatism in emmetropes, myopes, hyperopes, and WTR myopic astigmats. Stimuli were presented to subjects in an AO simulator, while correcting native aberrations and inducting astigmatism (+1 D, 6-mm pupil). Each subject was asked to search best focus for different images under different conditions (with or without aberrations; with or without astigmatism induction). The induction of aberrations shifted the subjective best focus and significantly correlated with the best focus shift predicted by optical simulations. The induction of astigmatism caused a shift of the best focus in all groups under natural aberrations, and in emmetropes and WTR astigmats under conditions with corrected aberrations. With induction of astigmatism, best focus shifted in opposite directions in WTR and ATR astigmats, symmetrically with respect to the shift in best focus in non-astigmatic myopes. The authors concluded that the observed shifts are consistent with a bias towards vertical and horizontal retinal blur in WTR and ATR astigmats, respectively, suggesting an adaption to native astigmatism.[41]

2.2.2 Higher-order aberrations

HOAs can be measured by devices based on one of three principles - Tscherning's aberroscopes, Hartmann-Shack's aberroscopes or ray tracing. The results of these measurements are often presented in the form of Zernike polynomials, described by

Frits Zernike (1888-1966), a Dutch Nobel prize in physics. They may be used to represent the optical aberrations of the entire optical pathway or any of its components.

The first orders of the Zernike polynomials (Z_0^0, piston and Z_1^1, Z_1^{-1}, tilt), have little direct impact on refraction. The second order aberrations (Z_2^0 and Z_2^2, Z_2^{-2}) correspond to the refractive error (sphere and cylinder), and can be corrected with spherocylindrical spectacle lenses. The higher orders of the Zernike polynomials represent the HOAs. By definition, HOAs cannot be corrected by spherocylindrical lenses. Correction of corneal HOAs is only possible by using rigid contact lenses, performing wavefront optimized or guided excimer laser ablations, or implanting IOLs that correct, for example, spherical aberration (Z_4^0).

Different representations of the refractive qualities of an optical system exist, such as the Fourier analysis, named after Jean Baptiste Fourier (1768-1830), a French mathematician and physicist, who showed that representing a function by a trigonometric series simplifies its study. A Fourier series is composed of trigonometric sine and cosine functions with increasing coefficients. By applying Fourier analysis to polar data of corneal power for each mire, it is possible to separate corneal topographic information into components – spherical, regular and irregular astigmatism, and decentration. For representing the eye's optical system, Zernike polynomials are generally more adequate than Fourier analysis. Zernike polynomials from the second to the fifth order are sufficient to outperform Fourier analysis in most populations. However, polynomials up to the ninth order may be required to accurately describe the simulated wavefront in some abnormal eyes.[42]

The magnitude of total aberrations is measured as a Root Mean Square (RMS) error, with most normal patients having RMS values of less than 0.3 µm. Higher RMS values indicate a more aberrated optical system.

Among the HOAs present in the human eye, spherical aberration, coma and trefoil (third and fourth order aberrations) are the most visually significant.[43, **Erro! Marcador não definido.**]

Spherical aberration is a fourth order aberration causing halos around point images. In photopic conditions, when the pupil constricts, the more peripheral light rays are

blocked, minimizing the effect of spherical aberration. In low-light conditions, as the pupil dilates, more peripheral rays enter the eye and the focus shifts anteriorly, inducing slight myopia. In general, the increase in overall wave aberration with pupil size has been reported to increase to approximately the second power of the pupil radius.[44] This is because most wave aberration is due to second order aberrations, which have a square radius dependency.[Erro! Marcador não definido.] The effect of spherical aberration increases as the fourth power of the pupil diameter (i.e. doubling the pupil diameter increases spherical aberration sixteen times).[45] Thus, a small change in pupil size may cause a significant change in refraction. This possibility should be considered in patients with fluctuating vision despite well-healed corneas after keratorefractive surgery, as spherical aberration generally increases after myopic excimer laser refractive surgery.[46] Coma is a third order aberration that causes an effect of smearing an image or making it appear to have a tail similar to that of a comet. It is a HOA common in patients with decentered excimer laser ablations or corneal grafts, and corneal ectasia. Trefoil, other third order aberration, produces less degradation in image quality when compared with coma of a similar RMS magnitude.[Erro! Marcador não definido.]

The relationship of light conditions and accommodation with HOAs astigmatism is well established. In low light conditions, the increase in HOAs may induce a higher cylinder power in manifest refraction. Increasing coma is correlated with higher magnitudes of astigmatism.[47] On the contrary, pupillary constriction with accommodation reduces HOAs and lenticular astigmatism.[48]

It has been demonstrated that certain combinations of non-rotationally symmetric aberrations (coma and astigmatism) can improve retinal image quality over what is achieved with the same magnitude of astigmatism alone. A study using AO simulated retinal image quality and measured visual acuity while varying defocus (between -1 and 1 D), astigmatism (between 0 and 1.5 D), and coma. They showed that the amount of coma producing the best retinal image quality (for a given relative angle between astigmatism and coma) was different from zero in all cases (except for 0 D of astigmatism). For example, for a 6-mm pupil, in the presence of 0.5 D of astigmatism, a value of coma of 0.23 µm produced a peak improvement in Strehl Ratio by a factor of 1.7 over the presence of astigmatism alone. These improvements were maintained

across a range of more than 1.5 D of defocus, with peak improvements being found for values of coma between 0.15 µm and 0.35 µm. However, the author also concluded that, for the typical normal levels of HOAs, this effect of coma/astigmatism interaction is considerably reduced.[49]

2.3 Importance of the posterior corneal surface

With the development of technologies that allow measurement of the posterior corneal curvature, knowledge of total corneal astigmatism has evolved. Posterior corneal astigmatism is clinically relevant. It reduces total corneal astigmatism by 13.4%, on average and, in 28.8% of eyes, causes total corneal astigmatism to differ from anterior corneal astigmatism by more than 0.5 D or more than 10 degrees.[50] Savini et al. showed that, in eyes with moderate to high astigmatism, a difference of 0.5 D or more in the magnitude of keratometric and total corneal astigmatism is present in 16.6% of cases, while a difference of 10 degrees or more in the location of the steep meridian exists in 3.8% of cases. In the same study, a high positive correlation was found between the magnitude of keratometric and posterior corneal astigmatism (Figure 3).[51]

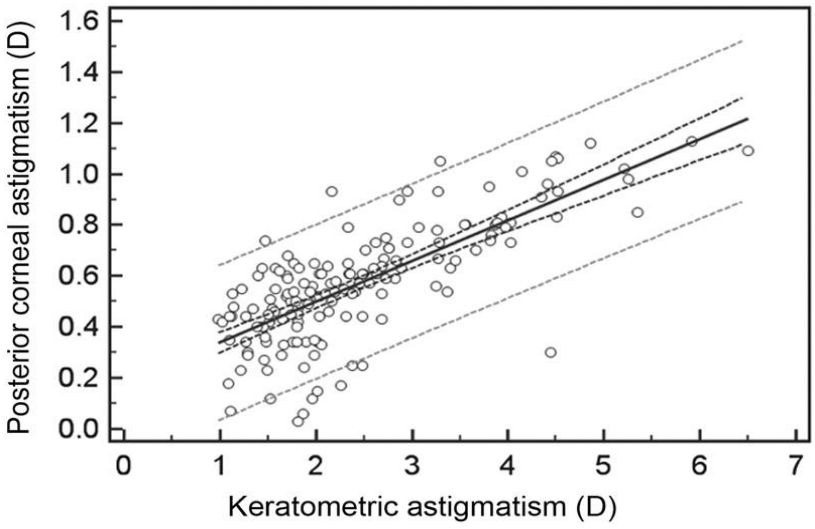

Figure 3 – Correlation between the magnitude of posterior corneal astigmatism and keratometric astigmatism across the whole sample. The outer dotted lines represent the 95% prediction. The inner dotted lines represent the 95% confidence interval.

Reprinted with License from Elsevier and Copyright Clearance Center.

Koch et al. showed that the posterior cornea is steeper along the vertical meridian in more than 86.6% of eyes (Figure 4).[52] Because the posterior corneal surface adds negative power along the vertical meridian, plus power is created in the horizontal meridian (i.e. ATR refractive astigmatism). The same authors showed that the average magnitude of posterior corneal astigmatism is 0.5 D in corneas with anterior WTR astigmatism and 0.3 D in corneas with anterior ATR astigmatism.[52]Also, that there is a positive correlation between the magnitudes of anterior and posterior corneal astigmatism when the anterior corneal astigmatism is WTR but not when it is ATR (Figure 5).[52]

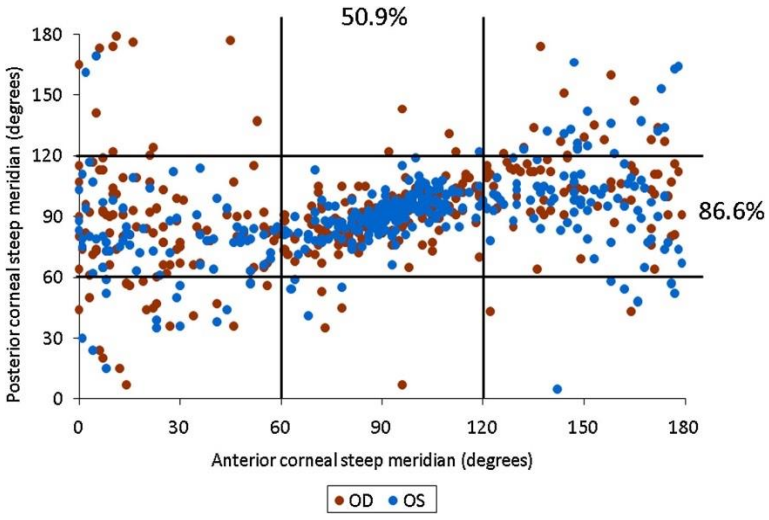

Figure 4 - Location of steep meridian on anterior and posterior corneal surfaces.

Reprinted with License from Elsevier and Copyright Clearance Center.

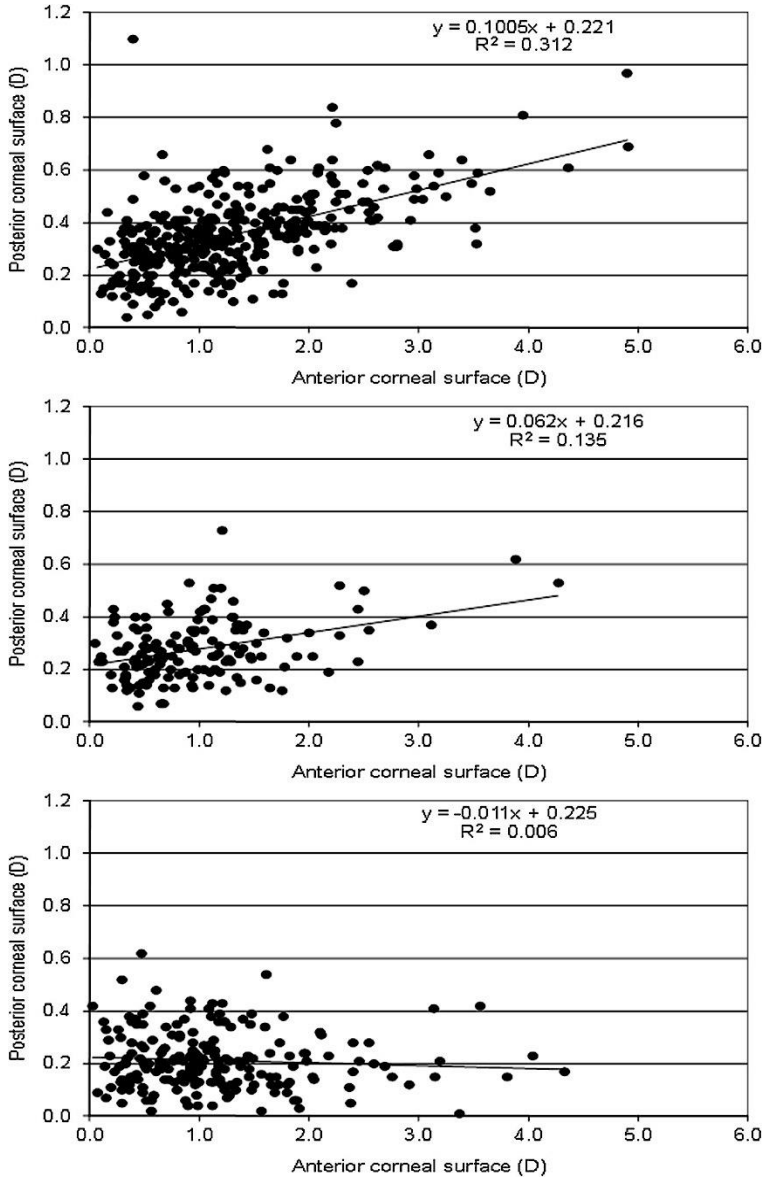

Figure 5 - Magnitude of astigmatism on the anterior corneal surface and posterior corneal surface grouped according to the orientation of the steep meridian on the anterior cornea.

Top: Vertical (r = 0.56, P<.001). *Middle*: Oblique (r= 0.37, P<.001). *Bottom*: horizontal (r= −0.08, P = .26).

Reprinted with License from Elsevier and Copyright Clearance Center.

Tonn et al. found that, in patients with WTR anterior astigmatism, posterior astigmatism is vertical in 97% of cases, with the corneal power being overestimated by 0.11 D. When anterior astigmatism is ATR, 18% of eyes have horizontal posterior astigmatism, and total corneal power is underestimated by 0.26 D.[53] A recent study by LaHood et al., using

the IOLMaster 700 (Carl Zeiss Meditec, Jena, Germany), a biometer based on swept-source optical coherence tomography (OCT) technology, that allows measurement of total corneal astigmatism, found a value of 0.24 D for the average magnitude of posterior corneal astigmatism and a lower value than previous studies for the proportion of eyes with vertical orientation of the posterior steep meridian (73%).[54]

Zheng et al. showed that the difference between keratometric and total corneal astigmatism is influenced by age, by the difference in the anterior to posterior astigmatism axis, by the magnitude of keratometric and posterior astigmatism and by the axial length.[55] In abnormal corneas, such as cases of corneal ectasia, posterior corneal astigmatism is highly variable, with a mean magnitude around 1 D.[56, 57]

Changes in astigmatism with aging are documented in numerous studies, although older studies were limited by the use of anterior corneal measurements only and by not directly studying the posterior corneal surface.[58,59,60,61]

More recent studies showed that total astigmatism varies from a mean of 0.62 D WTR in adolescence to 0.37 D ATR in older individuals.[62] The changing is mostly caused by the steep anterior corneal meridian rotating from horizontal to vertical with aging, while the steep posterior corneal meridian undergoes little change.[63] This means that the compensating effect of the posterior corneal surface on anterior corneal astigmatism decreases with advancing age.

Ho et al. showed that, for both anterior and total corneal astigmatism, the prevalence of WTR astigmatism decreases with age, while that of ATR and oblique astigmatism increases (Figure 6).[63] The mean changes towards ATR and oblique astigmatism are -0.18 D and -0.16 D for each 5 years of increase in age, respectively, whereas the mean increase in total corneal astigmatism is 0.16 D for each 5 years of aging.[63]

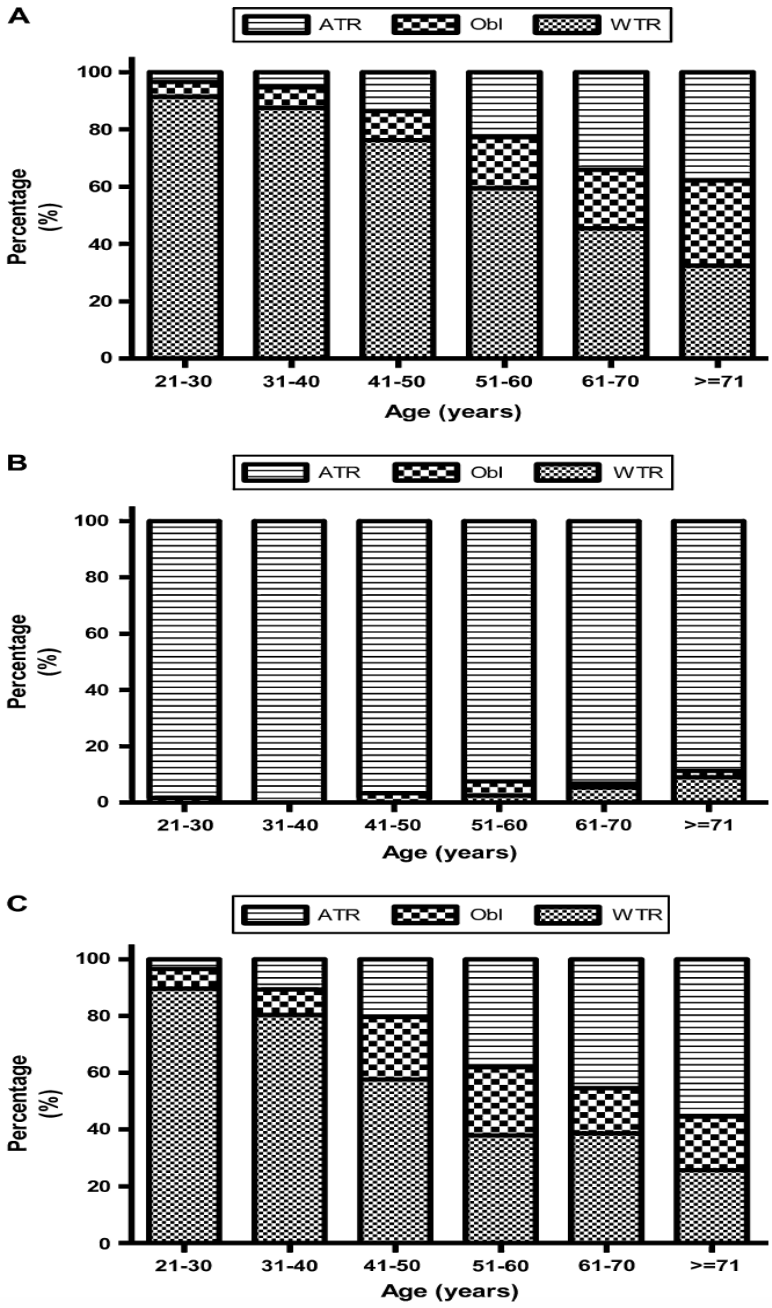

Figure 6 – Distributions of different kinds of astigmatism by age group. A, The anterior cornea. The proportions of WTR, OB, and ATR astigmatisms are 91.4%,

5.2%, and 3.4% in the 21–30 age group and 31.8%, 29.5%, and 38.6% in the ≧ 71 age group. B, The posterior cornea. The proportions of WTR, OB, and ATR astigmatisms are 0%, 1.7%, and 98.3% in the 21–30 age group and 9.1%, 2.3%, and 88.6% in the ≧71 age group. C, The total cornea. The proportions of WTR, OB, and ATR astigmatisms are 89.7%, 6.9%, and 3.4% in the 21–30 age group and 25.0%, 18.2%, and 56.8% in

the ≧71 age group (ATR: against-the-rule; OB: oblique; WTR: with-the-rule).

Reprinted with License from Wolters Kluwer Health, Inc. and Copyright Clearance Center

The findings by Ho et al. were recently confirmed by Naeser et al. (0.25 D of change in keratometric and total corneal astigmatism for each 10 years of aging).[64] Changes in posterior corneal astigmatism with age are almost negligible (0.044 D WTR for each 10 years of aging reported by Ho et al. and 0.03 D by Naeser et al.).[63,64] Hayashi et al. showed that eyes previously submitted to cataract surgery display similar changes to those described in non-operated eyes (towards ATR keratometric astigmatism) up to twenty years after surgery.[65,66]

2.4 Methods for correcting astigmatism

Non-surgical methods for correcting astigmatism include spectacles or contact lenses.

However, as technology evolved, interest in surgical techniques for correcting astigmatism during or after cataract surgery has grown. These techniques include manual or femtosecond laser-assisted corneal incisional surgery, excimer laser refractive surgery, and toric IOL implantation (Figure 7).

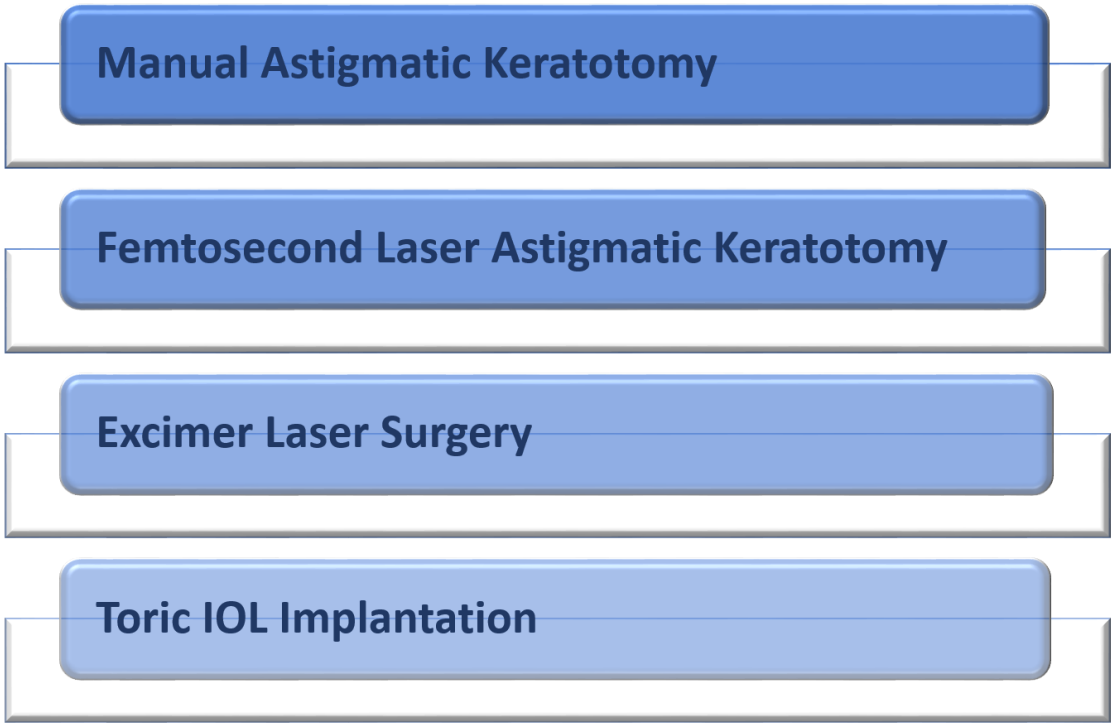

Figure 7 – Diagram illustrating the surgical techniques for the correction of astigmatism.

2.4.1 Astigmatic keratotomy

The history of surgery for correcting astigmatism dates back to the late 1800s. Several authors described numerous techniques of corneal incisional surgery, including limbal relaxing incisions (LRIs), CCIs (paired opposite incisions or an incision performed at the steep corneal meridian), anterior transverse incisions, and other non-penetrating corneal incisional techniques.[67] Modern corneal incisional surgery was introduced in the 1980s. In recent years, among corneal incisional techniques, one of the most widely spread is the execution of LRIs at the time of cataract surgery, according to different nomograms. As LRIs less central than other keratotomies, they have less of an effect, but advantages include a lower risk of inducing irregular astigmatism, ease of execution, a consistent 1:1 coupling ratio, and fewer complications.[68] However, the outcome of these interventions is, still today, variable and with questionable stability predictability.[69,70]

As with any other any other incisional keratotomy, older age amplifies the effect of LRIs. LRIs with longer arc lengths result in greater effect. Peripheral corneal thickness and corneal diameter and eccentricity also play a role on the final effect, and the lower the magnitude of the targeted astigmatic reduction, the more the results are inconsistent and unpredictable.[71]

An alternative incisional technique is performing paired opposite clear corneal incisions (OCCIs). A study evaluating the correcting effect of OCCIs performed on the steep axis during cataract surgery, found this technique to be useful for the correction of astigmatism, with the advantages of requiring no extra surgical skills or instrumentation.[72] A prospective randomized study reported on the correction of corneal astigmatism with OCCIs versus toric IOL implantation. Greater efficacy was found for toric IOLs over OCCIs.[73]

Femtosecond laser is a technology increasingly adopted by surgeons performing cataract and/or refractive surgery. It contributes to improve both safety and clinical outcomes. For corneal surgery, most surgeons use the femtosecond laser for the creation of LASIK flaps. Other potential applications include creating tunnels for implanting intrastromal corneal ring segments in cases of corneal ectasia, performing

different keratoplasty techniques, transepithelial or intrastromal astigmatic keratotomy or pockets for presbyopia-correcting intrastromal implants.[74] For cataract surgery, studies show that the femtosecond laser (femtosecond laser-assisted cataract surgery – FLACS) results in increased precision and reproducibility for the creation of corneal incisions, capsulotomy, and in a reduction of the ultrasound energy required for nucleus removal. The complication rate is low, and similar to that of manual cataract surgery.[75] The femtosecond laser is able to perform penetrating or intrastromal astigmatic keratotomy. In the latter, the absence of an open wound avoids infection, wound gape, or epithelial ingrowth.[76] A recent review revealed both techniques of astigmatic correction during FLACS are safe and effective, but recommended reserving these techniques to treat low amounts of astigmatism (<1.50 D) until better nomograms are available.[77]

2.4.2 Excimer laser refractive surgery

Excimer laser refractive surgery, including laser in-situ keratomileusis (LASIK) or photorefractive keratectomy (PRK), among other common techniques, is another option to treat residual refractive errors, including astigmatism, after cataract surgery. They are predictable and stable long-term procedures in most patients.[78] Zaldivar et al. suggested the creation of a transient corneal flap during cataract surgery. After postoperative stabilization of refraction, this flap could be used for residual spherical and/or cylindrical corrections.[79] An alternative option is the creation of the flap after the cataract surgery, at the time of the excimer laser surgery. Compared with LASIK, PRK may be a superior option for cataract patients, considering these are usually old patients, with a high prevalence of dry eye and ocular surface diseases.[80,81] Even though safe and predictable, excimer laser refractive surgery may be accompanied by postoperative pain or discomfort, potential flap complications (LASIK), and photic phenomena, such as glare or haloes. These eventual complications, in addition to requiring a separate surgical procedure, add significant expense or may need further surgery.[82]

2.4.3 Toric intraocular lenses

A toric IOL is designed to minimize image distortion by focusing the light that would otherwise be scattered by corneal astigmatism. Toric lenses are available with a wide

range of spherical and cylindrical powers to simultaneously correct aphakia and pre-existing corneal astigmatism. They avoid the variability associated with manual incisional techniques, do not require additional operative skills (besides those detailed in Topic 2.10), and offer highly predictable outcomes.**Erro! Marcador não definido.**

Furthermore, multifocal toric IOLs offer patients with corneal astigmatism the possibility of achieving spectacle independence not only for distance but also for near and intermediate vision.

The first toric IOL was introduced by Shimizu et al. in 1992.[83] It was a non-foldable three-piece toric IOL made from poly-methyl methacrylate (PMMA). About 20% of the IOLs rotated 30 degrees or more and almost 50% 10 degrees or more.[83] Since then, many advancements occurred not only in IOLs material and design and but also in the surgical technique. These advances led to improved rotational stability and excellent visual outcomes.

2.4.3.1 Toric intraocular lenses designs

The IOL biomaterial is of great importance on the postoperative rotation of the IOL. Hydrophobic acrylic IOLs material show the highest adhesive properties to the capsular bag, followed by hydrophilic acrylic IOLs, PMMA IOLs and finally silicone IOLs.[84,85] Currently available toric IOLs however have a total diameter ranging from 11 mm to 13 mm, which is effective in avoiding IOL rotation.[86,87,88]. Regarding haptic design, both plate haptic IOLs, and loop haptic IOLs are available. Even though Patel el al. showed plate haptic IOLs had better rotational stability than loop haptic IOLs[89], this finding was later contradicted in studies where the IOLs with different loop designs were both made of acrylic material.[90]

In the optic of a toric IOL, the toric surface may be located on the anterior surface of the lens, as is the case of the Tecnis Toric IOLs (Johnson & Johnson Vision), that have a proprietary wavefront-designed toric aspheric optic[91] or on the posterior surface (eg. Acrysof Toric IOLs; Alcon Laboratories Inc.).[92] A different toric IOL design is a bitoric lens (e.g. AT Torbi 709M IOLs, Carl Zeiss Meditec AG), with equiconvex toric anterior and posterior optics. This characteristic allows the production of IOLs with high cylindrical

powers.[93] A unique design is the incorporation of a transitional conic surface (Precizon Toric IOLs, Ophtec BV) on the lens. This surface has a consistent power from the center to the periphery and a broader toric meridian; a characteristic that allows the IOL to be more tolerant to tilt and/or misalignment.[94]

It is known that the presence of spherical aberration after non-aspheric IOL implantation results in worse optical outcomes.[95,96] The majority of toric IOLs available nowadays have an aspheric optic, either with a negative spherical aberration (with the objective of compensating the positive corneal spherical aberration) or with zero spherical aberration,[92] While negative spherical aberration IOLs have the advantage of improving contrast sensitivity, they are also more sensitive to the effects of tilt or decentration. In this case, decentration induces coma, a horizontal or vertical decentration over 0.6 mm may degrade visual quality. [97,98] On the other hand, aspheric IOLs with zero spherical aberration have the advantage of being more tolerant to tilt or decentration, in which case they do not induce other aberrations.[99]

2.4.3.2 Clinical outcomes of toric intraocular lenses

Studies show that toric IOLs are the most effective and predictable of astigmatic during cataract surgery.[73,100] A recent meta-analysis including thirteen randomized trials, with a total of 707 eyes randomized to toric IOL implantation and 706 eyes randomized to non-toric IOL implantation (in 225 eyes, the non-toric IOL was combined with a relaxing incision) found high-quality evidence that toric IOL implantation results in a better uncorrected visual acuity, a higher rate of spectacle independence and in less residual astigmatism than non-toric IOL implantation, even when the latter is combined with relaxing incisions.[100]

The combination of a toric IOL implantation LRIs was studied in twenty-two eyes with cataract and more than 2.50 D of corneal astigmatism. Results showed that the combined approach was effective in patients with high astigmatism. Although predicted residual astigmatism after implantation of the toric IOL was 1.42 ± 0.76 D, pre- and postoperative subjective cylindrical error and keratometric cylinder improved, respectively, from 3.90 D to 0.94 D and from 3.46 to 1.80 D.[101]

Despite their efficacy and predictability, implantation of a toric IOL is a complex process in which multiple steps must be optimized to avoid errors. However, these steps are not perfect nowadays. The diagram in Figure 8 illustrates the steps involved in the planning and implantation of a toric IOL.

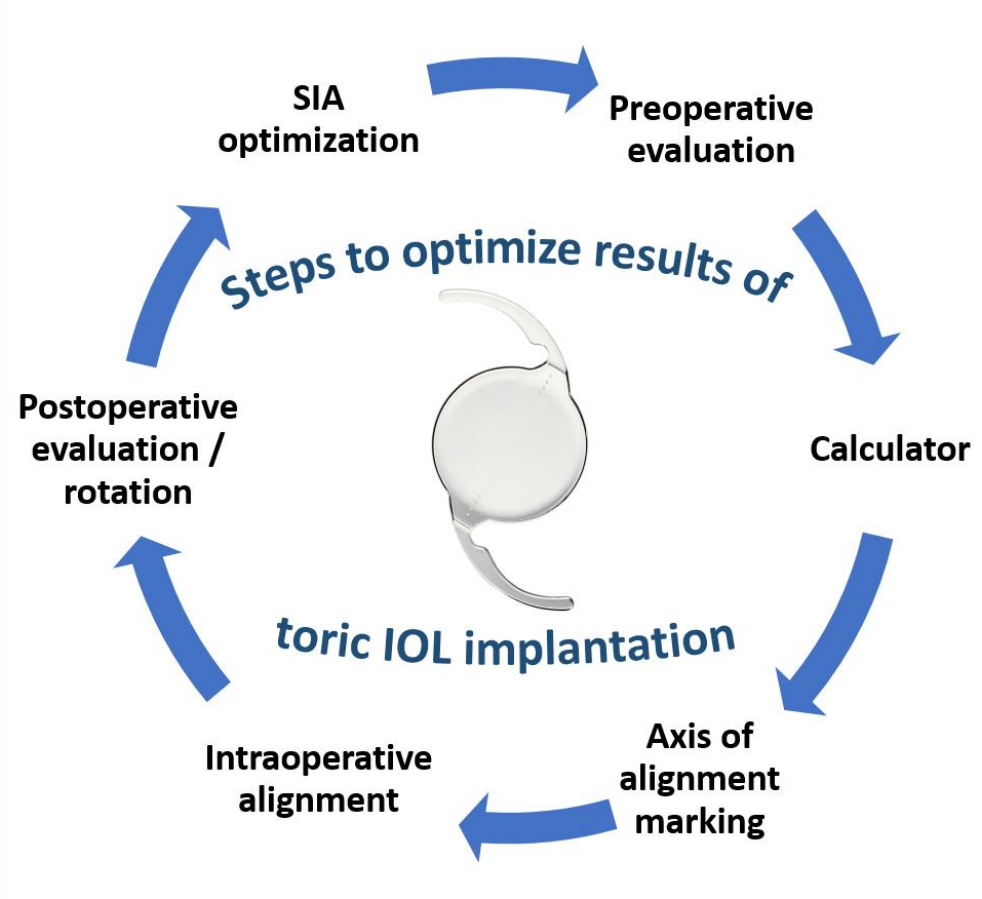

Figure 8 – Steps involved in the pre-, intra- and postoperative study for implanting a toric IOL.

Below, after describing how to analyze astigmatic data, we will further detail each of these steps (Topic 2.6 – 2.11).

2.5 Analysis of astigmatic data

Introduction to vector analysis

Although the vector analysis concept is seldom used in clinical practice, difficulties arise when astigmatism is represented in the traditional polar form (magnitude and axis) rather than the Cartesian form, which permits mathematical analysis. Statistical analysis of angular data, such as astigmatism axes, is distinct from the analysis of nondirectional

data. Applying conventional statistical methods to directional data is theoretically wrong, and its results may be misleading. However, when representing astigmatism in rectangular vector form, scalar methods can be applied to each vector component and standard multivariate statistics can be correctly used to calculate the sample mean and standard deviation, confidence intervals, and test hypotheses.[102]

The basis for vectorial analysis is the theory of obliquely crossed cylinders, originally described by Stokes.[103] Naylor suggested that the formula could be used to determine the difference in refraction caused by a surgical procedure.[104] The principle assumes that a theoretical spherocylinder, the surgically induced astigmatism (SIA or C_{SURG} x β°) is "crossed" with the preoperative refraction to produce the postoperative refraction (Figure 9).

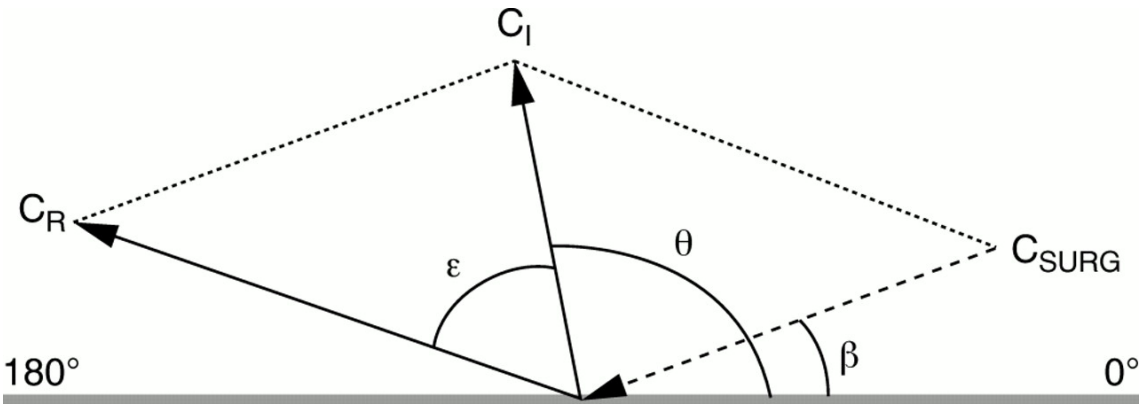

Figure 9 - Diagram demonstrating the principle of vector analysis of the change in the astigmatic refraction following surgery. The arrow direction represents the axis of astigmatism and the length the magnitude. The principle assumes that a theoretical spherocylinder, the surgical induced astigmatism (SIA or C_{SURG} × β°) is "crossed" with the preoperative refraction to produce the postoperative refraction: $S_I/C_I \times \theta° + S_{SURG}/C_{SURG} \times \beta° = S_R/C_R \times (\theta + \varepsilon)°$, $C_{SURG} = (C_I^2 + C_R^2 - 2\, C_I\, C_R \cos 2\varepsilon)$, $S_{CYL} = (C_I + C_{SURG} - C_R)/2$, $\sin 2\beta = (C_R/C_{SURG}) \sin 2\varepsilon$, $S_{SURG} = S_R - S_I - S_{CYL}$; C_I is the initial or preoperative astigmatism vector at θ° axis (in "plus" cylinder notation), C_R is the resultant or postoperative astigmatism vector at θ + ε° axis ("plus" cylinder notation), C_{SURG} is the surgically induced astigmatism vector (SIA, a theoretical construct) at β° axis (in "minus" cylinder notation), S_{CYL} is the spherical equivalent of all the cylindrical components.

Reprinted with License from BMJ Publishing Group Ltd. *and Copyright Clearance Center*

The above relation known as “law of cosines” was further promoted by Jaffe and Clayman[105] and has resulted in numerous subsequent publications on methods for SIA calculation. The main problem encountered is that the standard axis notation for cylinders (Axint, adopted at the 1950 International Federation of Ophthalmic Societies) ranges from 0 to 180°. The formula (Figure 9; $C_{SURG}^2 = (C_1^2 + C_R^2 - 2C_1C_2\cos 2\varepsilon)$) overcomes this limitation by doubling the angle of astigmatism into the 0 to 360° range required for vector addition and subtraction (polar coordinates). The mapping makes further sense in that cylinders at the same axis add and cylinders at cross axes (90° apart) cancel each other.

While vector analysis is the correct mathematical method for describing the relation between the pre- and postoperative cylinder, the surgical vector alone does not provide the surgeon with practical information about surgical precision and future refinements. To be meaningful, vectorial analysis of surgical results requires further translation. Given this, different investigators developed methods for characterizing the astigmatic change with ocular surgery.

The most widely used methods of vector analysis for astigmatic data will be described below.

2.5.1 Thibos et al. method

Thibos et al. developed a method of vector analysis with the objective of reducing the astigmatic component of refractive errors. The authors propose power vectors to help the visualization of complex changes in refractive errors by tracing a trajectory in a uniform dioptric space. The Cartesian components of a power vector are mutually independent.[106] This simplifies the mathematical and statistical analysis of refractive errors. In a broader sense, the HOAs of the eye can be similarly transformed into orthogonal components that are mutually independent. Thus, power vectors also provide a natural link to a comprehensive description of wavefront aberration functions and Zernike polynomials. This link will become increasingly important as refractive surgery aims to correct not only refractive error but also HOAs.

Thibos et al. method decomposes refractive data into three power vectors: the spherical equivalent and two Jackson crossed cylinders (JCC), separated by 45 degrees. Thibos et al. method was essentially developed to characterize refractive errors. The proposed method represents refractive astigmatism, including any spherical component, if present, in rectangular vector form as follows[107]:

- A spherical lens of power *M*, equal to the spherical equivalent of the refractive error (M = Sphere + Cylinder / 2);
- If the spherical power is removed from the prescription, the result is a JCC equivalent to a conventional cylinder of positive power *J* at axis α + 90° crossed with a cylinder of negative power –*J* at axis α. The astigmatic component is described as a JCC of power *J* at axis α (by convention, the meridian of maximum positive power);
- The vector component along the 0-180° axis (J_0) is calculated by: $J_0 = -\frac{C}{2} \times \cos 2\alpha$

The vector component along the 45° axis (J_{45}) is calculated by: $J_{45} = -\frac{C}{2} \times \sin 2\alpha$

- Any spherocylindrical refractive erro can be expressed by the three dioptric powers: *(M, J_0, J_{45});*
- The overall blur vector (B) is the vector drawn from the coordinate origin to the point *(M, J_0, J_{45})* and is calculated by $B = \sqrt{M^2 + {J_0}^2 + {J_{45}}^2}$

An additional index, the astigmatic power vector (APV), was described and is calculated by: APV = ${J_0}^2 + {J_{45}}^2$. The APV is an unsigned scalar metric, representing the magnitude but not the axis/meridian of astigmatism.

It is convenient to interpret (*M, J_0, J_{45})* geometrically as coordinates (*x, y, z,* respectively) of a point in a three-dimensional dioptric space. B is the vector drawn from the

coordinate origin to the point (M, J_0, J_{45}) and APV is the point (J_0, J_{45}) at the astigmatic plane. Figure 10 shows the graphic representation of these vectors.

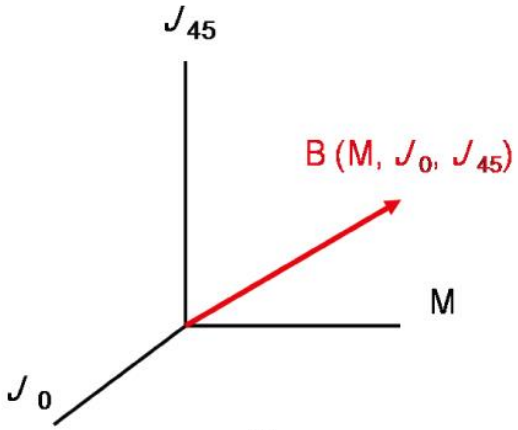

$$M = S + C/2$$
$$J_0 = (-C/2)\cos(2\alpha)$$
$$J_{45} = (-C/2)\sin(2\alpha)$$
$$B = \sqrt{M^2 + J^2{}_0 + J^2{}_{45}}$$

(B)

Figure 10 - (A) The three Cartesian coordinates (x, y, z) of each power vector correspond to the powers of three lenses: a spherical lens of power M, a JCC of power J_0 with axes at 90° and 180°, and a JCC of power J_{45} with axes at 45° and 135°. The Pythagorean length of the power vector, B, is a measure of overall blurring strength of a spherocylindrical lens or refractive error. (B) Power vector analysis (S = spherical diopters, C = cylindrical diopters, α = axis (°), Power vector = (M, J_0, J_{45})).

The concept of vector orthogonality simplifies practical problems involving the combination, comparison, and statistical analysis of spherocylindrical lenses or corneal astigmatic errors. In other words, the method of Thibos et al. is convenient for a descriptive analysis of astigmatism.[108]

The authors also enumerate the advantages of their method of representation of a spherocylindrical lens for the purposes of analyzing ophthalmic data involving lens combinations, comparing different lenses or studying the statistical distribution of refractive errors.[109]

2.5.2 Holladay et al. method

In 1992, Holladay et al presented a method specifically designed to calculate the surgically induced refractive change (SIRC) in sphere and cylinder after corneal refractive surgery for an individual patient.[110] This approach was posteriorly extended to also include analysis of aggregate data.[111] By 2001, a new publication further clarified some aspects of their method and the authors' tested it in a dataset of one hundred eyes previously submitted to corneal refractive surgery.[112] Holladay et al. method is suitable for analyzing the SIRC by any type of corneal surgery and consists of ten steps, each of them with specific equations. In addition to the calculation of SIRC via pre- and postoperative refraction (sphere and/or cylinder) or keratometry, Holladay et al. method is appropriate for other applications, such as the calculation of the prediction error (as the difference between the targeted and the final refraction), the addition of an overrefraction to a spectacle correction, the determination of the power of the meridians oblique to the principal meridians of a spherocylinder, and the calculation of the coupling ratio or average axes.

When reporting results of astigmatism correction, the authors suggest using doubled-angle polar plots.[112] The differences between single- and doubled-angle polar plots for reporting astigmatic data are illustrated in Figure 11.

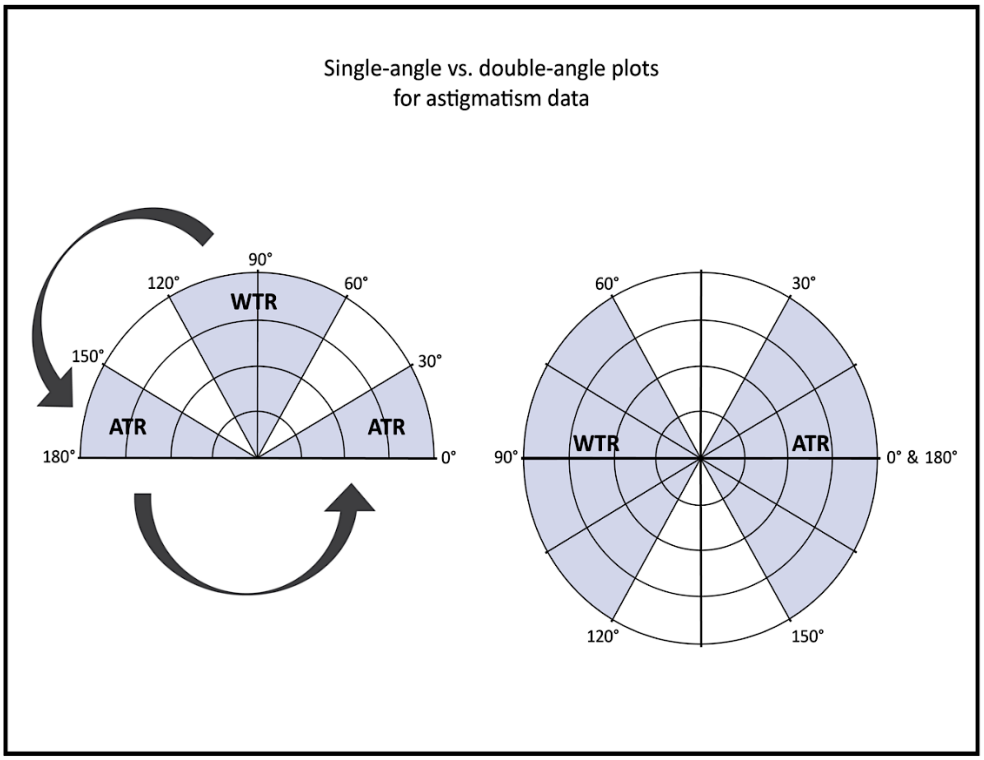

Figure 11 – differences between single- and doubled-angle plots for reporting astigmatism data.

On a single-angle plot, horizontal (0°; ATR) astigmatism is represented in the areas near the x-axis (blue shaded areas on the plot), vertical (90°; WTR) astigmatism is represented in the areas near the y-axis (blue shaded areas), and oblique astigmatism (45°; 135°) is represented between the blue shaded areas (non-shaded areas). The mean of a dataset of x and y values is usually represented in the plot by a dot, which is called the "centroid".

On a doubled-angle plot, the y-axis corresponds to the axis of oblique astigmatism, and the x-axis corresponds to the axis of vertical and horizontal astigmatism. The standard deviation (SD) is pictured by an ellipse. If a population with a higher percentage of WTR or ATR astigmatism is represented, the ellipse is oriented horizontally, if a population with mostly oblique astigmatism is represented, the ellipse is oriented vertically and if the of oblique and non-oblique astigmatism is uniform, the SD is represented by a circle. The centroid is represented as in single-angle plots.

While single-angle plots may be easier to understand for any ophthalmologist, as they are closer to clinical practice, double-angle plots have two advantages. The first is that the ellipse representing the SD can be displayed. On single-angle plots, data for the x and y SD values needs to be included in a box, outside area of the graphic. The other advantage of double-angle plots is that data points at 0° and 180° are visually grouped together, whereas they are on opposite sides on a single-angle polar plot. However, to simplify visualization shaded areas may be added, as displayed in Figure 11.

The method of vector analysis for aggregate data by Holladay et al was used for calculating the prediction error in residual astigmatism of the available toric IOL calculators in the publications by Ferreira and colleagues detailed in Chapter 6.

2.5.3 Alpins Method

An alternative vector analysis method was published by Alpins.[113,114] Alpins method uses different indices to fully describe astigmatic outcomes of surgery for astigmatism.

Alpins method is based on three main vectors: one represents the intended effect of the astigmatism surgery (i.e., the magnitude and axis of astigmatism targeted for treatment), and is referred to as target induced astigmatism vector (TIA); other represents the actual effect achieved by the surgery – surgically induced astigmatism vector (SIA), and the third is called the difference vector (DV). It provides a measure of the magnitude and axis of error and its ideal value is zero. The principles of calculation of these three vectors are detailed in Figures 12 and 13.

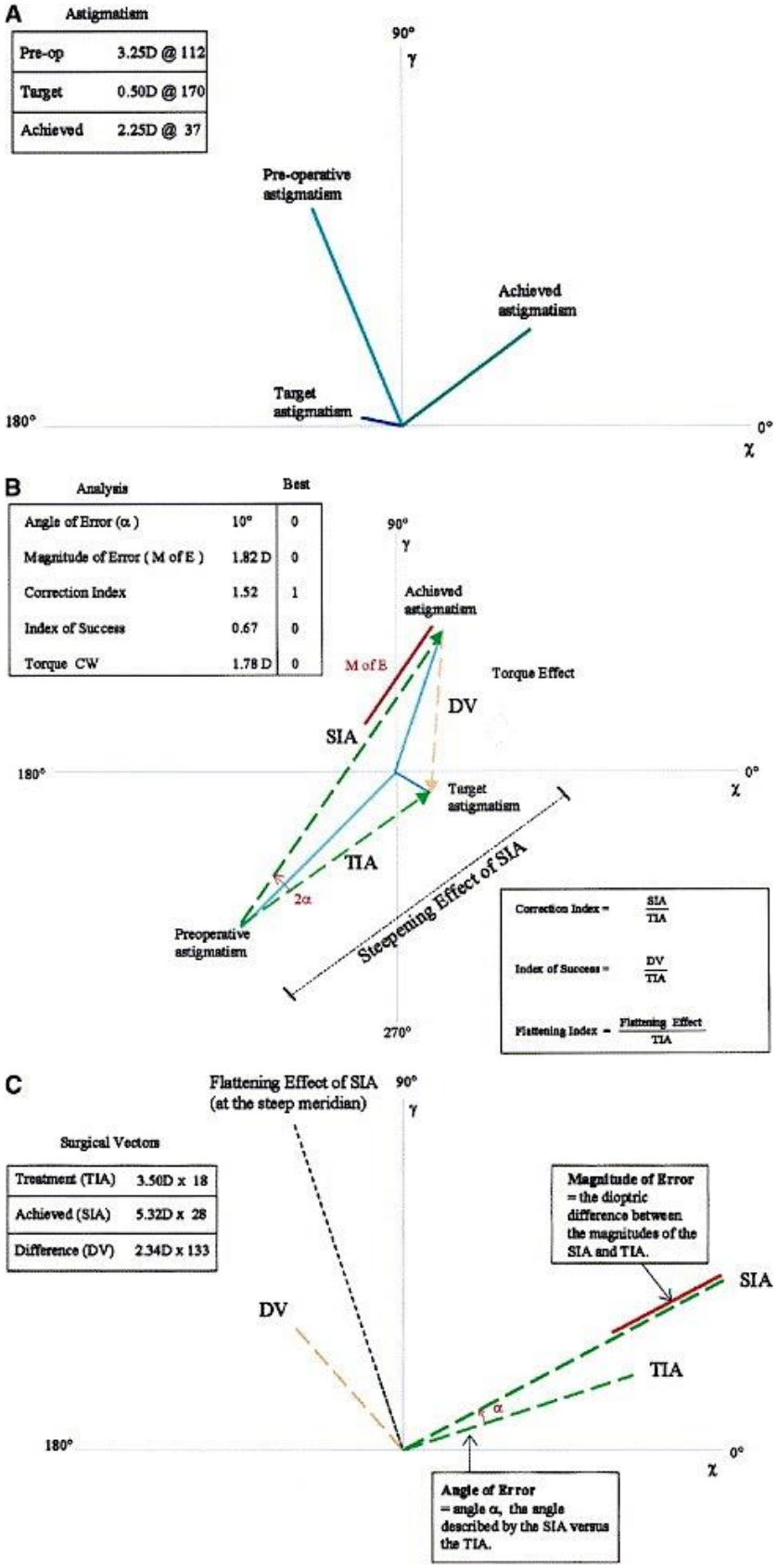

Figure 12 - A: Polar astigmatism diagram: displaying pre-operative, post-operative, and target astigmatism magnitudes at their actual orientation (steep corneal meridian or

power axis of negative cylinder). B: Double-angle vector diagram (DAVD): astigmatism axis values have been doubled, but the magnitudes are unchanged. The dashed lines are vectors, with arrowheads indicating their orientation, when connecting the continuous lines displaying the astigmatisms in this double angled mathematical construct. C: Polar surgical vector diagram: The vectors (dashed lines) are now displayed at their actual orientation by transposing them to the origin and then halving their axes derived on the DAVD.

Reprinted with License from Elsevier and Copyright Clearance Center.

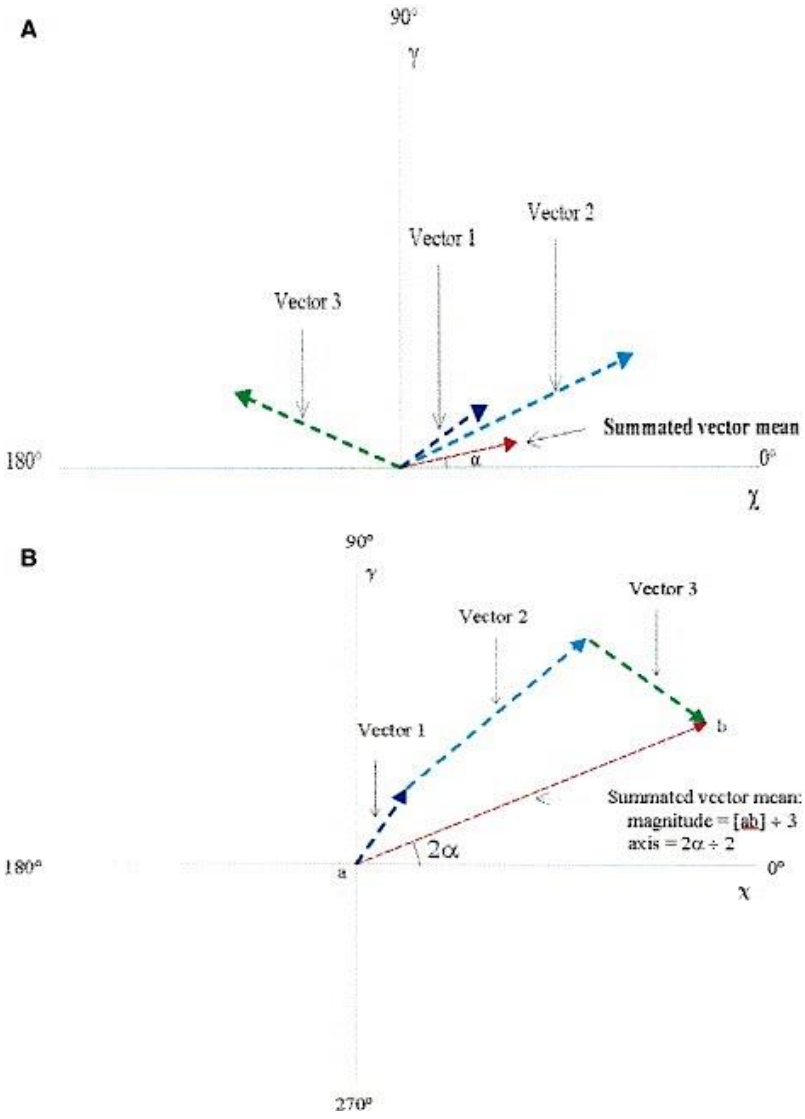

Figure 13 - A: Polar analysis of vectors. Multiple vectors are present on a polar diagram at their actual orientation, as they would appear on an eye. The summated vector mean resultant, determined in Fig. 9B, is shown in red at its orientation. B: The vectors

displayed on the polar diagram have their axes doubled to be displayed on a DAVD, and then are transposed in a head-to-tail summated fashion. The red dashed line connects the first tail at the graph origin to the last vector head. To determine the magnitude of the summated vector mean, the total length is divided by the number of component vectors and its axis is then halved to return to a polar diagram display as in Fig. 10A.

Reprinted with License from Elsevier and Copyright Clearance Center.

The relationships between these vectors provide parameters indicating if the treatment was on- or off-axis, over- or undercorrection occurred, and of the changes required if the same astigmatic correction were to be performed again. Besides the TIA, SIA and DV, and among other parameters described by Alpins, the most commonly used are:

Correction index (CI): calculated by determining the ratio of SIA to TIA. CI is preferably 1.0 (>1.0 represents over- and <1.0 represents undercorrection);

- Magnitude of error (ME): arithmetic difference between the SIA and TIA vectors (the ME is positive for over- and negative for undercorrection);
- Angle of error (AE): angle described between SIA and TIA vectors. The AE is positive if the achieved correction is on an axis counterclockwise to where it was intended, and negative if the achieved correction is clockwise to the intended axis;
- Index of Success (IS): calculated by dividing the DV by the TIA vector. The IS is a measure of surgical accuracy. The ideal value is zero;
- Coefficient of Adjustment (CA): The inverse of the CI, calculated by dividing the TIA by the SIA vector. The CI was developed to adjust future TIA magnitudes. The CI value is, ideally, 1.0.

Specifically for studying corneal incisional surgery,[115] in addition to the other vectors, Alpins suggested two indices: the flattening effect (FE), which is the parameter that effectively reduces astigmatism at the surgical meridian, and the torque, a component

of the SIA vector that does not contribute to reduce astigmatism but only causes a change in its orientation.

Although both Alpins and Thibos et al. methods allow the evaluation of corneal and refractive astigmatism, the method of Thibos et al. is adequate when an objective description of astigmatism, preferably refractive, is desired. However, to study required modifications in astigmatism, Alpins method provides more data.[108]

Alpins method of vector analysis was used by Ferreira et al. for comparing the morphologic features and the SIA resulting from femtosecond laser and manually-created clear corneal incisions (CCIs) for cataract surgery.[116]

2.5.4 Other methods of vectorial analysis

Additional vectorial calculation methods for analyzing astigmatic data have been published. One of these methods, making use of polar coordinates analysis instead of cartesian vectorial analysis, was proposed by Naeser and Hjortdal. In this approach the change in astigmatism is characterized by two polar values, separated by 45 degrees.[117] In subsequent publications, Naeser and Hjortdal extended this methodology to trivariate analysis, which is able to provide a three-dimensional representation displaying both the polar values and the spherical equivalent.[118]

2.6 Preoperative evaluation for toric intraocular lens implantation

2.6.1 Candidate assessment

As with any other intraocular procedure, a careful patient assessment must be conducted before cataract surgery. Special attention should be given to any relevant medical history that may compromise the success of the surgery due to an increased risk of intra- or postoperative complications or be an independent cause of decreased vision, such as diabetes, prostatic disease (tamsulosin and other alpha-adrenergic receptor antagonists for benign prostatic hyperplasia have been associated with intraoperative floppy iris syndrome and an increased rate of intraoperative complications. Moreover, poor pupillary dilatation is also a relative contraindication, as it may hamper the visualization of the alignment marks in the periphery of the toric IOL,[119,**Erro! Marcador não definido.**,**Erro! Marcador não definido.**,**Erro! Marcador não definido.** or psychiatric disorders, such as

dementia or Parkinson's disease, which may compromise cooperation during surgery or postoperative care.

A complete ophthalmologic examination must be performed, with evaluation of uncorrected and corrected distance and near visual acuity (UDVA, CDVA, UNVA, CNVA, respectively), manifest refraction, slit-lamp and fundus examination with special attention to conditions with prognostic relevance such as corneal endothelial dystrophies (patients with endothelial dystrophies may later require a keratoplasty, which may change their refraction) or the presence of a narrow anterior chamber, pseudoexfoliation or phakodonesis (zonular instability and posterior capsular dehiscence are contraindications for implanting toric IOLs, as a stable capsular bag-IOL complex is essential for guaranteeing the rotational stability of the IOL), elevated intraocular pressure and optic disc or retinal diseases.

If a multifocal toric IOL is being considered, it is especially important to rule out relative or absolute contraindications for these lenses, in particular amblyopia, corneal pathology, macular disease or glaucoma, since these can affect visual acuity and/or quality.[119,120]

Patients' profiles must also be considered and their expectations properly assessed and managed.[120]

In all toric IOL candidates, it is advisable to perform corneal topography or tomography before surgery. This is important, as we will discuss, not only for keratometry and IOL power calculation, but also to rule out relative contraindications for toric IOLs. These include irregular astigmatism, which may be secondary, for example, to keratoplasty, and ectasic disorders such as keratoconus or pellucid marginal degeneration. Although regular astigmatism is most suitable for toric IOL implantation[121], good outcomes may be achieved with toric IOLs implanted in eyes with irregular astigmatism.[122] However, the expected results should be carefully discussed with the patient and corneal disease progression should be ruled-out.

In recent years, increased importance has been given to a careful evaluation of the ocular surface before cataract surgery, particularly when implanting premium IOLs. It is

recognized that the integrity of the ocular surface has a strong correlation with visual quality. For its evaluation, several tests may be used. On the slit lamp, the tear meniscus height may be measured. A height inferior to 0.2 mm is indicative of dry eye and a foamy tear film of Meibomian gland disease (MGD). Also, tear film break-up time should be measured after fluorescein instillation, with a time of less than ten seconds being considered abnormal. [123,124,124] For many years, Schirmer's test was the gold standard for dry eye evaluation. Schirmer I test is performed without topical anesthetic and measures both basic and reflex tearing combined (less than 5 mm of wetting of the thin paper strip used after five minutes is diagnostic of dry eye). Schirmer II is performed after the instillation of topical anesthetic and evaluates reflex secretion (less that 15 mm after two minutes is considered abnormal).[125] Other more complex tests, including the evaluation of tear film osmolarity, lysozyme or lactoferrin levels, the use of imaging technologies or impression cytology are less used in clinical practice.

As with any other surgical procedure, patients should be warned about the general risks and complications of cataract surgery and of the possibility, albeit careful biometry and IOL calculation, of postoperative refractive surprises and, in the particular case of a toric IOL, lens misalignment. If significant and associated with decreased visual acuity (if the lens is 30 degrees off the intended axis, it will have no effect on astigmatism correction), may justify a secondary procedure to realign the IOL.

Finally, as in any other medical procedure, informed consent must be obtained from the patient or guardian.

2.6.2 Biometry and intraocular lens power calculation

The main factor for achieving a good refractive outcome in cataract surgery is precise IOL power calculation.

Although there are several techniques to measure axial length (AL), optically based systems, such as partial coherence interferometry (PCI) or optical low-coherence refractometry (OLCR) have gained increased popularity in recent years. These systems are more accurate than applanation ultrasound biometry, especially because they are easy to perform and avoid possible artifacts such as overestimation of IOL power due to

the measurement of an artificially shorter AL secondary to unintended corneal compression.[126,127] Immersion ultrasound (IUS) may also yield precise results, but is a time-consuming technique and requires an experienced operator.[128,129] Optical biometry is less dependent on the operator[130,131], while also avoiding potential infection, since it is a non-contact technique. In addition, most optical biometers evaluate additional parameters, including corneal curvature, anterior chamber depth (ACD), lens thickness (LT) and corneal diameter (CD). Software systems allow the calculation of IOL power using different formulae, which the surgeon can choose according to the patients' individual characteristics.

In patients with dense cataracts, corneal edema or vitreous hemorrhage, optical biometry may not be possible,[128,132] If feasible, IUS should be carried out since, as previously mentioned, it results in less AL shortening when compared to applanation ultrasound.

When considering the correction of astigmatism during cataract surgery, the targeted astigmatic correction must be determined. The surgeon must consider the refraction of the fellow eye and the desire of the patient to be spectacle independent. With the presence of high astigmatism in the fellow eye, and if second eye surgery is not planned, it might not be advisable to eliminate all astigmatism in the surgical eye.

Several publications support the finding that, after monofocal IOL implantation, distance and near visual acuity is typically better in patients with residual ATR than in those with WTR or oblique astigmatism.[133,134] Also myopic astigmatism causes more deterioration in distance visual acuity than hyperopic astigmatism, regardless of the axis.[135]

When implanting a multifocal IOL correction of astigmatism over 0.75-1.00 D is mandatory, as any residual astigmatism over these values deteriorates visual acuity.[13,136] Furthermore, residual astigmatism is one of the main causes of dissatisfaction after multifocal IOL implantation.[137] Finally, if avoiding flipping of the axis is considered relevant (even though the discomfort this may cause in a spectacle prescription by altering meridional magnification and spatial distortion do not apply to toric IOL implantation), it is advisable to err on the side of under-rather than overcorrecting pre-existing astigmatism.

2.6.3 Evaluation of corneal astigmatism

Several intrinsic factors affect the accuracy of corneal astigmatism measurements. As previously stated, tear film and ocular surface status can alter the accuracy of corneal astigmatism evaluation. A stable tear film and absence of corneal epitheliopathy are essential to obtain accurate measurements.[138,139,140] Moreover, patients wearing contact lenses should cease their use for a given period before astigmatism evaluation.

A multiplicity of instruments was developed for evaluating corneal astigmatism, including manual and automated keratometers, Placido-based corneal topographers, scanning-slit based tomographers, systems based on the Scheimpflug principle, and anterior-segment optical coherence tomography (AS-OCT) devices.

2.6.3.1 Reflection-based technology

A keratometer, also known as ophthalmometer, is a diagnostic instrument for measuring the curvature of the anterior surface of the cornea, in particular for assessing the magnitude and axis of astigmatism.

In 1779, Ramsden and Home attempted to measure the corneal curvature with a telescope that examined an image reflected on the cornea. However, inaccuracies caused by the eye and head movements were a limitation with this and subsequent designs. These were address by optically doubling the image with prisms.[141]

In 1853, the German physiologist Hermann von Helmholtz developed a keratometer that doubled the images with two glass plates instead of prisms. Since the images move together, head or eye movements have the same effect on both, not affecting the measurements. [141]

As a general principle, a keratometer uses the relationship between object size (O), image size (I), the distance between the reflective surface and the object (d), and the radius of the reflective surface (R). If three of these variables are known (or fixed), the fourth can be calculated by using the formula:

$$R = 2d\frac{I}{O}$$

There are two distinct variants of determining R: Javal-Schiotz type keratometers have a fixed image size and are typically 'two position', whereas Bausch and Lomb type keratometers have a fixed object size and are usually 'one position'. The most common, the Javal-Schiotz keratometer uses two self-illuminated mires (O), a red square and a green staircase, maintained at a fixed distance from the eye. It uses the Scheiner principle, in which the converging reflected rays coming towards the eyepiece are viewed through (at least) two separate symmetrical apertures.

Keratometers have several limitations. They measure only a small central area of the cornea (approximately 3-4 mm, with variations in corneas of different powers), not providing peripheral information and presuming the cornea is symmetrical, with the two main meridians separated by 90°. Moreover, they only evaluate the anterior corneal surface, assuming a fixed ratio between the curvature of both corneal surfaces. In most cases, a standard keratometric index of 1.3375 is used for converting anterior surface measurements in total corneal power and astigmatism.

According to Gaussian optics, the equation:[142]

$$P = \frac{(n_1 - n_2)}{r}$$

describes the refracting dioptric power (*P*) of a spherical surface of a transparent medium, given the index of refraction of the medium (n_1), the index of refraction of the optical medium adjacent to the surface (n_2), and the radius of curvature of the surface (*r*), in meters:

However, various keratometric indices are used by different manufacturers, such as 1.332 or 1.336, inducing variability. These last indices are considered by several authors to be more precise, as they are closer to the real lacrimal film and aqueous humor indices. In fact, a keratometric index of 1.3375 overestimates the total corneal power in about 0.56 D.[111]

The Lenstar LS900 is an OLCR biometry device. For evaluating astigmatism, it uses the reflection of thirty-two measuring points arranged in two concentric rings (outer 2.3 mm, inner 1.65 mm of diameter) of sixteen points each. Each displayed keratometry

measurement is a composite of the mean of four measurements, totaling 128 measuring points. Therefore, if the five scans recommended by the manufacturer are performed, keratometry is calculated on the basis of 640 measuring points. Once the data is captured, the spherical equivalent radius is calculated for each individual measuring point. The keratometric calculation considers the best-fit ellipsoid built by the reflected points to determine the radii of the circumscribed ellipsoid.[143]

Keratometry readings of the Lenstar are highly precise and repeatable, show good agreement with those from the IOLMaster (Carl Zeiss Meditec, Jena, Germany) and the Pentacam (OCULUS Optikgeräte GmbH, Wetzlar, Germany) and their use in toric IOL calculation yields better clinical outcomes than manual keratometry readings.[144,145,146]

This device was used by Ferreira et al. in a study to evaluate the mean biometric values in cataract surgery candidates in Portugal[147], in a study to assess the accuracy of corneal astigmatism by three different devices in pseudophakic eyes[148], in a study assessing comparability and repeatability of keratometric and astigmatism readings using three different devices[149], as well as for preoperative assessment of astigmatism in three other recent studies.[150,151,152]

Corneal topographers expand the cornea evaluation, overcoming some of the keratometer limitations. Moreover, corneal topography/tomography and aberrometry have allowed topography‐guided and wavefront‐guided customized corneal ablations with the excimer laser, improving the results not only of standard refractive surgery but particularly in highly aberrated eyes.[153]

2.6.3.2 Placido disk technology

In 1847, Henry Goode, described the first keratoscope, which used the reflection of a square object from the cornea from the side of the target. Ferdinand Cuignet coined the term “keratoscopy” in 1874 to describe the technique which now is known as “retinoscopy”. Seven years later, António Plácido da Costa (1840–1916), a Portuguese ophthalmologist, developed his keratoscope, called the Placido disk, with a central aperture for observing and photographing the corneal reflections (Figure 14).

Figure 14 – The Placido disk.

The Placido disk was the first attempt to qualitatively assess the shape of the entire cornea. Placido-based devices are, still today, widespread topographic instruments in clinical practice. They project a disk of concentric dark and light rings on the corneal suface, with the center of the disk having a convex lens for the visualization of its reflection on the cornea. The initial devices evolved onto photokeratoscopy and videokeratoscopy.

In 1896, Allvar Gullstrand (1862–1930) quantitatively analyzed photokeratoscopic images of the cornea. Photokeratoscopy provided qualitative information about the anterior corneal surface (the reflected rings appear noncircular in cases of high astigmatism or other corneal abnormalities). The development of computerized analysis at the end of the 20th century allowed computerized videos, with keratoscopes becoming capable of analyzing information from thousands of points on the anterior cornea to describe the anterior corneal curvature. The union of computer software analysis with high-resolution concentric ring keratoscopic images allowed the creation of color-coded topographic maps of the cornea. On these maps low dioptric powers are represented by blue and green (cold colors) and high dioptric powers are represented by yellow, orange, and red (warm colors). The smaller the radius of curvature of the anterior corneal surface, the higher the refractive power, derived considering the refractive index.[153]

Unlike keratometers, which only measure the central cornea, keratoscopy-based instruments cover the central 7-8-mm zone of the cornea. The main disadvantage of these devices is their inability to evaluate the posterior surface of the cornea, with the astigmatism value obtained being dependent on a given keratometric index. Another

limitation of this technique results from the operation of its algorithms, which may not accurately characterize the morphology of the anterior corneal surface when the cornea is too irregular or presents too many elevations, since the projection of rings is more difficult on corneal surfaces that have higher curvatures and are not rotationally symmetric. Placido-based techniques are also very susceptible to errors in patients with dry eye. This condition leads to a distorted image of the rings, resulting in the detection of false corneal surface irregularities and inaccurate measurements.[154] In order for the evaluation to be correct, Placido-based techniques require very precise alignment between the instrument and the patient's eye, which is not always easy to achieve. Skew ray errors and lack of reliability in information from the central corneal are other limitations inherent to this technique.[153] Nevertheless, Placido-based devices provide a repeatable anterior cornea analysis, including the anterior corneal shape (central power, simulated keratometry, corneal asphericity, etc.) and anterior corneal aberrometry. Placido-disk technology is nowadays combined with other technologies, including slit-scanning topography, Scheimpflug imaging, and aberrometry through ray tracing.

2.6.3.3 Slit-scanning technology

Slit-scanning elevation topography employs a projection of slit of light (same principle as the slit-lamp) to obtain corneal curvature measurements. This imaging technology was developed at end of the 1990s and was the first to evaluate both the anterior and posterior corneal surfaces. Mathematical analysis of the slit of light reflected by both corneal surfaces allows the reconstruction maps of anterior and posterior corneal surfaces (ray tracing triangulation) and, because both surfaces are measured at the same time, maintaining the relationship to each other, pachymetry of the entire cornea is also provided. To increase the robustness of data capture in cases with reduced transparency (edema, scars, haze, etc.), when the quality of the slits of light could introduce errors in the analysis, a Placido-disk is incorporated.

Corneal surface elevation is measured from a reference sphere that is freely adjusted to each patient’s cornea to reach the best fit in diameter and position to produce a “best-fit sphere” (BFS) surface (Figure 15). [155]

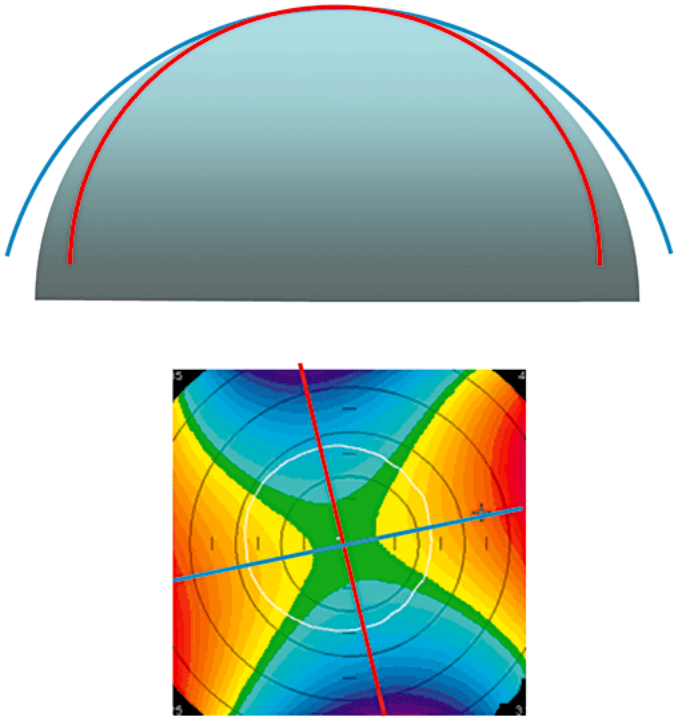

Figure 15 - The figure depicts elevation data of a cornea with regular astigmatism. The upper image shows the flat and steep meridians as compared with a best-fit-sphere in profile view. The steep meridian (red) is below the best-fit-sphere, and the flatter meridian (blue) falls above the best-fit-sphere. The elevation subtraction map below shows the flatter meridian elevated above the best-fit-sphere (warm colors) and the steeper meridian below the best-fit-sphere (cool colors).

Reprinted with License from John Wiley and Sons and Copyright Clearance Center.

Corneal power is represented with the same color code used by Placido-based devices.

Finally, pachymetry is also represented in a color-coded map, where green represents the normal range of corneal pachymetry, purple, and warm colors indicate thicker areas and red indicates thinner areas. This map also includes the values for corneal pachymetry. Optical power maps of the cornea, the anterior chamber depth, the corneal white-to-white distance, and other data from the iris and lens are also assessed and represented with this technology.

The Orbscan II series (Bausch and Lomb Inc., Rochester, NY, USA) is the only device commercially available based on this technology. During image acquisition, fourty slits are projected sequentially on the cornea (twenty from each side) at a 45° angle and the

anterior and posterior edges are captured and subsequently analyzed. Images are taken from 9.000 points in two-time ranges of 0.75 seconds. The last version (Orbscan IIz) can be integrated with the Zywave II wavefront aberrometer in the Zyoptix workstation.

The Orbscan IIz device was used by Ferreira et al. in the studies reporting on use of a novel color-LED corneal topographer to assess astigmatism in pseudophakic eyes and evaluating comparability and repeatability of different devices for corneal astigmatism assessment.[148,149] In these studies, keratometry from the central 3.0 mm zone was used to maximize comparability between the devices.

Because a full three-dimensional reconstruction of the cornea is possible, these devices, together with Scheimpflug imaging-based and AS-OCT devices are called corneal tomographers, to differentiate them from corneal topography, that just assesses the anterior corneal surface.[153]

2.6.3.4 Scheimpflug imaging-based technology

Scheimpflug imaging-based devices use sub-pixel edge detection for the cornea, anterior chamber and lens. Through one or various rotating cameras, these instruments obtain scans of sections of the cornea and rebuild its surfaces.

This technology presents the outcomes in a similar way to slit-scanning devices, measuring elevation from a BFS reference. Global pachymetry maps are also represented similarly. In addition, a complete analysis of the anterior segment is possible providing corneal topography data (anterior and posterior corneal surface), corneal eccentricity, anterior chamber depth, pupil diameter, iridocorneal angle width, lens density, and lens thickness.

As previously mentioned, evaluating both corneal surfaces provides a more accurate representation of corneal astigmatism than that obtained by extrapolating the total corneal power using a conventional keratometric index. In the past, the contribution of posterior corneal astigmatism for the refractive power of the cornea was underestimated, because of the small difference in the refractive index between the cornea and aqueous humour. For the posterior corneal surface to produce the same magnitude of astigmatism as the anterior surface, the difference in curvature between

the steepest and flattest meridian would have to be ten times larger. Furthermore, the normally employed standard keratometric index of 1.3375 assumes that the anterior and posterior astigmatism have a standard and linear relationship. This is, in fact, not true for many eyes.[156,157,158]

The Pentacam HR (Oculus Optikgeräte GmbH, Wetzlar, Germany) is one of the imaging devices based on the Scheimpflug principle. The device captures up to fifthy slit images of the anterior segment of the eye in less than two seconds using a single Scheimpflug camera to construct a three-dimensional image of the anterior segment.[153] It generates highly repeatable values of magnitude and axis for anterior and total corneal astigmatism.[158]

Several maps may be selected to represent total corneal astigmatism. The True Net Power (TNP) map measures the total corneal power using real keratometric indices (1.376 for the anterior and 1.336 for the posterior surface). A study investigating the use of this map in IOL power calculation in in eyes with previous laser refractive surgery reported the TNP of the Pentacam is a reliable alternative to determine the IOL power in cases where historical data is not available. They recommended implementing the TNP to obtain precise IOL power calculations after refractive surgery.[159]

The Total Corneal Refractive Power (TCRP) map is calculated by ray tracing.[160] When parallel light passes through the cornea, light rays are refracted according to the true refractive indexes of each surface, their curvature and the exact location of the refraction. Theoretically, this map is the most realistic to represent TCA.

The Holladay Equivalent K Readings map adapts total corneal power values to be used in conventional IOL calculation formulas. Calculation is made with the real refractive indices of the cornea and aqueous and Snell's law is used for calculating TCA.

The Pentacam HR tomographer was used by Ferreira et al. in the studies comparing astigmatic prediction errors associated with new calculation methods for toric intraocular lenses as well as comparing methodologies using estimated or measured values of total corneal astigmatism for toric IOL power calculation.[150,151,152]

Scheimpflug based devices have known limitations, including their high sensitivity to the pupil diameter, which interferes with the sampling of the instrument, and the inability to evaluate the density of the central nucleus of the lens in the presence of mature cataracts.[161] The acquisition time of a corneal elevation map is another shortcoming, since involuntary ocular movements may degrade the reliability of the examination.[154,Erro! Marcador não definido.]

2.6.3.5 Point-source light-emitting diodes technology

Accounting for the limited precision in evaluating corneal astigmatism, a distinct technology was recently developed, color point-source light-emitting diodes (LED) topography. The only device using this technology is the Cassini (i-Optics, The Hague, The Netherlands).

The Cassini uses multi-color point-to-point (up to seven hundred) forward ray tracing imaging for evaluating the anterior corneal surface combined with second Purkinje imaging reflection of seven monochromatic LEDs, arranged in a circular shape, to evaluate the posterior corneal surface (again, using forward ray tracing). The operation principle of the algorithm used in color-LED topography is shown in Figure 16.[162]

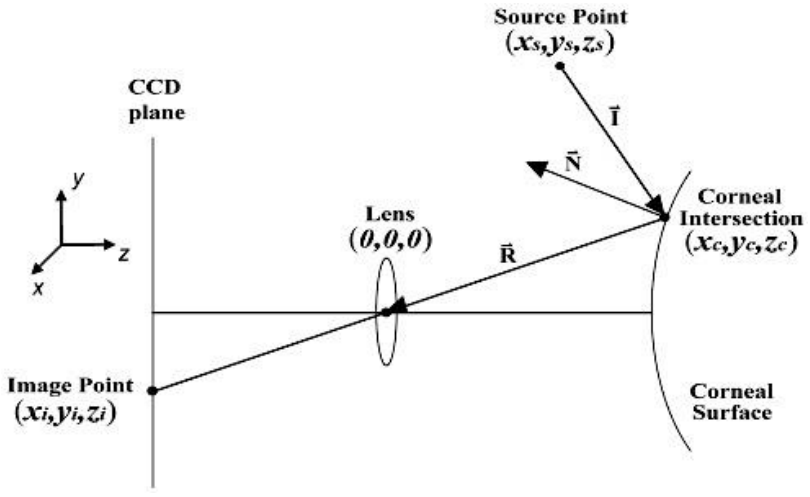

Figure 16 – Diagram of forward ray tracing model.

Reprinted under License CC BY 4.0.

On this algorithm, each point of LED projected on the anterior corneal surface is modeled as a light source to which coordinates (x_s, y_s, z_s) are assigned. These are traced

towards the intersection points on the corneal surface (x_c, y_c, z_c), and proceed with the reflected ray towards the image points (x_i, y_i, z_i), which are capture by a camera Because only the chief ray is considered, the reflected ray is constrained to pass through the nodal point (0, 0, 0). So, a point system with well-defined coordinates is established, allowing the reconstruction of a model of the anterior corneal surface.

In essence, forward ray tracing methods aim to determine the position of the image by knowing the position of the light source and the shape of the reflecting surface (in this case the cornea). However, in color-LED topography, the objective is to reconstruct the surface of the cornea by knowing the positions of the source and the image. This is possible by introducing some changes in the equations associated with the method considering that any corneal surface can be characterized by an expansion of the Zernike polynomials, provided that a sufficient number of coefficients is used. Thus, by knowing the position of the point image and the point of the light source and describing the vectors formed between them, it is possible, through a step-by-step and iterative algorithm, to obtain the Zernike polynomials coefficients that can model the anterior corneal surface.[162]

The posterior corneal surface is evaluated by the previously mentioned second Purkinje image light points. The position of these points in space is also obtained through a point-to-point ray tracing algorithm. In this model, the rays from each light point are propagated to the posterior corneal surface, where they are reflected, considering the refractive effect of the already reconstructed anterior cornea. After the reflection on the posterior corneal surface, the rays are again propagated to the position of the image on the sensor. The Cassini does not perform pachymetry, so a corneal thickness of 550 µm is assumed. The software accounts for smearing and deformation in irregular corneas and provides parameters to estimate the quality of the scans.

When compared with other systems, color-LED topography has the advantage, over Placido-based devices, of not being affected by the Placido mismatch, given the reconstruction algorithm employs data that assures there is no mismatch between the source and image points, even in non-rotationally symmetrical corneal surfaces, and over Scheimpflug-based systems, of not having to compensate for motion artefacts,

since the acquisition is instantaneous. Moreover, the precision of its measurements is not so affected by dry eye, due to the employed multicolor LEDs.[163,164]

In a recent study, the Cassini was compared with Placido-based topography (Keratron), automated keratometry (Lenstar) and Scheimpflug-based topography (Pentacam), showing improved reliability compared to the Pentacam and to the Keratron. No difference in corneal astigmatism measurements was found compared with the Lenstar. However, measurements were less precise at lower levels of astigmatism.[165]

Being a recent technology, the precision, repeatability, agreement with other devices and clinical implications of color-LED topography have yet to be fully investigated. This was the basis for the studies discussed in Chapter 5.

2.6.3.6 Anterior segment-optical coherence tomography technology

One limitation of Scheimpflug imaging is the low resolution of the anterior segment scans. This is greatly improved by AS-OCT, particularly with the introduction of spectral-domain OCT devices (SD-OCT). These new devices are capable of generating corneal curvature and pachymetric maps while also evaluating total corneal astigmatism. Recent studies show that AS-OCT provides repeatable measurements of corneal power, thickness, diameter and aqueous depth.[166,167]

2.7 Toric IOL power calculation

With the increasing importance of a precise refractive outcome in cataract surgery, accuracy in planning of astigmatic correction became critical. However, there are several limitations in the calculation of the cylindrical power of toric IOLs.

Firstly, for each cylindrical power at the IOL plane, a corresponding magnitude of astigmatism is corrected at the corneal plane. This variability depends on the distance between the cornea and the IOL. Most toric IOL calculators (e.g. the original, still available online, toric calculator from Alcon (Alcon Laboratories Inc., Fort Worth, TX, USA))[168] assume a fixed ratio (in Alcon's case, 1.46) between the cylindrical power at the corneal and IOL plane. This results in undercorrections in long eyes and overcorrections in short eyes (e.g. in an eye with an axial length of 20.0 mm the real ratio is 1.29 and in an eye with an axial length of 30.0 mm the real ratio is 1.86).[169,170]

Recently, strategies to overcome this limitation, such as including the anterior chamber depth and pachymetry in toric IOL power calculation were described.[171,172]

Moreover, although scientific literature is scarce on the subject, the cylindrical power of the IOL at the corneal plane also depends on the IOL's spherical power, due to the different vergence of the rays. Not considering the spherical power when calculating a toric IOL may also induce errors, especially in toric IOLs with higher cylindrical powers. For example, considering the same effective lens position (ELP) of the manufacturer (5.2 mm for Alcon), an Acrysof Toric SN60T3 IOL (1.50 D of cylinder at the IOL plane and 1.03 at the corneal plane, according to the manufacturer) has a true cylindrical power of 1.32 D at the corneal plane for a 17.0 D lens and of 1.22 D for a 28.0 D lens. In the case of a SN60T9 IOL, the error induced by not considering the spherical power, may be greater than 1 D.[173]

However, the most important source of error when calculating a toric IOL is not considering the astigmatism of the posterior corneal surface.[171] As mentioned previously, ignoring its power in toric IOL calculation results in overcorrection in eyes with WTR astigmatism and undercorrection in eyes with ATR astigmatism.[52,174]

Considering this, to account for posterior corneal astigmatism when it is not directly measured, several nomograms and mathematical models were developed.

The first to be published, in 2013, was the Baylor nomogram.[175] Later, Goggin et al. developed two coefficients of adjustment (for WTR and ATR eyes) to alter the anterior keratometric power while also considering the spherical power of the IOL.[176] Abulafia et al. published the Abulafia-Koch formula, a mathematical regression formula to estimate total corneal astigmatism based on standard keratometric measurements. The formula was developed by back-calculating the real IOL cylindrical power in a series of eyes that had been subjected to cataract surgery with toric IOL implantation.[177] Several other calculators were recently developed, accounting for ELP, spherical power of the IOL and/or total corneal astigmatism. These include Holladay's toric calculator (available in the software "Holladay IOL consultant & surgical outcomes assessment"), which takes the predicted ELP into account, adjusting the cylinder ratio according to the Holladay 2 formula, and the Barrett toric calculator,[178] which considers the ELP (with Barrett

Universal II formula), while also adjusts the cylindrical power and axis of alignment of the toric IOL according to a mathematical model and a regression formula for the posterior corneal surface.[179] The Barrett toric calculator is incorporated in the new calculator recently introduced by Alcon for their toric IOLs.[180]

A different strategy for IOL power calculation is the use of ray tracing. Ray tracing overcomes problems related with simplifications (such as the conversion of effective powers in different planes). Ray tracing uses measured instead of presumed geometry, not including keratometric indices but only the corneal refractive index. This avoids the overestimation of corneal power by using the common 1.3375 refractive index and the variability caused by the use of different keratometric indices in different devices.[158]

Ray tracing to calculate total corneal astigmatism is a method for calculating the path of a single ray of light through a given optical system. As a ray passes through an optical system, starting at a given point and angle relative to the system's optical axis, it is refracted at each optical surface, causing the ray to change direction. The angles of these direction changes can be calculated according to Snell's law, although it is impossible to calculate the final direction of a ray that has passed through an optical system with more than one refractive surface using closed formulas.

The principles of ray tracing were developed in the early 17th century, but it was not until 150 years later, when Karl Friedrich Gauss developed a simplified calculation method, that optical calculations became practicable. In Gaussian optics, the sine is approximated by the first element of series expansion of the sine; that is, the angle (arc) itself. With this approach, for the first time, optical systems with more than one refractive surface could be calculated with a closed formula. These are principles that have been used in recent decades for the creation of new IOL power calculation formulas. When applied to IOL formulas, ray tracing uses a pseudophakic eye model, and ideally anterior and posterior corneal surfaces should be measured using topography. In this power calculation strategy, anterior and posterior central curvature radii, asphericity of the surfaces, central IOL thickness, and index of refraction are all used to describe the IOL. The position of the IOL in this calculation is not a fictitious ELP but the true geometrical position, as defined by the distance between the posterior

corneal apex and the anterior IOL surface. The downside of ray tracing is that the postoperative position of the IOL cannot be determined before surgery. Therefore, ray tracing is no more advantageous than third-generation IOL formulas to predict the accuracy of postoperative IOL position. However, prediction methods for postoperative ACD should be directly compared with corresponding ACD measurements. This is possible with ray tracing but not with the fictitious ELP calculated with third-generation formulas using Gaussian optics. With ray tracing the postoperative ACD can be determined using partial coherence interferometry and directly compared with the preoperative estimation. With third generation IOL formulas, the ELP can be back-calculated from the postoperative refraction; however, the latter is less accurate due to errors in subjective or objective refraction and IOL mislabeling. Although many surgeons rely on the use of third-generation formulas for IOL calculation, ray tracing should be considered a potentially useful strategy.[181] A Danish study evaluated 767 pseudophakic eyes (583 patients) to describe a method for back-solving the power of an IOL *in situ* based on optical biometry and ray tracing analysis. Assuming a 3.0 mm pupil, the mean prediction error between the labeled and the calculated IOL power was -0.26 D ± 0.65 (range -2.4 to +1.8 D). The prediction error showed no bias with IOL power or AL. The authors concluded that the optics of the pseudophakic eye can be accurately described using exact ray tracing and modern biometric techniques.[182]

Recently, Abulafia et al. published a case series comparing the precision of some of the new calculation methods.[11] However, there were no studies comparing all the recently developed nomograms and calculators.

This was the basis for conducting the studies described in Chapter 6.

2.8 Surgically induced astigmatism

The astigmatism generated by the creation of a clear corneal incision (CCI) during phacoemulsification and that is present postoperatively is named surgically induced astigmatism (SIA). The effect of SIA must be considered in any toric IOL calculation for determining the correct cylindrical power and axis of alignment of the IOL. This type of astigmatism can be WTR or ATR, according to the corneal meridian of the incision. SIA is related to the process of healing and scar reshuffling taking place at the surgical incision.

SIA depends on factors related to the individual (such as age, pre-existing corneal astigmatism, and ocular morphometry)[183,184], the type of surgery (bimanual or coaxial microincision cataract surgery, manual or FLACS)[185,186], and the CCI (use of sutures, incision location, and incision size).[187]

Regarding the factors related to patient, an older age at the time of surgery is associated with higher SIA.[183,188] A higher magnitude of preexisting corneal astigmatism is also correlated with a higher SIA[188]One study examined the influence of ocular features on SIA. Not only higher preoperative corneal astigmatism but also a shallower ACD, shorter AL, and lower intraocular pressure were associated with higher SIA (for an incision width of 2.75 mm but not 2.2 mm).[188] Central corneal thickness is negatively correlated to the SIA magnitude.[188] Corneal biomechanical properties also play a role, with corneas with lower hysteresis and resistance factor resulting in higher SIA.[189]

The type of surgery also influences the SIA. One study showed that bimanual microincision cataract surgery (MICS) induced slightly more SIA than coaxial MICS,[185] although another study contradicts this finding, showing similar SIA values with both techniques.[190] SIA is similar in manual and FLACS.[186]

Finally, factors related to the incision influence SIA. These include the use sutures, the incision location relative to the limbus, the meridian of the incision and the incision width. In the case of a suture, the operative wound astigmatism is dependent on the length, depth and tightness of the suture. Sutures in the anterior portion of the cornea compress more tissue from the anterior part than the posterior part of the cornea, producing a depression of the limbal cornea towards the anterior chamber and steepening the central cornea in the meridian of surgery. The corneal diameter decreases in that meridian. In the opposite meridian, the cornea flattens, the corneal diameter increases, and the sagittal depth decreases.[191] An incision more into clear cornea determines a higher SIA and vice versa.[192] However, the effect of anatomical location is less pronounced in the case of small incisions.

For oblique CCIs, SIA is similar in superotemporal and superonasal incisions.[193] Horizontal CCIs induce WTR astigmatism. For this meridian, SIA is lower in temporal than

in nasal incisions.[194,195] Temporal CCIs induce less astigmatism than on-axis oblique incisions.[196]

Finally, the width of the incision is one of the main factors influencing SIA. As shown in several studies, a smaller incision width is associated with less SIA.[187,188,197,198]

Knowledge of SIA is still limited. There is scarce literature, and with several methodological limitations, comparing SIA in manual and femtosecond-laser created CCIs. Also, although literature on the influence of incision width and meridian on SIA is extensive, the association of SIA with other ocular features is less well known. This was the basis for conducting the study detailed in chapter 7.

2.9 Preoperative marking of the IOL axis of alignment

As toric IOLs are increasingly used, accurate alignment of the lens inside the eye remains a concern. For each degree of toric IOL misalignment, about 3.3% of the efficacy in cylinder correction is lost.[197] If the lens is 30 degrees off axis, it will have no effect on astigmatism correction. If it is more than 30 degrees off, postoperative astigmatism is increased relative to the preoperative. Hence, accurate marking and IOL alignment are mandatory.

2.9.1 Manual marking techniques

Several methods for marking the calculated toric IOL axis of alignment are available.

In any marking method (for manual methods, axis marking and, for digital methods, image capturing), the axis of toric IOL alignment should be marked with the patient seated, as changing from an upright to a supine position can induce ocular cyclotorsion (mean of 0.4 - 4.2 degrees; range 0 - 16 degrees).[198,199,200] Care must be taken to ensure the patient's head is not tilted.

One method of freehand marking is the placement of two marks on the horizontal meridian with the patient on the slit-lamp. With this approach, execution of both marks exactly 180 degrees apart is difficult. Specially designed tonometers can be adapted to the slit-lamp for this purpose. Alternatively, a weighted thread, pendulum marker or Nuijts-Solomon bubble marker can be used. Yet another option is utilizing electronic

markers. These markers display a green light when the marker is in the horizontal position. With any of these methods, two other steps are necessary. The second step involves the intraoperative alignment of the horizontal reference marks with the marks on a degree gauge and the third step, the marking of the targeted axis using a corneal meridian marker. Although involving three-steps, this marking method is fairly accurate, with a mean error in axis marking of 2.4 degrees, which results in a combined error of 4.9 degrees in toric IOL alignment.[201] In a study comparing four marking methods (marking at the slit-lamp, bubble marker, pendular marker, and tonometer marker) the pendular marker showed the least rotational deviation, and the slit-lamp marking technique the least vertical misalignment.[202]

To avoid ink diffusion, a specially designed wet-field cautery tips (Osher ThermoDot Marker) was developed as an alternative.[203]

One-step manual marking systems include, among several pendular devices, the Robomarker (Surgilum, Wilmington, NC, EUA). In a previous study, our group demonstrated this device is highly precise (mean error in axis marking of 1.2 degrees) and reproducible.[204]

Besides ink smudging, irregular or broad marks, manual marking has the limitations of any manual technique, including a significant learning curve, and intersurgeon variability.

2.9.2 Digital marking techniques

To overcome the limitations of manual marking, digital marking systems have been introduced. With these systems, a preoperative reference image is captured and posteriorly used intraoperatively, after limbal landmarks are matched to the reference image, to overlay an image of the targeted axis of implantation on the surgical microscope and guide toric IOL alignment. These systems include the Verion Image Guided System with VerifEye (Alcon), the Callisto Eye with Z align (Carl Zeiss Meditec), and the Truevision Digital Microscope Platform (TrueVision 3D Surgical, Santa Barbara, CA, USA).

Digital marking systems are more precise than manual techniques. Using the Verion system results in less postoperative deviation from the TIA and less postoperative toric IOL misalignment than a manual-marking technique.[205] The accuracy of Callisto Eye with Z align is similar to that of the Verion system.[206] A recent study showed that, despite increased precision in IOL alignment, digital systems do not result in significantly better UDVA or less residual refractive astigmatism.[207]

2.9.3 Intraoperative aberrometry

The most recent alternative approach for toric IOL alignment is the use of intraoperative aberrometry. The Optiwave Refractive Analysis system (ORA; Alcon) was the first commercially available intraoperative aberrometer. It utilizes the principle of Talbot-Moire interferometry to perform IOL power calculation based on the aphakic refraction.[208] Furthermore, it allows refinement of toric IOL alignment axis by indicating the direction and degrees of rotation required to achieve minimum residual astigmatism. More recently, VerifEye was incorporated into the ORA system, integrating a fast imaging processor that confirms the stability of the system before measurements are taken. Other system of intraoperative aberrometry is the Holos IntraOp (Clarity Medical Systems, Inc., Pleasanton, CA, USA). The Holos uses a rapidly rotating micro electro-mechanical system (MEMS) mirror and quad detector to measure the magnitude of wavefront displacement. Like the ORA, it attaches to the operating microscope to provide intraoperative refractive measurements.[209]

The use of intraoperative aberrometry results in a 2.4 times increased likelihood of a postoperative residual astigmatism of 0.50 D or when compared with standard methods (biometry assessment, conventional IOL power formula, Alcon toric calculator, and ink marking).[210] In patients with prior myopic keratorefractive surgery, intraoperative aberrometry is also superior to conventional methods.[211] However, a recent study comparing the Callisto with the ORA reported less residual astigmatism when the Callisto was used.[212]

2.10 Intraoperative technique

An adequate injector should be used to implant the chosen toric IOL. Injection may be performed by two techniques: cartridge-assisted (with full introduction of the cartridge

tip into the anterior chamber) or wound-assisted (in which the cartridge tip is inserted in the CCI but not into the anterior chamber). The latter results in less incision enlargement, regardless of the biomechanical properties of the cornea, which may be important to generate less SIA.[213]

As previously stated, surgery with toric IOL implantation must be meticulous. A capsulorhexis overlapping the optic of the IOL in the 360 degrees is essential to ensure IOL stability; a complete aspiration of the OVD, including from behind the IOL to avoid postoperative rotation and guaranteeing a meticulous IOL alignment.[214]

2.11 Postoperative astigmatism evaluation and measures to optimize outcomes

Complementing the usual ophthalmologic examination after cataract surgery, when refractive outcomes are sub-optimal, the axis of alignment of the toric IOL must be evaluated.

As stated before, even minor degrees of misalignment can cause a significant loss of the cylinder correction efficacy with subsequent residual astigmatism and reduced UDVA.[215,216]

Toric IOL misalignment can occur by an imperfect alignment during surgery or postoperative rotation, which is much less frequent with newer lens' designs.[217,218] However, other causes of residual astigmatism exist: the variability in the SIA generated by the CCI, a different toric power at the IOL plane than predicted (nonoptimized constants[219], unexpected ELP[220] or different IOL power than labeled[221]). Furthermore, there are other sources of postoperative astigmatism that remains unexplained after the postoperative keratometry or the toric effect of the IOL has been accounted for. This is termed non-lens ocular residual astigmatism. Causes include pre-existing non-lens astigmatism, including posterior corneal astigmatism[52], IOL tilt[222] or changes in the patient's subjective perception of astigmatic neutralization.[223]

Residual astigmatism may be corrected by repositioning the IOL or exchanging the IOL (depending on the magnitude of the residual refractive error), excimer laser touch-up or femtosecond laser arcuate keratotomy.

Any misalignment greater than 10 degrees is generally regarded as an indication for surgical repositioning, although this must always be considered in light of the individual visual requirements of each patient. In case IOL realignment is necessary, it should be performed in the first two to three weeks after surgery. Early intervention facilitates rotating the IOL, as there is less capsular fibrosis and adhesion, with lower probabilities of capsular rupture/tear, IOL decentration/(sub)luxation or vitreous loss.[224] However, a sufficient time period (about 2-3 weeks) after the surgery is to be observed before the secondary intervention. This time allows early capsule fibrosis and shrinkage to commence and a precise manifest refraction to be determined. The lens may be rotated through the original incision with the help of an OVD.

To determine the ideal IOL rotation, Alpins et al. described how to calculate the angle of rotation, which is the toric IOL rotation, to minimize the amount of manifest refractive cylinder in any eye using optimized lens constants to account for eye-specific and surgeon-specific factors that affect the equivalent power of the toric IOL at the corneal plane.[225]

Using an online calculator (e.g. Berdahl and Hardten Toric results analyzer[226] or Barrett Rx Formula – Outcome Analysis[227], both freely available online) helps determining which orientation axis would result in a lower residual astigmatism.

Chapter 3: Objectives

3.1 General objective

The main objective of this research was to minimize the errors involved in each step of toric IOL power calculation, ultimately contributing to refine the refractive results and improve clinical outcomes of cataract surgery with toric IOL implantation.

3.2 Specific objectives

In detail, the specific objectives were as follows:

- Characterize the ocular biometric parameters and investigate the prevalence of preoperative corneal astigmatism in the Portuguese population submitted to cataract surgery (**Chapter 4**);

- Investigate the precision, repeatability and comparability of different measurement methods, including the recently introduced color-LED topography, for evaluating total corneal astigmatism (**Chapter 5**);

- Assess the precision of the available new toric IOL calculators and compare direct measurements of total corneal astigmatism with its estimation with mathematical models (**Chapter 6**);

- Improve knowledge of SIA, by analyzing its value and its correlations with ocular and individual characteristics in manually and femtosecond laser-created clear corneal incisions (**Chapter 7**).

All the studies included in the thesis were conducted in accordance with the principles of the Declaration of Helsinki, approved by Hospital da Luz Ethics and Investigation Committees and NOVA Medical School Ethic Committee and all the participants provided written informed consent for the respective study.

Chapter 4: Prevalence of astigmatism in the Portuguese population

This chapter is based on the papers:

- "Ocular Biometric Measurements in Cataract Surgery Candidates in Portugal", published by Ferreira et al. in 2017 in PLOS ONE (12(10):e0184837), and;

- "Distribuição e determinantes de parâmetros biométricos oculares em candidatos a cirurgia de catarata em Portugal", published by Ferreira et al. in Oftalmologia in 2017;41(4):17-26.[228]

- Since results from both in this chapter studies were similar, we will only focus on the paper reporting data from the larger cohort

4.1 Introduction and objectives

With the increase in life expectancy of populations, there has been a progressive increase in the volume of cataract surgery performed worldwide, and it is the most common elective surgery in many countries. The introduction of less invasive techniques, new IOLs, and the achievement of more predictable refractive outcomes have been accompanied by an increase in patients' expectations of good visual outcome without the use of spectacles. Accurate biometric measurements are therefore essential. Knowledge of these measures is fundamental for obtaining precise calculations for the IOL power, which is primarily based on formulas derived from normative ocular biometric parameters.

It is known that ocular biometric parameters such as AL, K, and ACD (corneal epithelium to anterior lens) vary with gender, age, and ethnicity, and hence are different among different populations.[229,230,231,232,233,234] Although there are many studies that describe these mean parameters in the European Caucasian population, there has been little attention to those studies carried out in Asian, Black and Hispanic populations.[229] In addition, many of the published studies were conducted using contact applanation ultrasound biometry, a method limited by several measurement errors limiting its use prior to cataract surgery, particularly when premium lenses are implanted. It is known that optical biometry offers several advantages even over immersion ultrasound biometry, including its non-contact method, greater reproducibility and accuracy, and application in particular cases such as posterior staphyloma and eyes filled with silicone oil.[235,236] Published studies of ocular biometric parameters using optical biometry are scarce, and this technology is constantly evolving and allows the evaluation of new parameters, such as measurement of the LT. Among various optical biometry devices available, Lenstar (Haag-Streit AG, Koeniz, Switzerland) has proved to be highly accurate in biometry measurements.[237]

There has not before been a large study of biometric values for the Portuguese population. The objective of the present study is to characterize the ocular biometric

parameters and their associations in a population of cataract surgery candidates in Portugal.

4.2 Material and methods

A retrospective study of 13,012 eyes of 6,506 patients who underwent cataract surgery was performed at the Hospital da Luz in Lisbon.

Ocular biometric parameters, including AL, mean corneal power K and astigmatism, ACD, LT, and CD were studied by optical low-coherence reflectometry using the Lenstar LS900 (Haag-Streit AG, Köniz, Switzerland). Examinations that yielded poor quality or uncertain results were excluded as were those of patients with previous ocular surgeries. Astigmatism was studied using the automatic keratometry of the same device. Keratometry with this system demonstrated high precision and repeatability and has been shown to produce better clinical results with toric IOLs than manual keratometry.[144]

Statistical analysis

One eye was randomly chosen for each patient. The biometric data measured were entered into an Excel spreadsheet (Microsoft Office 2010; Microsoft, Redmond, WA).

The statistical analysis was performed according to E9 guidelines of the ICH principles of statistics for clinical trials, using SPSS for Mac (version 21.0, Chicago, IL). The normality of the data was accessed with the Kolmogorov–Smirnov test. Since none of the studied variables had a normal distribution, nonparametric statistics were used. The Mann–Whitney U test was used for comparisons between groups. Correlations were performed using the Spearman coefficient. Regression models considering age, gender, LT, and CD were constructed to determine associations with the most relevant ocular biometric parameters (AL, ACD, and K). The results are expressed as the parameter mean value ± standard deviation (SD), and those with a value of $p < .05$ were considered statistically significant.

4.3 Results

Demographic data and biometric parameters

The demographic data and ocular biometric parameters of the patients are presented in Table 1.

The mean AL was 23.87 ± 1.55 mm. 241 (7.4%) eyes had an AL < 22.0 mm, 2,111 (64.9%) between 22.0 and 24.5 mm, 612 (18.8%) between 24.5 and 26.0 mm and 289 (8.9%) > 26.0 mm. A positive deviation and a leptokurtic distribution (kurtosis 2.804) were observed, with a significant deviation from normality, as in the other measured parameters ($p < .001$ in all cases except for CD, $p = .049$). The histograms of the distribution of the measured values of AL, K, corneal astigmatism, ACD, LT and CD are shown in Figures 17 to 22.

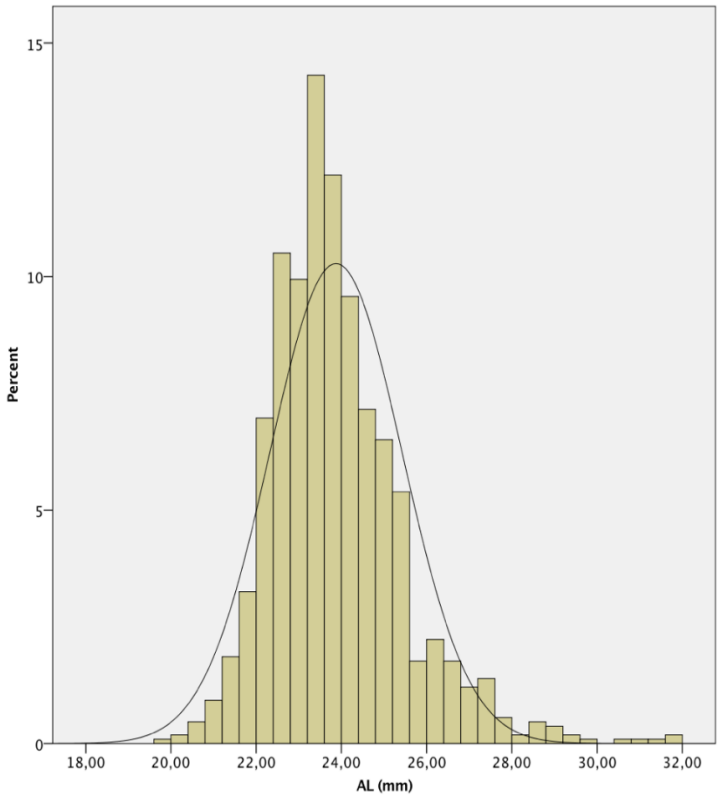

Figure 17 - histogram of axial length (AL) of the study population.

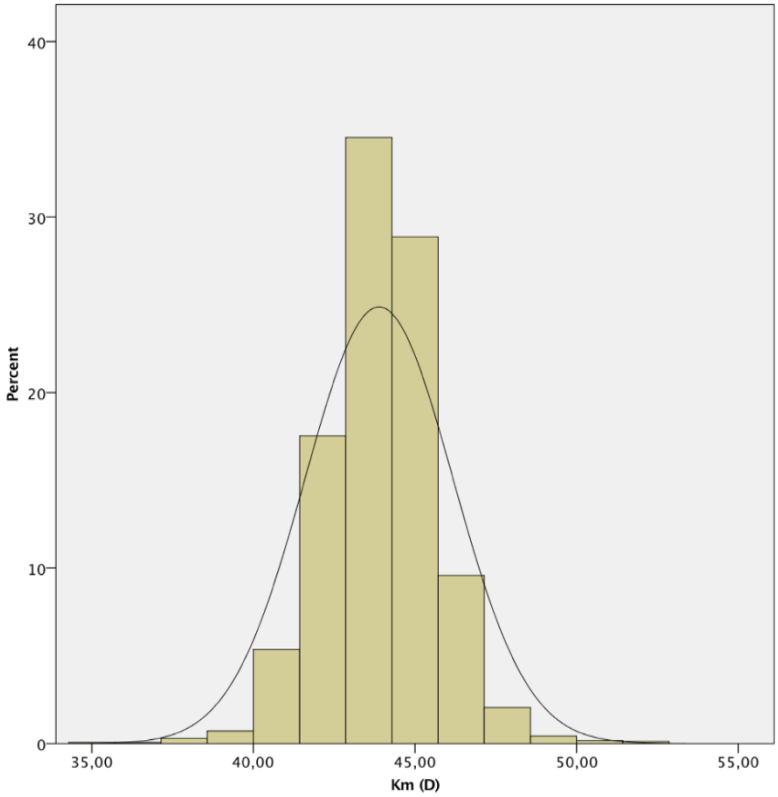

Figure 18 - histogram of mean keratometry (Km) of the study population.

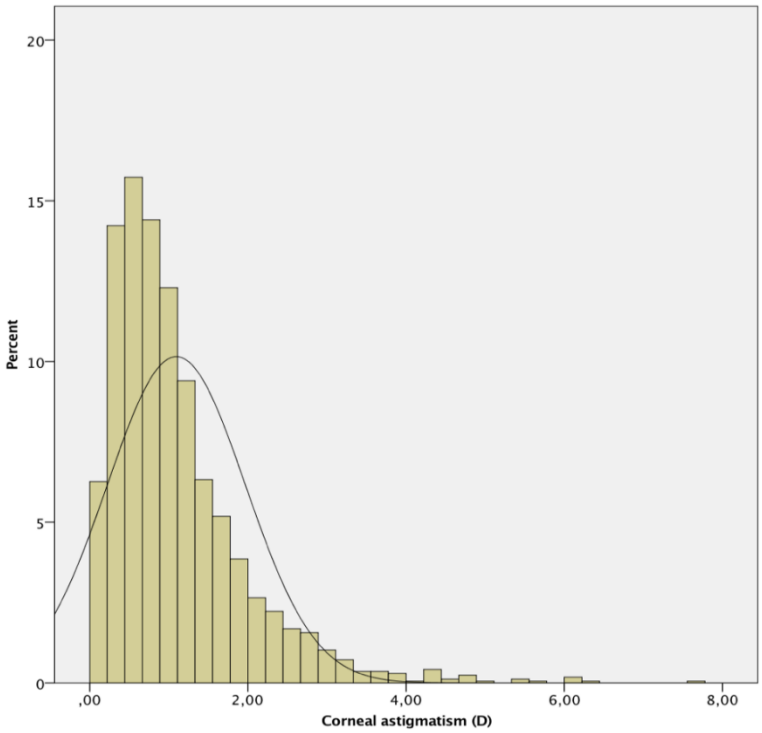

Figure 19 - histogram of corneal astigmatism (D) of the study population.

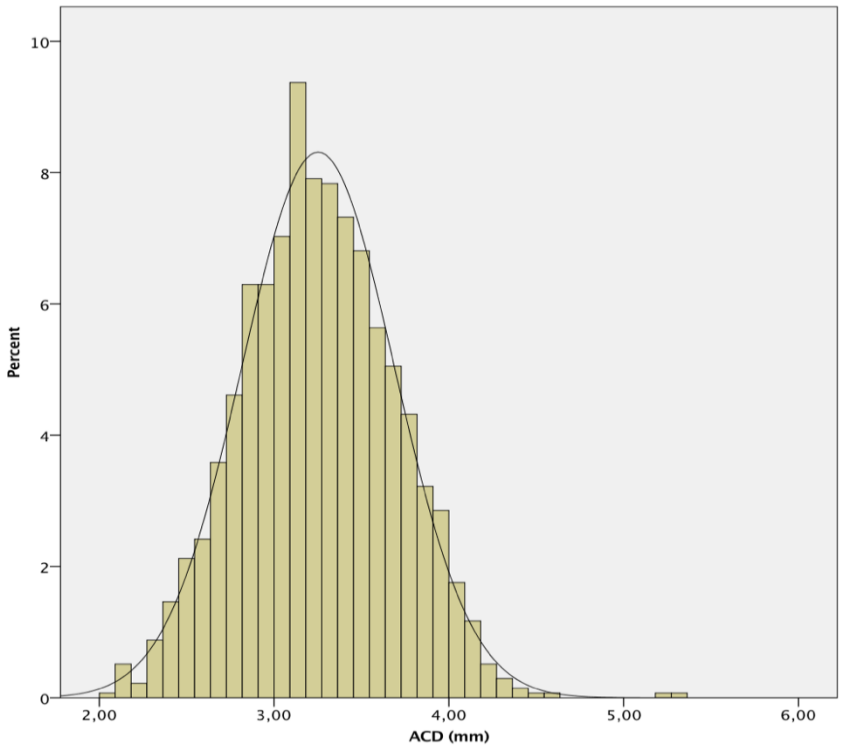

Figure 20 - histogram of mean keratometry (Km) of the study population.

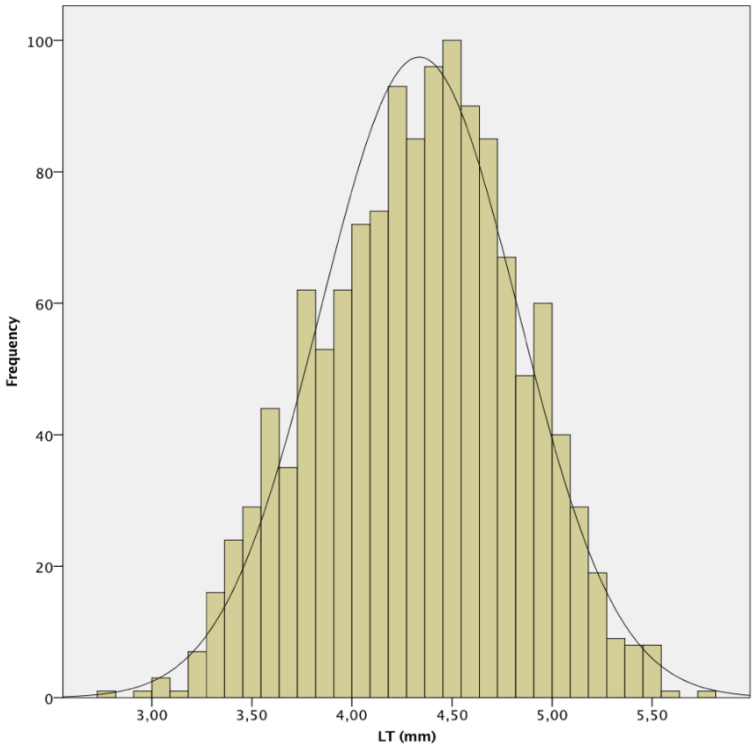

Figure 21 - histogram of lens thickness (LT) of the study population.

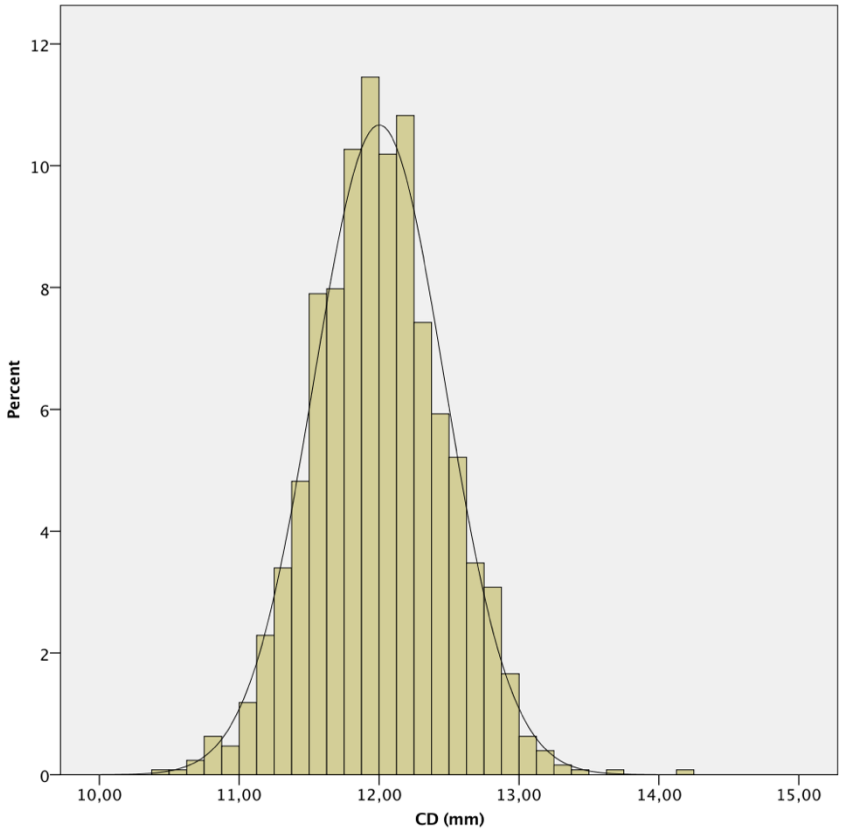

Figure 22 - histogram of corneal diameter (CD) of the study population.

Male eyes had longer ALs, deeper ACDs and flatter corneas than female eyes ($p < .001$); however, there were no statistically significant differences in the other parameters evaluated.

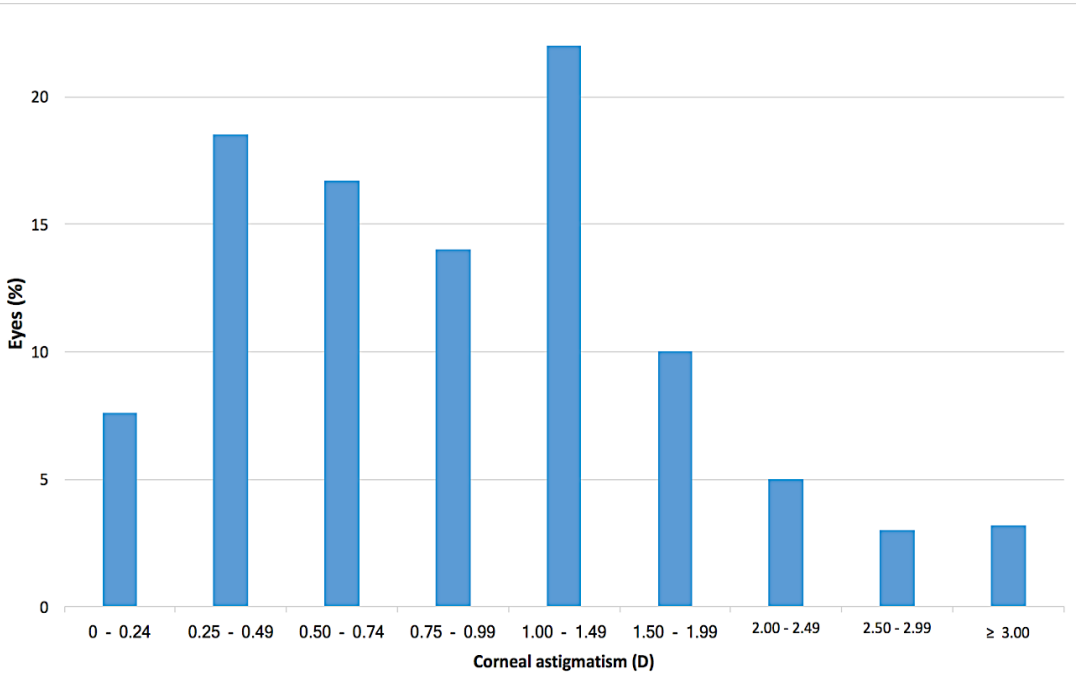

Figure 23 - distribution of corneal astigmatism in the study population.

The distribution of corneal astigmatism is shown in Figure 23. The mean corneal astigmatism was 1.08 ± 0.84 D (range 0–7.58), with 1,415 (43.5%) eyes showing astigmatism ≥ 1 D. 1,513 (46.5%) eyes presented against-the-rule (ATR) astigmatism (steep meridian 0-30 degrees or 150-180 degrees), 1,077 (33.1%) eyes with-the-rule (WTR) (60-120 degrees), and 663 (20.4%) eyes were oblique (31-59 degrees or 121-149 degrees).

Table 1 - Demographic data and mean ocular biometric parameters in Portuguese population.

Parameter	**Mean ± SD (range)**
Eyes (*n*)	6,506
Patients (*n*)	6,506
Age (years-old)	69 ± 10

Range	(44 – 99)		
Females, *n* (%)	3,721 (57.2%)		
Right eyes, *n* (%)	1,678 (51.6%)		
	Total	**Males**	**Females**
Axial length (mm) ± SD	23.87 ± 1.55	23.99 ± 1.47	23.68 ± 1.46
Range	(19.8 – 31.92)	(20.03 – 31.92)	(19.8 – 29.99)
Mean keratometry (D) ± SD	43.91 ± 1.71	43.46 ± 1.11	44.20 ± 1.29
Range	(40.61 – 51.14)	(40.93 – 51.14)	(40.61 – 49.93)
Mean corneal astigmatism (D) ± SD	1.08 ± 0.84	1.09 ± 0.92	1.12 ± 0.86
Range	(0 – 7.58)	(0 – 7.58)	(0 – 6.27)
Anterior chamber depth (mm) ± SD	3.25 ± 0.44	3.30 ± 0.40	3.14 ± 0.43
Range	(2.04 – 5.28)	(2.06 – 5.42)	(2.04 – 4.99)
Lens thickness (mm) ± SD	4.32 ± 0.49	4.35 ± 0.49	4.38 ± 0.41
Range	(2.73 – 5.77)	(2.75 – 5.77)	(2.73 – 5.42)
Corneal diameter (mm) ± SD	12.02 ± 0.46	12.03 ± 0.43	11.98 ± 0.49
Range	(10.50 – 14.15)	(10.51 – 14.15)	(10.50 – 14.09)

Correlations

The AL, ACD, LT and CD were all significantly correlated between each other ($p < .001$). There was no significant correlation between age and any of the biometric parameters investigated ($p > .05$). The complete matrix of correlations is presented in Table 2.

Table 2: Matrix of correlations of ocular biometric parameters in Portuguese population.

			ACD	LT	CD	Mean K	Age	AL
Rho Spearman	ACD	Correlation coefficient	1.000	-.633**	.484**	-.045	-.018	.571**
		Sig.	.	<.001	<.001	.281	.500	<.001
	LT	Correlation coefficient	-.633**	1.000	-.245**	.032	-.001	-.334**
		Sig.	<.001	.	<.001	.256	.979	<.001
	CD	Correlation coefficient	.484**	-.245**	1.000	.048	-.009	.454**
		Sig.	<.001	<.001	.	.098	.761	<.001
	Mean K	Correlation coefficient	.040	.032	.048	1.000	-.035	.040
		Sig.	.148	.256	.098	.	.150	.150
	Age	Correlation coefficient	-.018	.012	-.009	-.035	1.000	-.007
		Sig.	.500	.443	.761	.150	.	.804
	AL	Correlation	.571**	-.334**	.454**	.040	-.007	1.000

coefficient						
Sig.	<.001	<.001	<.001	.150	.804	.

***. Significant correlation (0.01).*

Sig. = significance, ACD = anterior chamber depth (epithelium to lens), LT = lens thickness, CD = corneal diameter, Mean K = mean keratometry, AL = axial length.

Regression models

Regression models were constructed for AL, ACD, and K considering age, gender, K, ACD, LT, and CD. A longer AL was associated with male gender (β = .082, p = .018), and deeper ACD (β = 0.512, p < .001), LT (β = .105, p = .007), and CD (β= .171, p < .001). A deeper ACD was associated with male gender (β = .571, p < .001), longer AL (β = .298, p < .001), wider CD (β = .253, p < .001), and thinner LT (β = − .496, p < .001). For K, there was a significant association with male gender (β = .313, p < .001) and no significant associations with the other studied parameters.

4.4 Discussion

This study presents the normative values of the biometric parameters evaluated using optical biometry in a Portuguese population of candidates for cataract surgery. To our knowledge, this is the first study to characterize these parameters in this population.

Mean values of biometric parameters

The mean values of the biometric parameters published in the different studies in the literature are described in Table 3.

Table 3: Mean values of biometric parameters published in previous studies

Study	**Country**	**Race**	**Measurement method**	**AL (mm)**			**ACD (mm)**			**Km (D)**		
				Total	Males	Females	Total	Males	Females	Total	Males	Females
Ferreira et al.	Portugal	Caucasian	Lenstar	23.87	23.99	23.68	3.25	3.20	3.09	43.91	43.46	44.20
The Tanjong Pagar Survey	Singapore	Chinese	US Contact	23.23	23.54	22.98	2.90	2.99	2.81	44.12	43.66	44.47
Cao et al.	China	Chinese	US Contact	23.04	-	-	3.03	-	-	44.24	-	-
Los Angeles Latino Eye Study	USA	Hispanic	US Contact	23.38	23.65	23.18	3.41	3.48	3.36	43.72	43.35	43.95

Hoffer	USA	Caucasian	US Immersion	23.65	-	-	3.24	-	-	43.81	-	-
Jivrajka et al.	USA	Caucasian	US Immersion	23.46	23.76	23.27	2.96	3.05	2.90	-	-	-
The Reykjavik Study	Finland	Caucasian	US Contact	-	23.74	23.20	-	3.20	3.08	-	43.41	43.73
The Singapore Indian Eye Study	Singapore	Indian	IOLMaster	23.45	23.68	23.23	3.15	3.19	3.10	44.35	43.94	44.70
The Singapore Malay Eye Study	Singapore	Malay	IOLMaster	23.55	-	-	3.10	-	-	44.12	-	-

The Blue Mountains Eye Study	Australia	Caucasian	IOLMaster	23.44	23.75	23.20	3.10	3.16	3.06	43.42	43.01	43.74
The Beaver Dam Eye Study	USA	Caucasian	IOLMaster	23.69	23.92	23.51	3.11	3.14	3.09	43.83	43.44	44.12
Hoffmann et al.	Germany	Caucasian	IOLMaster	23.43	23.77	23.23	3.11	3.12	3.02	43.89	43.44	44.12
Knox Cartwright et al.	United Kingdom	Caucasian	IOLMaster	23.40	23.76	23.20	-	-	-	43.90	43.45	44.18
Siahmed et al.	France	Caucasian	IOLMaster	23.46	-	-	-	-	-	43.97	-	-
Olsen	Denmark	Caucasian	IOLMaster	23.45	-	-	-	-	-	-	-	-
Aristodemou	United Kingdom	Caucasian	IOLMaster	23.50	-	-	-	-	-	43.84	-	-

US = A-scan ultrasound biometry, AL = axial length, ACD = anterior chamber depth, Km = mean keratometry (values converted to D using the given refractive index)

In our study, we found that AL had a non-normal distribution with positive deviation and high kurtosis. This deviation and kurtosis are in accordance with the findings described in the Reykjavik Eye study,[238] Singapore Malay Eye study[239], and the Blue Mountains Eye Study.[240] The normality of the distribution is variable in several studies. The mean AL in our study (23.87 ± 1.55 mm) is longer than the one reported in the Singapore and Chinese populations using applanation contact ultrasound.[241,242] It is still slightly longer than that reported in the Hispanic population of Los Angeles and Singapore Malay[239] and in the studies of Hoffer[243] and Jivrajka et al.[244] both in the USA and using immersion ultrasound. When compared with studies using optical biometry, the mean AL in our population is longer than that of the Caucasian population in Australia[234] and USA.[240] Using optical biometry, the mean AL in our study is longer than that published in several studies of European populations.[5,238,239,240] Although there may be differences explained by the AL measurement method, the AL in our study is longer than that published in the literature for different populations in studies using optical biometry, being closer to that reported in the Caucasian population of the USA[243,245] than in European Caucasian populations.[5, 246,247,248] In the latter populations, there is great similarity in the AL values reported in different countries; hence, in our study is longer than all of them, with a difference in mean values of about 0.40 mm. Although the majority of these studies used the IOLMaster 500 (Carl Zeiss AG, Jena, Germany) and our study used the Lenstar, this does not explain the differences found, since it was demonstrated by Hoffer et al.[249] that the IOLMaster and Lenstar AL biometry are not significantly different. The mean difference found is relevant, since a 1 mm error in AL results in a residual postoperative refractive error of 2.35 D in a 23.5 mm eye, 1.75 D in a 30.0 mm eye and 3.75 D in a 20 mm eye or about 2.0-4.0 D in the power of the implanted IOL.[250] The mean keratometry in our study did not follow a normal distribution, with negative deviation and high kurtosis. These findings are similar to both the Singapore Malay Eye study[239] and the Blue Mountains Eye Study.[240] The mean keratometry in our study was 43.91 ± 1.71 D. This value is lower than that reported in the Chinese[229]and Singaporean[239] populations,

being closer to those reported in the Caucasian population in Europe[246,247] and USA.[243] Although the keratometry evaluation methods are different, there is a close relationship between the values reported in Caucasian populations, which are generally lower than in the Far Eastern populations. The difference observed with respect to Far Eastern populations is significant, representing a potential difference in the refractive error greater than 0.50 D.[250]

It is known that about 29 to 40% of patients undergoing cataract surgery have corneal astigmatism greater than 1 D, which is enough to prevent optimal visual acuity without optical correction.[4] In our series, the mean corneal astigmatism was 1.08 ± 0.84 D, with 43.5% of the eyes showing astigmatism ≥ 1 D. These values are higher than those reported in most studies, such as those by Ferrer-Blasco et al.[4] (34.8%) in Spain and by Hoffmann et al.[5] in Germany (36%). It is known that corneal astigmatism varies significantly with age, increasing the prevalence of ATR astigmatism.[58] In our study, the majority of eyes (46.5%) had ATR astigmatism, which is in agreement with the age range of the evaluated population, with a mean of 69 years-old.

The mean ACD in our population (3.25 ± 0.44 mm) was higher than that reported in most studies in Eastern[230,242] and in Western populations[5,234,238,240], and it is comparable with that reported by Hoffer in the USA.[243] The differences found may be partly because of the measurement method used, since Lenstar uses laser optical biometry to measure ACD, while the IOLMaster 500, uses an optical slit image. Hoffer et al.[249] have reported that ACD values with Lenstar are higher than those measured with IOLMaster 500.

In our series, the mean LT was 4.32 ± 0.49 mm, and it was directly proportional to age and inversely proportional to AL. These findings confirm those of the studies by Jivrajka et al.[244] and Hoffer[243], although LT in our study was thinner than those studies reported. The mean CD in our study (12.02 ± 0.46 mm) was similar to that reported in other series in the literature.[5,240]

Relationship with gender and age

In this study, male eyes had longer ALs, deeper ACDs and flatter corneas than female patients did, and a gender difference with respect to the other investigated parameters was not statistically significant. These results are in accordance with those in the literature, especially in populations from Germany,[5] Australia,[240] USA,[244,245] and Iceland.[238] It is interesting to note that in a paper to be published, Hoffer et al. found a constant 0.50 mm difference in AL between genders, much higher than the 0.31 mm we found in this study. According to the Beaver Dam Eye Study[234] the height adjustment of individuals can explain all the differences found between the genders, however other studies have adjusted for height and weight and found that the differences still existed. Since gender and race appear to be important determinants of ocular biometric parameters, it may be important to consider them in the calculation of the IOL for cataract surgery, as shown by the appearance of the first 5th-generation formula, the Hoffer-H-5, which uses the same basic structure as the Holladay 2 formula but considers gender and ethnicity to reduce the error associated with the use of generalized population regression factors.

In contrast with most studies[5,240] there was no significant correlation between age and AL, ACD, or K. In the study by Hoffmann et al.[5], the results were similar to those observed in our series, and no correlation was found between age and AL. The interpretation of these differences is complex and would require adjustments for the refraction, height, age, and even educational level of the studied population.

Correlations between parameters

In this series, there was a positive correlation between AL and ACD, and K (not statistically significant) and CD, and a negative correlation between AL and LT. These results are in agreement with those reported in the literature[240,243,246] except for K, whose correlation with AL is inverse in most series, showing the emmetropic relationship between AL and corneal curvature.[243] Although there may be population differences and the correlation with refractive error has not been addressed in this

study, the different published studies in the literature reported keratometry evaluated with manual, automatic, or IOLMaster keratometry, and these values cannot be directly compared with ours because of the different methods of measurement and refractive indices used.

Regression models

In regression models for AL, ACD, and K considering age, gender, K, ACD, LT, and CD, the major determinants of AL were ACD and CD, and gender was not significant. Unlike the finding in other series, age was not a significant determinant.[234] An association between ACD and CD and LT was also observed.

4.5 Conclusions

The present study presents normative biometric parameters and their relationships in a Portuguese population. These results may be relevant not only in the evaluation of the refractive error but also in the IOL calculation for cataract surgery. The obtained AL, ACD, and mean K values were closer to the US population than most published series in different European Caucasian populations, and the disparities found could represent differences greater than 1 D in both the refractive error and the IOL power. Corneal astigmatism in the present study was higher than that in most published series, which may affect the type of IOL to be implanted.

Chapter 5: Improving the evaluation of astigmatism

This chapter is based on the papers:

- "A novel color-LED corneal topographer to assess astigmatism in pseudophakic eyes", published by Ferreira et al. in Clinical Ophthalmology. 2016: 10:1521-29, and;

- "Comparability and repeatability of different methods of corneal astigmatism assessment", published by Ferreira et al. in Clinical Ophthalmology 2018;12:29-34.

Introduction

Based on the data from the cross-sectional study on ocular biometric measurements in a Portuguese population of cataract surgery candidates (Chapter 4), we found that there is a high prevalence of preoperative corneal astigmatism amongst these over 6500 patients.[147]

As the benefits of correcting astigmatism are well known, precise measurements of corneal astigmatism are of the utmost importance to accurately determine the adequate toric IOL power for each patient. Given the multiplicity of topography devices available, and the lack of a recognized gold standard, it is important to assess their comparability and repeatability.

Color-LED topography (Cassini; i-Optics) is a recent technology specifically developed to assess eyes before cataract surgery. Its principles are detailed in Chapter 2 – 2.6.3.5 (Theoretical Background).

The goal of our first study (Chapter 5 – 5.2) was to assess the accuracy of corneal astigmatism measured by four techniques: slit-scanning topography, automated keratometry, and color-LED topography (anterior corneal surface and TCA), using the subjective refraction of pseudophakic eyes as a comparator. It must be noted that, although there are further sources of astigmatism in these eyes, the most important is, by far, the cornea.[251]

Several studies investigated the comparability and repeatability of different topography devices, including the Cassini, to evaluate corneal power and astigmatism.[252,253,254,255] However, no study has compared it with the Orbscan IIz (Bausch & Lomb) and the Lenstar LS900 (Haag-Streit). This was the basis for conducting a subsequent study (Chapter 5 – 5.2), where we assessed the comparability and repeatability of these topography methods.

5.1 Comparison between four measurement techniques to assess astigmatism on pseudophakic eyes

5.1.1 Objectives

The goal of this study was to assess the accuracy of corneal astigmatism evaluation measured by four techniques, using subjective refraction of pseudophakic eyes as a comparator.

5.1.2 Material and methods

Population sample

30 patients (46 eyes), with an average age of 67.3 ± 7.3 years, 16 women and 14 men, who had undergone cataract surgery with the implantation of a monofocal non-toric intraocular lens (Alcon AcrySof IQ), were assessed at least three months after surgery. All eyes showed a well centered IOL with no tilt, a stable capsular bag, no posterior capsule opacification, and no retinal or corneal pathologies. All CDVAs were ≥ 20/30. Inclusion and exclusion criteria were those recommended for cataract surgery.

Subjective assessment of astigmatism

Subjective assessment of the astigmatism magnitude and axis was performed using trial frames at a nominal vertex distance of 12 mm, and under best spherical refractive error correction. Given subjective measurements are the true clinical evaluation, these were used as the comparator against all measurements taken by the automated topographers.

Automated topographers

Topography data was obtained with Orbscan IIz, Lenstar LS900 and Cassini. Minimum, maximum and mean keratometry, and astigmatism magnitude and axis were evaluated. For the Cassini, these values were recorded for the anterior corneal surface and for TCA (anterior + posterior surfaces). The evaluated systems are detailed in Chapter 2 – 2.6.3 (Theoretical Background).

Measurements

All measurements were taken by experienced technicians. Assessed parameters were astigmatism magnitude (D), axis (°), and vectors J0 and J45 (Chapter 2 – 2.5.1 Theoretical Background).

Statistical Analysis

All measurements were compared with the subjective measurements. When comparing axis, 180° was added to or subtracted from the measured axis so measurement differences between methods were never more than 90°.[148,255,256] For example, if one measurement was 11° and the other measurement 179°, either 11° was converted to 169° (180° - 11°) or 179° was converted to 1° (180° - 179°) so that measurements would be of the same magnitude and hence comparable. For the calculation of centroids, the difference between each method of assessment and the subjective value of vectors J0 and J45 was determined. After Shapiro-Wilk tests of all variables, Spearman ρ coefficients were determined to assess correlations between parameters. The Wilcoxon test was used to compare measurements performed on the same eye. Analysis of agreement between each device and subjective was performed using Bland-Altman plots. The limits of agreement (LoA) were calculated based on the mean and SD of the difference between each device and the subjective assessment, as mean ± 1.96 SD. Linear regressions of the form y = Bx+A were performed and standard errors σ of all parameters were calculated. Regression coefficients, slopes and intercepts between the different regression models were compared. Tests were considered significant at $p < 0.05$ significance level (two-tailed). Data were processed using IBM SPSS 21 software.

5.1.3 Results

Comparison between assessment methods

Univariate analysis comparing axis, J0 and J45 as assessed by Total Cassini, Cassini, Orbscan and Lenstar with subjective assessment showed that vector J0 measured by Cassini, Orbscan and Lenstar were statistically different when compared to subjective assessment (Table 4).

Table 4: Comparison between astigmatism assessment methods.

	Subjective	Cassini	Total Cassini	Orbscan	Lenstar
Axis (º)	57.50 [0.00-180.00)]	68.50 [2.00-180.00]	108.50 [1.00-177.00]	73.00 [1.00-180.00]	66.00 [0.00-179.00]
J0 (D)	0.760 [-4.970-1.970]	0.735* [-5.800-1.690]	0.845 [-5.400-1.950]	0.215* [-5.720-1.610]	0.600* [-2.950-1.740]
J45 (D)	0.045 [-1.950-1.130]	0.150 [-1.820-2.260]	-0.080 [-1.730-2.130]	0.100 [-3.300-1.480]	0.245 [-2.670-1.780]

*D=Diopters. All groups compared with subjective. *Wilcoxon sign rank test, p<0.001 for Cassini and Orbscan, p=0.001 for Lenstar. All other comparisons were not statistically significant.*

However, when comparing differences in astigmatism value for patients in whom the difference between axis was ≤10°, no method showed differences from subjective assessment (Table 5).

Table 5: Comparison between assessment methods for patients with difference in axis ≤10°.

	Median (D)	Two-sided Wilcoxon p value	n
Subjective	1.250		
Cassini	1.090		
Difference from Subjective	0.160	0.773	23
Lenstar	1.080		
Difference from	0.170	0.429	23

Subjective			
Subjective	1.125		
Orbscan	1.000		
Difference from Subjective	0.125	0.320	16
Subjective	1.000		
Total Cassini	1.210		
Difference from Subjective	-0.210	0.135	25

All groups compared with subjective measurements.

Agreement between assessment methods and subjective assessment for J0 and J45 is further illustrated in the Bland-Altman plots (Figure 24).

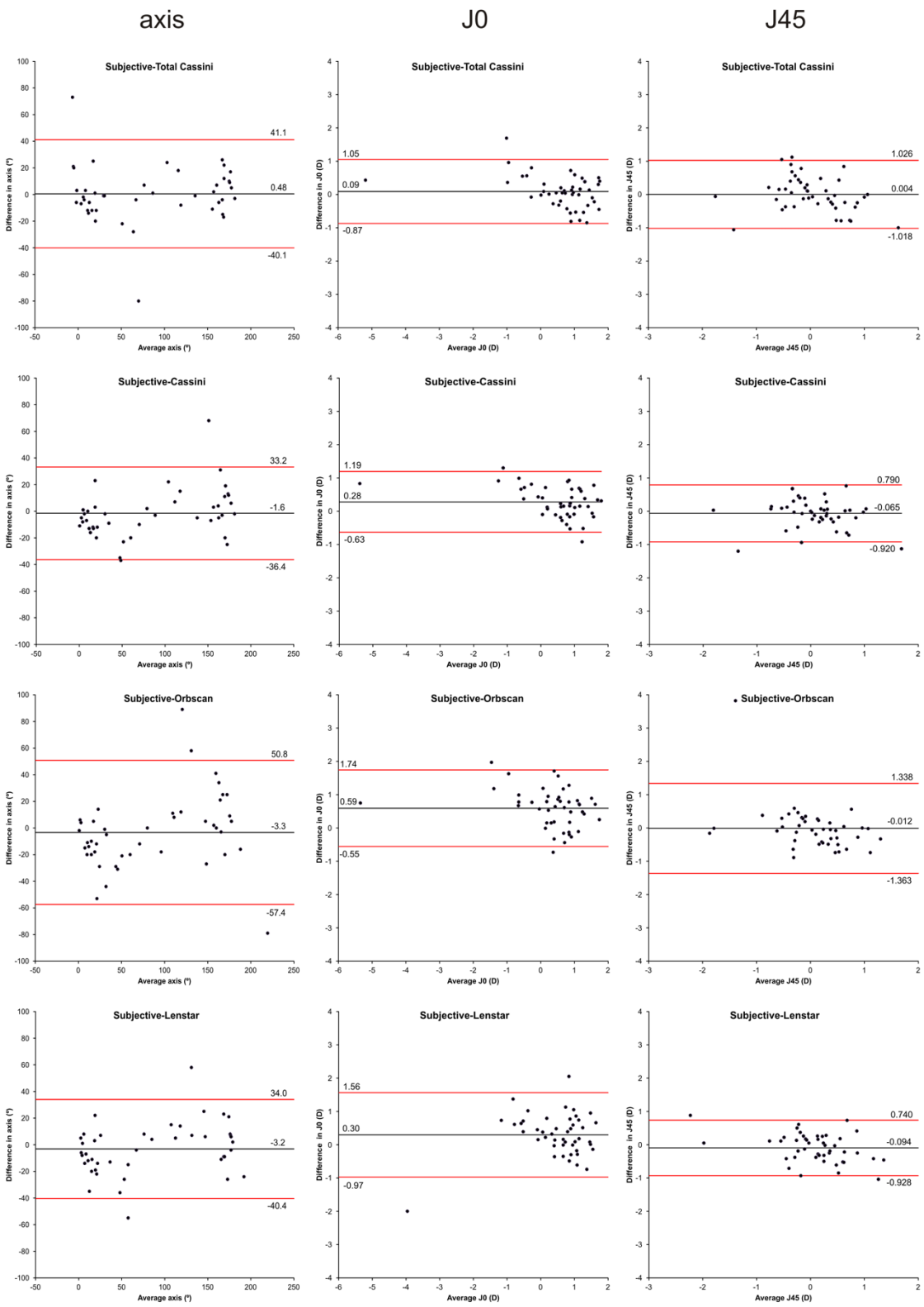

Figure 24 - Bland–Altman plots for astigmatism axis, J0 and J45. **Note:** The limits of agreement are shown by the red lines.

Linear Regression analysis

Linear regression analysis of axis considering subjective assessment as the independent variable is shown in Figure 25. Linear regression analysis of astigmatism value, for cases in which the difference between axis was ≤10°, is shown in Figure 26. For astigmatism axis models, all models showed a very high R^2 (Orbscan < Total Cassini < Lenstar < Cassini) with Total Cassini having the least difference to the unit slope (0.052) and to a null constant (3.790). However, and although the higher R^2 in the Total Cassini model points to a best fit, this comparison is observational, since there were no statistical differences between regression coefficients, slopes or intercepts between models. Regarding astigmatism value, Total Cassini model showed the highest R^2 (0.808), although the Cassini model showed the least difference to the unit slope (0.031) and the least difference to a null constant (0.034). Regression coefficients, slopes and intercepts were not statistically different between the Total Cassini and the Cassini models. However, regression coefficient was lower for the Lenstar model than for Total Cassini ($Z=2.019$, $df=41$, $p<0.05$), and the Lenstar model slope was also lower than both Total Cassini and Cassini ($t=3.323$, $df=44$, $p<0.002$ and $t=2.972$, $df=42$, $p<0.005$, respectively). Orbscan is not shown in Figure 25 because the regression was not statistically significant.

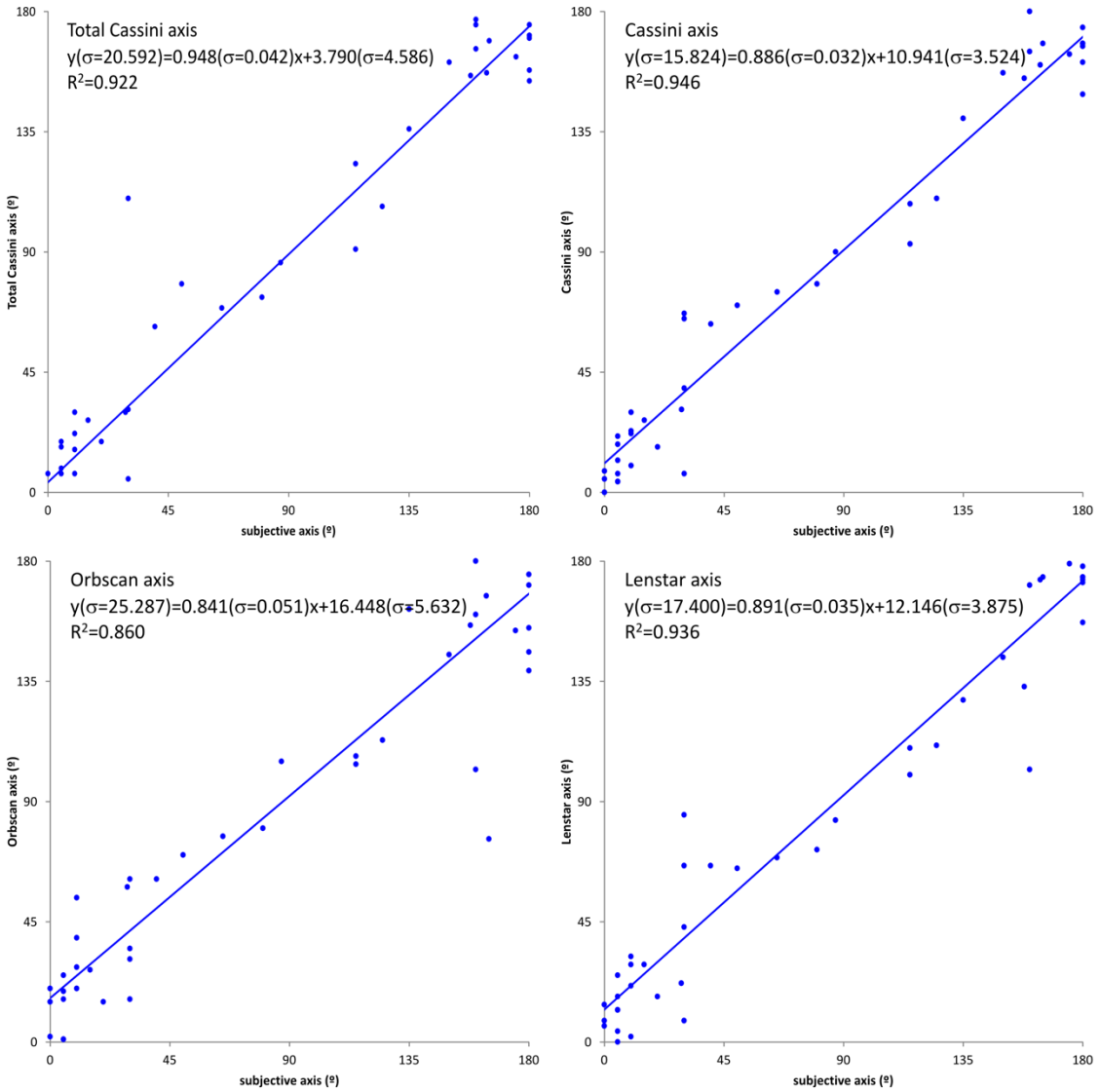

Figure 25 - Linear regression models for astigmatism axis assessment by (**A**) Total Cassini, (**B**) Cassini, (**C**) Orbscan, and (**D**) Lenstar methods. Notes: Astigmatism axis subjective assessment as independent variable. All models with *P*<0.001.

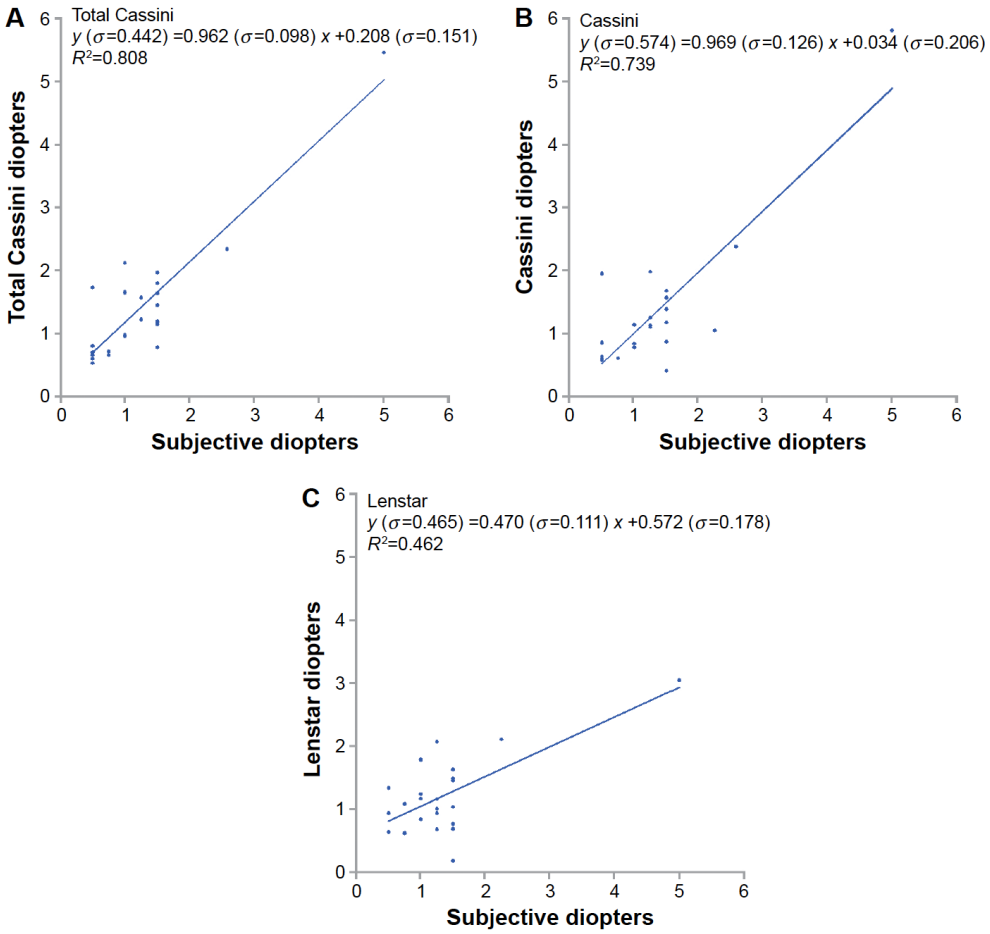

Figure 26 - Linear regression models for astigmatism value assessed by (**A**) Total Cassini (n=25), (**B**) Cassini (n=23), and (**C**) Lenstar (n=23) for patients with axis difference ≤10°. Note: Astigmatism subjective diopters was the independent variable in all models.

Centroids

Table 6 and Figure 27 A-D show the centroids according to all assessment methods. J0 vectors were better for Cassini and Total Cassini when compared to Orbscan, with no difference from Lenstar. There were no differences for J45 assessed by the four measurement techniques.

Table 6: J0 and J45 vectors assessed by Total Cassini, Cassini, Orbscan and Lenstar.

Method	J0 (mean±SD) Diopters	J45 (mean±SD) Diopters

Total Cassini	0.0907±0.490*	-0.0037±0.521
Cassini	0.2798±0.465*	-0.0652±0.436
Orbscan	0.5939±0.486*	-0.0120±0.689
Lenstar	0.2967±0.647	-0.0941±0.425

SD=standard deviation; *p=0.041 between Orbscan and Cassini; p<0.001 between Orbscan and Total Cassini. Results from ANOVA with post-hoc Sidak.

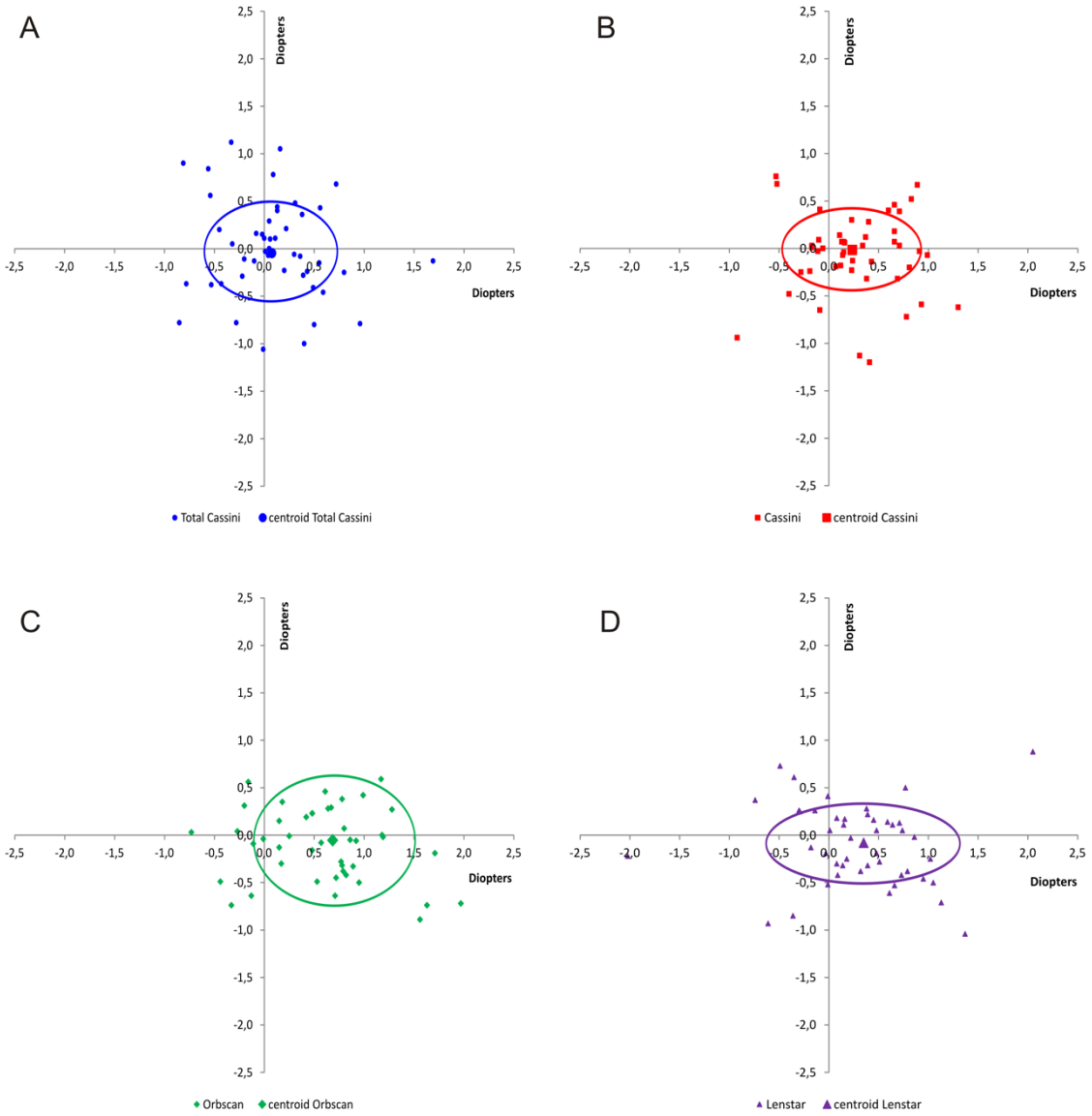

Figure 27 - Centroids of the difference between each method of assessment and the subjective value of vectors J0 and J45 for (A) Total Cassini, (B) Cassini, (C) Orbscan, and (D) Lenstar.

5.1.4 Discussion

Most of the effort regarding the correction of LOAs in cataract surgery relies on accuracy on diagnosis, stratification, and correction of astigmatism, as it is the most prevalent residual postoperative LOA. Although there is a known error associated to the subjective evaluation of astigmatism, and a poor correlation with K values,[12] this remains the standard for postoperative evaluation and the most important measure of therapeutic success.

There is an ongoing debate on which instrument is more accurate for the evaluation of anterior and posterior corneal surfaces.[257,258] Also, if measurement of the anterior corneal surface will suffice, or if the posterior corneal surface should also be directly measured to improve accuracy.[50,52] Classically, corneal power calculation is based on anterior corneal surface measurements, assuming a constant and linear relationship between anterior and posterior corneal curvatures[259] to estimate posterior corneal curvature and corneal refractive power. However, recent technologies allow direct measurement of posterior corneal curvature, giving a more precise corneal power calculation. The importance of the posterior corneal surface for toric IOL power calculation is discussed in detail in Chapter 2 – 2.3 (Theoretical Background).

As a continuing emerging field, different keratometers are available for the diagnosis and stratification of astigmatism. However, previous studies are not consistent regarding the hypothesis that no significant differences exist between keratometers, [255,257,260] and even small differences between different methods may be of concern.[261,262] Given the previous published data, no recommendation can be done regarding one specific device. However, there are several limitations associated with those comparative studies, namely their retrospective nature and the inclusion of healthy volunteers only, making it difficult to create specific recommendations based on sound evidence. Based on clinical sense and expert opinions, recommendation is that the device with which one has more experience should be preferably used.[255]

In the present study, subjective astigmatism was compared with four methods of astigmatism assessment: Orsbcan, Lenstar, Cassini and Cassini TCA. Cassini is a new method of evaluation of corneal anterior and total (anterior+posterior) astigmatism.

Although recent, several studies have demonstrated its high repeatability, both in normal corneas, [254,255,256,263] and in post-LASIK,[253,256] post-cataract,[252] post-keratoplasty and post-crosslinking corneas.[256]

Our results show that astigmatism value and axis assessment by each of the tested methods was not different from subjective assessment. Although not statistically significant, the axis difference between Total Cassini and Cassini may have implications when implanting toric IOLs, given precise IOL alignment is crucial. According to linear regression models for astigmatism axis, all models showed a high R^2. Cassini and Total Cassini presented with the highest R^2, with Total Cassini showing the least difference to the unit slope (0.052) and the least difference to a null constant (3.790). However, these comparisons are observational, given there were no statistical differences between models regarding regression coefficients, slopes or intercepts. These data suggest that measuring both the anterior and posterior corneal surfaces translates into a more accurate measurement, as this model points to a best fit regarding subjective assessment of astigmatism axis. Although not statistically significant, an observational comparison suggests that Orbscan was the method with the lowest value, which may be explained by the fact that the posterior corneal measurement accuracy of Orbscan has not been fully validated.[264,265]

Also, it has been previously reported that, after keratorefractive surgery, Orbscan produces inaccurate measurements.[266,267]

As for astigmatism value, both Cassini and Total Cassini have very high R^2 values in linear regression models. Statistically, both models were comparable, and with better prediction than Lenstar, suggesting that these are the best methods when compared to subjective assessment. The Orbscan model was not statistically significant for astigmatism value. Centroid analysis led us to conclude that J0 from Total Cassini and Cassini have the less *x* deviation from the Cartesian origin when compared with Orbscan, which shows the highest *x* deviation from the Cartesian origin. J45 values did not differ between assessment methods.

These results confirm the importance of measuring total astigmatism and not just anterior astigmatism. A future work assessing the prediction error of Cassini total

astigmatism measurements in patients with toric IOLs would be interesting and add to these results.

This study has the following limitations. The confounders and bias associated to all observational studies, and the number of patients needed to achieve a 90% power to assess differences between very similar measuring instruments with small effect differences; the fact that measurements were taken by two technicians, although very experienced and using automatic software; the inherent subjectivity of subjective refraction; and the fact that an initial version of the Cassini software was used.

5.2 Comparability and repeatability of different methods of keratometric assessment

5.2.1 Objectives

The goal of this work was to assess the comparability and repeatability of keratometric and astigmatism values measured by four techniques: slit-scanning topography, automated keratometry, and color-LED topography (anterior corneal surface and TCA), in healthy volunteers.

5.2.2 Material and methods

This was an institutional cross-sectional study that included 15 healthy volunteers (30 eyes). Three consecutive measures (10 minutes apart) were performed in each eye by the same operator, using the four techniques. Keratometric and astigmatism values were recorded. Inclusion criteria were healthy individuals aged 18-50 years with a corrected visual acuity of 0.00 logMAR or better. Exclusion criteria were a history of ocular pathology, trauma, contact lens wear, systemic or local medications, and ocular surgery. In addition, patients with anterior segment pathologies such as dry eye, Meibomian gland disease, corneal disease or abnormal topographies were excluded from this study. All participants were in the proper head positioning, and targets were positioned as instructed by the manufacturer of each device. The sequence of the measurements with the three devices was randomly chosen.

Topography data was obtained with Orbscan IIz, Lenstar LS900 and Cassini. All systems are described in Chapter 2 (Theoretical Background).

Assessed parameters were minimum (K1), maximum (K2) and mean keratometry (Km), astigmatism magnitude (D) and axis (°). For the Cassini, these values were recorded for the anterior corneal surface and for TCA (anterior+posterior surfaces). Also assessed were vectors J0 and J45 (Chapter 2 – 2.5.1 Theoretical Background).

Power vectors were conceived as a way of transforming conventional refractive error, or keratometric data, into mutually independent, orthogonal components, better suited to statistical analysis. Vector analysis permits a complete description of astigmatism characteristics[268] and allows the comparison of both orientation and power.

Statistical analysis

After Shapiro-Wilk tests of all variables, the Wilcoxon test was used to compare measurements performed on the different pairs of devices. The intraclass correlation coefficient (ICC) was used to assess comparability and repeatability. The ICC expresses the consistency of repeated measurements, ranging from 0 to 1. An ICC <0.75 indicates poor repeatability, from 0.75 to 0.89 moderate repeatability, and >0.90 high repeatability.[252]

As in study 5.1, when comparing axis, 180° was added to or subtracted from the measured axis, so measurement differences between methods were never more than 90°.[148,255] Analysis of agreement between each pair of devices was performed using Bland-Altman plots.[148,269] The 95% limits of agreement (LoA) represent the limits of the range for 95% of differences between each pair of devices. According to the Bonferroni correction, tests were considered significant at p<0.008 significance level (two-tailed). Data were processed using IBM SPSS 21 software.

5.2.3 Results

Comparability of keratometry readings

Univariate analysis comparing K1 and K2, as assessed by Total Cassini, Cassini, Orbscan and Lenstar showed that there were differences in the median values of K1 and K2

between Lenstar and Orbscan – Table 7. The ICC showed that comparability was high between all measurement techniques for K1 and K2. Agreement between assessment methods for Km is further illustrated in the Bland–Altman plots – Figure 1. The Cassini vs Lenstar agreement regarding Km showed the closest to 0 mean difference (-0.030) but the highest range of LoA (2.397). The Orbscan vs Lenstar agreement showed the highest mean difference (-0.143) and the lowest range of LoA (0.301).

Comparability of astigmatism evaluation

Univariate analysis comparing astigmatism magnitude, astigmatism axis, J0 and J45 as assessed by Total Cassini, Cassini, Orbscan and Lenstar showed that there were differences in the median values of J0 between Cassini total and Cassini, and of J45 between Cassini and Lenstar – Table 7.

Table 7: Descriptive statistics

Parameter	Cassini total	Cassini	Orbscan	Lenstar
K1 (D)		42.77 (36.93–46.06)	42.90* (36.90–45.70)	42.82* (36.86–45.76)
K2 (D)		44.31 (41.24–47.06)	44.17* (40.87–46.43)	44.06* (41.32–46.63)
Astigmatism (D)	0.88 (0.44–2.04)	0.89 (0.25–5.80)	0.80 (0.27–2.17)	0.87 (0.34–3.04)
Axis (°)	89.33 (11.33–147.50)	91.92 (10.67–167.00)	93.00 (16.00–167.00)	94.33 (12.67–163.00)
J0 (D)	0.23* (-0.92–0.72)	0.30* (-0.86–2.87)	0.33 (-0.78–2.82)	0.32 (-0.82–1.48)
J45 (D)	-0.01 (-0.76–0.36)	0.03* (-0.79–0.56)	0.04 (-0.54–1.63)	0.05* (-0.45–1.34)

*All values presented as median (maximum-minimum). D=diopters; °=degrees. *p<0.005. Orbscan showed higher values of K1 and K2 compared to Lenstar. Cassini showed a higher value of J0 compared to Cassini total and a lower value of J45 compared to Lenstar.*

The ICC used to assess comparability was high between all measurement techniques for astigmatism magnitude and astigmatism axis, with ICC>0.900, except for astigmatism magnitude measured by Cassini compared to Lenstar (ICC=0.798) and Orbscan compared to Lenstar (ICC=0.810). For J0 and J45 comparability was only high for J0 between Cassini and Orbscan (ICC=0.989), with all other comparisons showing ICC<0.900. Although all comparisons showed a p<0.001, J45 between Cassini and Orbscan and between Orbscan and Lenstar were notably low (ICC=0.522 and ICC=0.690, respectively). When comparing Cassini and Cassini total regarding both astigmatism magnitude and astigmatism axis, comparability was high (ICC=0.941 and ICC=0983, respectively, p<0.001).

Agreement between assessment methods for astigmatism magnitude and astigmatism axis is further illustrated in the Bland-Altman plots – Figure 28. The best agreement for astigmatism magnitude was between Cassini Total and Cassini, having the closest to 0 mean difference (0.014) and the lowest range of LoA (0.862). The agreement between Cassini and Lenstar showed the highest mean difference (0.201), and the Orbscan vs Lenstar the highest range of LoA (2.923). Regarding astigmatism axis, all comparisons showed a wide data spread, with the agreement between Cassini Total and Lenstar showing the closest to 0 mean difference (0.802), and the Cassini Total vs Cassini the lowest range of LoA (34.385). The agreement between Cassini Total and Cassini showed the highest mean difference (2.928), and the Cassini Total vs Orbscan the highest range of LoA (63.564).

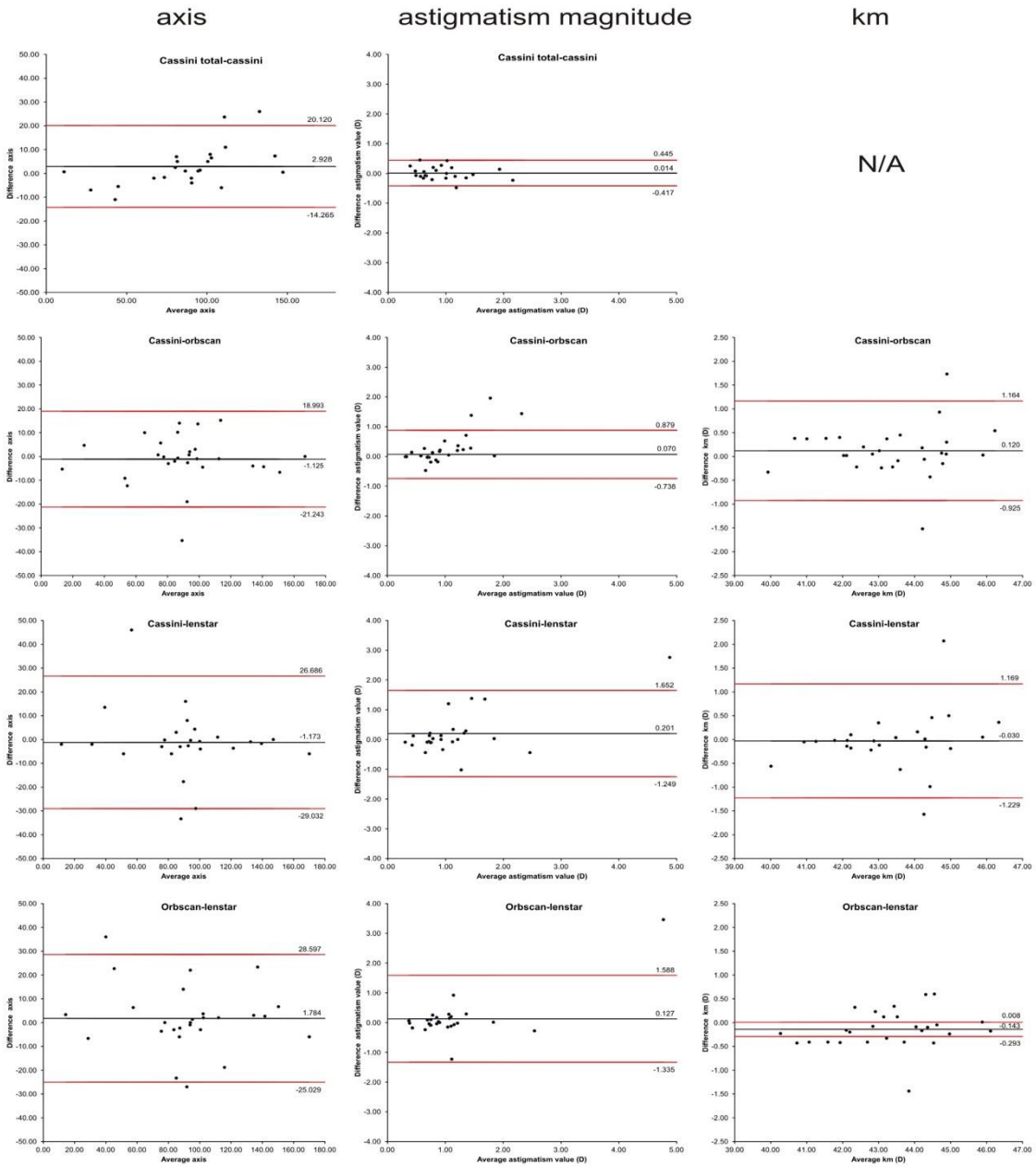

Figure 28 - Bland–Altman plots for astigmatism axis, astigmatism magnitude, and Km. The limits of agreement are shown by the red line. For astigmatism axis, the best agreement was between Total Cassini and Lenstar LS900 and the worst was between Total Cassini and Cassini. For astigmatism magnitude, the best agreement was between Total Cassini and Cassini, and the worst was between Cassini and Lenstar. Regarding Km, the best agreement was between Cassini and Lenstar, and the worst was between Orbscan IIz and Lenstar. Abbreviation: Km, mean keratometry.

Repeatability

ICC to assess repeatability showed that this was high for all measurement techniques and assessed parameters, with ICC>0.900, except for K2 and J45 measured by Cassini (ICC=0.814 and ICC=0.621, respectively) ¬ Table 8.

Table 8: Repeatability and comparability

	Intra-keratometer (ICC, 95% CI)			**Inter-keratometer (ICC, 95% CI)**		
Parameter	**Cassini**	**Orbscan**	**Lenstar**	**Cass-Orb**	**Cass-Lens**	**Orb-Lens**
K1	0.954	0.982	0.997	0.979	0.947	0.969
	0.893–0.980	0.959–0.992	0.993–0.999	0.954–0.990	0.882–0.976	0.932–0.986
K2	0.814	0.979	0.997	0.954	0.949	0.968
	0.609–0.918	0.953–0.991	0.993–0.999	0.901–0.979	0.886–0.977	0.930–0.985
Astigmatism	0.913	0.955	0.942	0.964	0.798	0.810
	0.806–0.963	0.901–0.980	0.859–0.977	0.922–0.983	0.550–0.910	0.583–0.913
Axis	0.984	0.970	0.978	0.976	0.960	0.964
	0.962–0.993	0.933–0.987	0.945–0.991	0.948–0.989	0.911–0.982	0.921–0.984
J0	0.918	0.984	0.984	0.989	0.891	0.893
	0.825–0.963	0.963–0.993	0.960–0.994	0.976–0.995	0.761–0.950	0.766–0.951
J45	0.621	0.920	0.950	0.522	0.815	0.690
	0.313–0.812	0.827–0.965	0.877–0.980	-0.018–0.776	0.593–0.915	0.320–0.859

All ICC, both intra-keratometer and inter-keratometer, have p<0.001. Repeatability was high for all measurement techniques and assessed parameters, with ICC>0.900, except for K2 and J45 measured by Cassini (ICC<0.900). Comparability was also high for most parameters (ICC>0.900), but several inter-keratometer comparisons showed ICC<0.900.

5.2.4 Discussion

Given the importance of evaluating the potential exchangeability of corneal power and astigmatism measurements,[252] we assessed the comparability and repeatability of keratometric and astigmatism values measured by four techniques – Orbscan IIz, Lenstar LS900, Cassini, and Total Cassini (anterior+posterior surfaces) – in 30 eyes of 15 healthy volunteers.

Comparability

The results reported in the literature concerning comparability between devices are not in agreement. Ventura et al found no differences in mean values of corneal power when comparing Cassini with Lenstar, but reported a significant difference in corneal power between Cassini and a Placido-based topographer.[252] However, Klijn et al reported differences in corneal power between Cassini and Lenstar and Cassini and a Placido-based topographer, although the authors considered the differences to be of negligible clinical relevance.[254] In addition, a comparison between Cassini and a Placido-based corneal topographer showed no differences in corneal power,[253] although another study comparing Cassini and a Placido-based corneal topographer showed differences in both K1 and K2.[255] We found no differences in the median values of K1 and K2 between Cassini and Orbscan or Lenstar, although the median values of K1 and K2 between Lenstar and Orbscan were different. Comparability was high between all assessment methods, with ICC>0.900.

Agreement analysis showed that the Cassini vs Lenstar agreement regarding Km showed the closest to 0 mean difference, but it also showed the highest range of LoA (2.4), which is clinically relevant, while Orbscan vs Lenstar agreement showed the highest mean difference and the lowest range of LoA. Similar or higher ranges of LoA have been reported for Cassini-Placido and Cassini-Lenstar for corneal power, leading the authors to discourage the interchangeable use of these devices.[252,253,255]

We also evaluated the median values of astigmatism magnitude and axis between Cassini and Orbscan or Lenstar and they showed no differences. Comparability was also high regarding astigmatism magnitude and astigmatism axis for all paired devices,

except for astigmatism magnitude measured by Cassini compared to Lenstar (ICC=0.798) and Lenstar compared to Orbscan (ICC=0.810). Once again, results reported in literature are different. Ventura et al found no differences in mean values of astigmatism magnitude when comparing Cassini with Lenstar,[252] in contrast with two studies comparing Cassini and two different Placido-based corneal topographers, both showing differences in astigmatism magnitude.[253,255] Our results are further supported by agreement analysis, which showed that, for astigmatism magnitude, the agreement between Cassini and Lenstar had the highest mean difference, with the agreement between Orbscan and Lenstar showing the highest range of LoA. Similar or higher ranges of LoA have been reported for Cassini-Placido and Cassini-Lenstar for astigmatism magnitudes.[252,253,255] Regarding astigmatism axis, comparisons showed a wide data spread.

As for J0 and J45, our results showed differences of J45 between Cassini and Lenstar, with Lenstar showing higher values. There were also differences in the median values of J0 and J45 between Total Cassini and Cassini. However, Ventura et al. found no differences in the mean values of J45 when comparing Cassini with Lenstar.[252] As for comparability, it was only high for J0 between Cassini and Orbscan (ICC=0.989), with all other comparisons showing an ICC<0.900. Although all comparisons showed a p<0.001, J45 between Cassini and Orbscan and between Lenstar and Orbscan were notably low (ICC=0.522 and ICC=0.690, respectively).

These different results may be accounted for due to the different population samples, different operators, and different Placido-based devices. Given there is no gold standard device for these measurements, no conclusions can be drawn regarding which device is the most accurate. Agreement analysis showed a wide data spread, suggesting that these devices should not be used interchangeably, despite the high ICC values.

Repeatability

Repeatability was high for all measurement techniques and assessed parameters, with ICC>0.900, except for K2 and J45 measured by Cassini. Two studies assessing Cassini repeatability concluded that Cassini has enhanced precision, further improving astigmatism magnitude, astigmatism axis repeatability[256] and keratometry, even in

LASIK-treated, keratoconic, and crosslinked corneas.[263] Other studies have shown different results. One study concluded that, although Cassini provided highly repeatable measurements, it had worse repeatability than Lenstar in all parameters, with Lenstar showing the best repeatability of all studied devices.[252] However, another study reported a relatively low repeatability of corneal power measurements with Cassini, but a higher repeatability of cylinder measurements compared both to Lenstar and a Placido-based topographer.[254] In contrast, Hidalgo et al showed a good repeatability for Cassini and a Placido-based device for both keratometry and astigmatism.[255]

A comparison between Lenstar and two Placido-based topographers showed that Lenstar and one of the Placido-based topographers showed a reasonable repeatability for corneal power, J0, and J45, while the other Placido-based topographer showed poor repeatability for J45.[158] This same study showed that one of the corneal Placido-based topographers had statistically higher repeatability for corneal astigmatism and Lenstar had lower repeatability[158], but another study concluded that Lenstar showed acceptable repeatability.[270] Other authors have reported a very high repeatability for Placido-based topographers, with ICC>0.990 for K1, K2[176,271] and Km.[271] Analysis of our results shows that the best repeatability for K1 and K2 was achieved by Lenstar, and the worst for K2 and J45 measured by Cassini. All other 95% CI show overlap.

In conclusion, the best repeatability for K1 and K2 was achieved by Lenstar.

5.3 Summary of conclusions of the two studies evaluating color-LED topography

In conclusion, our first study (5.1) showed that measurements of the anterior corneal surface and TCA by color-LED topography (Cassini) have no statistically significant differences when compared to subjective cylinder in pseudophakic patients. Together with automated keratometry (Lenstar), they have the highest R^2 values on linear regression models with subjective assessment as the independent variable. However, measurements of TCA by the Cassini showed better performance than the Lenstar, for both astigmatism axis and magnitude, as well as better J0 when compared to Orbscan

and the least centroid deviation from the Cartesian origin. On the other hand, Orbscan had the lowest performance in astigmatism evaluation.

Our study in healthy volunteers (5.2) showed the same topography devices have high comparability regarding K1, K2 and astigmatism axis. However, the wide data spread suggests that these devices should not be used interchangeably.

In summary, total corneal measurement with the color-LED topographer seems to be a better technique for astigmatism assessment and is not interchangeable with the other studied devices.

Chapter 6: Overcoming the current limitations on toric intraocular lens calculation

This chapter is based on the papers:

- "Comparação do erro de predição do astigmatismo residual entre dois calculadores de uma lente intraocular tórica", published by Ferreira et al. in Oftalmologia 2017;41(4):55-62;
- "Comparison of the astigmatic prediction errors associated with new calculation methods for toric intraocular lenses", published by Ferreira et al. in J Cataract Refract Surg 2017; 43:340-347. This paper was followed by a letter from Dr. M. Goggin and our reply in:
    - Goggin M. Back calculation of prediction error compared with controlled trial prediction error of Goggin nomogram for toric intraocular lens cylinders. J Cataract Refract Surg. 2017 Jun;43(6):863-864, and;
- "Comparison of Methodologies Using Estimated or Measured Values of Total Corneal Astigmatism for Toric Intraocular Lens Power Calculation" published by Ferreira et al. in J Refract Surg. 2017;33(12):794-800.

The introductory publication to this Chapter (Oftalmologia 2017;41(4):55-62) presented preliminary data comparing two toric IOL calculators (Original vs. New Alcon toric calculator). It clearly showed the advantage of considering the ELP, the SE IOL power and posterior corneal surface power in toric IOL calculation. This paper created the base for conducting the subsequent studies.

Introduction

With the identification of the importance of considering the posterior corneal surface in toric IOL power calculation in order to avoid under- or overcorrections of astigmatism, several technologies capable of evaluating both corneal surfaces and thus directly calculate the total corneal power emerged. These include tomographers based on the Scheimpflug principle or color-LED technology (studied in the previous chapter), among others. These systems are detailed in Chapter 2 – 2.6.3 (Theoretical Background).

As an alternative strategy to the direct measurement of the posterior corneal surface, it is possible to estimate its power with newly developed nomograms, regression formulas, or mathematical models. These estimation models are described in Chapter 2 – 2.7 (Theoretical Background).

In our initial study on toric IOL calculators (Oftalmologia 2017;41(4):55-62), we compared the original, and still available online, with the recently updated Alcon calculator, incorporating the Barrett toric algorithm. This study clearly demonstrated the advantage of the latter, showing a reduction in the mean prediction error in residual astigmatism of about 50%.[272] However, given the multitude of new toric calculators and the absence of studies comparing their results, we saw the necessity to determine the optimal method(s). The new calculation methods for toric IOLs are listed in Table 9.

We compared the prediction error in residual astigmatism of each of the listed methods with that of the original Alcon calculator (J Cataract Refract Surg 2017; 43:340-347) – Chapter 6 – 6.1.

Table 9 - Toric IOL calculation methods compared in the study.

Characteristics	Calculator
Nomograms considering posterior corneal surface when it is not directly measured	Baylor nomogram Abulafia-Koch formula Goggin's coefficient of adjustment
Takes into account predicted ELP	Holladay toric calculator
Considers both ELP and a mathematical model for posterior corneal surface	Barrett toric calculator Alcon new calculator
Ray tracing calculation (real posterior corneal surface measurements)	Ray tracing software

ELP=effective lens position

We were somewhat surprised to find that direct measurements of total corneal astigmatism with a Scheimpflug camera had worse results than theoretical models estimating it, so we designed a study (J Refract Surg. 2017;33(12):794-800; Chapter 6 – 6.2) specifically to compare the calculators that showed the best results in the previous study (6.1) with direct measurements of total corneal power. In this follow-up study, we used the Barrett Toric Calculator and the Abulafia-Koch formula as calculation methods that estimate the power of the posterior corneal surface and a Scheimpflug camera for the direct measurements. Toric IOL cylindrical power calculation was performed through ray tracing and vectorial calculation of total corneal astigmatism (previously shown to be the most precise calculation method for toric IOLs when using a Scheimpflug camera).[273]

6.1 Comparison of astigmatic prediction error of new calculation methods for toric intraocular lenses

6.1.1 Objectives

The purpose of this study was to compare the new calculation methods for toric IOLs (listed in Table 9) with refractive results from the original Alcon calculator. To our knowledge, this is the first study to compare all available methods, including the latest nomograms, the new Alcon calculator, and ray tracing.

6.1.2 Material and methods

Patient Population

This retrospective case series was performed at Luz Hospital, Lisbon, Portugal.

Medical records were reviewed to identify patients who had cataract surgery with the implantation of a monofocal toric IOL (Acrysof IQ Toric SN6AT3-T9, Alcon Laboratories, Inc.) between January 2014 and January 2016. Patients with senile cataract who had regular corneal astigmatism between 1.0 D and 4.5 D and preoperative examinations with good quality were selected. Cases with other ocular pathologies, such as pseudoexfoliation, glaucoma, traumatic cataract, or other comorbidities, that could affect capsular bag stability or adequate manifest refraction evaluation were excluded, as were patients with systemic disease that might influence visual acuity or intraoperative or postoperative complications.

Preoperative Assessment

All patients had full preoperative ophthalmologic examinations, including UDVA and CDVA using logMAR acuity charts at 4 m under photopic conditions (85 candelas/m^2), manifest refraction using the cross-cylinder method, slit-lamp biomicroscopy, Goldmann applanation tonometry, and fundoscopy under mydriasis. Corneal astigmatism and curvature were evaluated using the automated keratometry feature of the Lenstar LS 900. As recommended by the manufacturer, five scans were performed in each case. The Lenstar LS 900 methodology for evaluating corneal astigmatism is described in Chapter 2 – 2.6.3 (Theoretical background). Corneal Scheimpflug

tomography (Pentacam HR) was performed in all cases to confirm the regularity of the astigmatism.

The IOL spherical equivalent power was calculated using the Hoffer Q formula[274] if the AL was less than 22.0 mm or with the SRK/T[275] if the AL was 22.0 mm or longer. The A-constant was 119.2. The refractive goal was emmetropia. The IOL cylindrical power was calculated using the manufacturer's online calculator[276] and automated keratometry (OLCR device).

Surgical Technique

With the patient seated to prevent cyclotorsion, the previously calculated implantation axis was marked using a Neuhann-Nuijts one step bubble marker. Two experienced surgeons (T.B.F., F.J.R.) performed all surgeries under topical anesthesia and a microcoaxial phacoemulsification technique with a temporal 2.4 mm clear cornea incision. After IOL implantation and complete aspiration of the OVD, the IOL was rotated to its final position by aligning the corneal marks with the reference marks in the IOL.

Postoperative Assessment

At the 3-month visit, refraction was evaluated by the same cross-cylinder method and OLCR keratometry and Scheimpflug tomography were repeated. Scheimpflug tomography was used to evaluate the curvature of the posterior corneal surface. These values were used for calculations performed with the ray tracing software.

The toric IOL alignment axis was recorded via a slit-lamp procedure incorporating digital photography after pupillary mydriasis, in accordance with a previously published method.[277] Eyes with IOL misalignment of more than 5 degrees were excluded from the final analysis, as were eyes with any visible IOL tilt or decentration.

Postoperative Calculations

Postoperatively, the preoperative calculation performed via the manufacturer's website was repeated for each case with and without Baylor nomogram adjustment, the Abulafia-Koch formula, and the Goggin coefficient. Calculations were also performed for each case using the Holladay IOL consultant calculator with and without the same

nomograms, the Barrett online calculator, the new Alcon calculator, and ray tracing software (PhacoOptics, IOL Innovations ApS) (Table 9). The postoperative K measurements, posterior corneal surface curvature, and measured IOL alignment axis were used for these calculations to distinguish the effects of SIA or IOL misalignment from the errors induced by each calculator.

The prediction error for each method was calculated as the difference between the postoperative manifest refraction corrected for the corneal plane and the predicted residual astigmatism. All calculations were performed in accordance with the method described by Holladay et al.[112] The manifest refraction was converted in a cross-cylinder format. Each cylinder was transformed for the corneal plane according to the following formula:

REFc = REFv/[1 - (REFv x V/1000)]

where REFc is the refraction at the corneal plane, REFv is the refraction at the vertex plane, and V is the vertex distance in millimeters.

The toric IOL cylinder power at the corneal plane was calculated as a fixed ratio for the original Alcon calculator. For the Holladay IOL consultant calculator, cylinder power was calculated using meridional analysis.[172] For the Barrett toric calculator and the ray tracing software, the value indicated in the calculation result was used.

Last, predicted residual astigmatism was calculated as follows: Predicted residual astigmatism = Calculated toric IOL cylindrical power (corneal plane) + Corneal astigmatism (derived from measured keratometry, with or without nomogram/coefficient adjustment). The error in predicted residual astigmatism was calculated as follows: Predicted error = Postoperative refraction (corneal plane) − Predicted residual astigmatism (corneal plane).

Vector analysis was used in all calculations.[112] The mean absolute error (MAE) and centroid error in predicted residual astigmatism were calculated.

Eyes were further divided into 3 groups: a with-the-rule (WTR) group if the keratometric steep meridian was oriented between 60 degrees and 120 degrees, an against-the-rule (ATR) group if the steep meridian was oriented between 0 degrees and 30 degrees or

150 degrees and 180 degrees, and an oblique group if the steep meridian was between 31 degrees and 59 degrees or 121 and 149 degrees.

Statistical Analysis

The sample size required to detect a prediction error in astigmatism of more than 0.125 D with a SD of 0.38 D (value obtained from primary calculator data) was determined using a power sample calculation incorporating a significance level of 5% and a power of 80%. According to this calculation, 73 eyes were required.

Excel software was used for major calculations (Office 2010, Microsoft Corp.). Statistical analyses were performed in accordance with ICH statistical principles for clinical trials E9 guidelines, using SPSS for Mac software (version 21.0, International Business Machines Corp.). The normality of the distribution of all data-sets was checked using the Kolmogorov-Smirnov test. Where parametric analysis was justified, a paired samples Student *t* was used for comparisons. Where parametric analysis was not justified, differences were evaluated using a nonparametric Wilcoxon rank-sum test. For multiple comparisons, Bonferroni correction was applied. Centroid SDs were calculated in accordance with the method described by Holladay et al.[111] Results are expressed as mean ± SD; a P value lesse than 0.05 was considered statistically significant.

6.1.3 Results

Patient Demographics

The analysis included 86 eyes of 86 patients. Table 10 shows the patients' demographics and the IOLs that were implanted. Of the eyes evaluated, 41 (47.6%) had WTR astigmatism, 36 (41.9%) had ATR astigmatism, and 9 (10.5%) had oblique astigmatism. Because of the low number of eyes in the oblique astigmatism group, only the eyes with WTR and ATR were included in subgroup analysis.

Table 10 – Patient demographics and clinical information.

Parameter		Mean ± SD (range)
Eyes (*n*)		86
Patients (*n*)		86
Age (y)		71 ± 10 (43, 90)
Male sex, *n* (%)		22 (25.6)
Right eyes, *n* (%)		56 (53.5)
Axial length (mm)		23.92 ± 1.79 (20.11, 29.14)
Corneal astigmatism (D)		2.16 ± 0.89 (1.00, 4.50)
IOL SE power (D)		20.28 ± 4.78 (8.00, 33.00)
IOL cylinder power (D)		2.85 ± 1.23 (1.00, 6.00)
Implanted IOL	SN6AT3	22 (25.6)
	SN6AT4	20 (23.2)
	SN6AT5	18 (20.9)
	SN6AT6	14 (16.3)
	SN6AT7	4 (4.6)
	SN6AT8	4 (4.6)
	SN6AT9	5 (5.8)

SE = spherical equivalent, IOL = intraocular lens

Absolute and Centroid Errors in Predicted Residual Astigmatism

Table 11 shows the MAE in predicted residual astigmatism for each calculator.

Table 11 - Mean absolute error in predicted residual astigmatism.

Calculator/Nomogram	Mean ± SD (range) Diopters	*p* value‡
Original Alcon calculator	0.64 ± 0.38 (0.02, 1.49)	-
Original Alcon calculator + Baylor nomogram	0.59 ± 0.36 (0.08, 1.47)	.233^
Original Alcon calculator + Abulafia-Koch formula	0.57 ± 0.34 (0.00, 1.23)	.010^
Original Alcon calculator + Goggin nomogram	0.65 ± 0.38 (0.08, 1.47)	.264^
Holladay toric calculator	0.61 ± 0.36 (0.01, 1.68)	.184^
Holladay calculator + Baylor nomogram	0.53 ± 0.33 (0.01, 1.42)	.001^
Holladay calculator + Abulafia-Koch formula	0.53 ± 0.26 (0.00, 1.07)	.010^
Holladay calculator + Goggin nomogram	0.63 ± 0.36 (0.01, 1.68)	.744^
Barrett calculator	0.30 ± 0.27 (0.00, 1.20)	<.001*
New Alcon calculator	0.33 ± 0.25 (0.00, 1.20)	<.001*
Ray tracing software	0.57 ± 0.35 (0.00, 1.65)	.053^

*‡Comparison with original Alcon calculator, ^Student t-test, *Wilcoxon rank-sum test*

The MAE for the Alcon original calculator was 0.64 D. When methods involving nomograms were used, this error decreased to 0.59 D (p = .233) for the Baylor

nomogram, 0.57 D for the Abulafia-Koch formula (p = .010) and remained stable (p = .264) with the Goggin coefficient. The MAE associated with the Holladay toric IOL calculator did not differ statistically significantly from that associated with the original Alcon calculator (p = .184). Applying the Baylor nomogram significantly reduced the MAE (p = .011 compared with the Holladay calculator alone). The Abulafia-Koch formula reduced the MAE to a similar value (p = .025), whereas the Goggin coefficient did not reduce the MAE (p = .083). The differences between the Holladay toric calculator and the original Alcon calculator were statistically significant only when the Baylor nomogram or Abulafia-Koch formula was applied (p = .001 and p = .013, respectively). In this case, the Abulafia-Koch formula and the Baylor nomogram showed similar results (p = .840).

The Barrett toric calculator yielded the lowest MAE. This calculator yielded significantly reduced error compared with the original Alcon calculator, the Holladay calculator, and all the nomogram methods (all p < .001). The new Alcon calculator yielded similar results, with a MAE that differed minimally from that of the Barrett calculator (p =.457). With the ray tracing software, the MAE was lower than that of the original Alcon calculator but significantly higher than that of the Barrett calculator and the new Alcon calculator (p < .001).

Table 12 shows the centroid errors in predicted residual astigmatism.

Table 12 - Centroid error in predicted residual astigmatism.

Calculator/Nomogram	Centroid (D @ angle) ± SD	*p* value *x* component‡	*p* value *y* component‡
Original Alcon calculator	0.43 ± 0.42 @ 170	-	-
Original Alcon calculator + Baylor nomogram	0.35 ± 0.54 @ 169	.155^	.692^
Original Alcon calculator r + Abulafia-Koch formula	0.34 ± 0.42 @ 170	.001^	.550^
Original Alcon calculator + Goggin nomogram	0.42 ± 0.56 @ 166	.906^	.077^
Holladay toric calculator	0.40 ± 0.40 @ 168	.346^	.534^
Holladay calculator + Baylor nomogram	0.35 ± 0.38 @ 169	.038*	.988^
Holladay calculator + Abulafia-Koch formula	0.25 ± 0.41 @ 158	.006^	.116^
Holladay calculator + Goggin nomogram	0.38 ± 0.39 @ 170	.744^	.940^
Barrett calculator	0.17 ± 0.33 @ 165	<.001^	.001^
New Alcon calculator	0.19 ± 0.32 @ 164	<.001^	.001^
Ray tracing software	0.32 ± 0.54 @ 171	<.001^	<.001^

*‡Comparison with original Alcon calculator, ^Student's t-test, *Wilcoxon rank-sum test*

The original Alcon calculator yielded an ATR centroid error that was reduced by the application of the Baylor nomogram (p =.155 and .692 for *x* and *y* components, respectively) and the Abulafia-Koch formula (p =.001 and .550 for *x* and *y*, respectively); however, the error was not reduced but not by using the Goggin coefficient (p = .906 and .077 for *x* and *y*, respectively). For the Holladay toric calculator, the application of the Abulafia-Koch formula resulted in the lowest centroid error of all the nomograms.

The Barrett toric IOL calculator yielded the lowest ATR centroid error of all calculators and differed statistically significantly from the original Alcon calculator ($p < .001$ and .001 for *x* and *y*, respectively). The combination of the Holladay calculator and the Abulafia-Koch formula yielded a similar performance to the Barrett calculator ($p = .388$ and .601 for *x* and *y*, respectively). The new Alcon calculator yielded an error in predicted residual astigmatism similar to that of the Barrett calculator ($p = .842$ and .942 for *x* and *y*, respectively). Ray tracing software yielded a higher prediction error and SD than the Barrett calculator or the new Alcon calculator, although in both cases the differences did not reach statistical significance in the *x* component for the Barrett calculator ($p = .566$ and .022 for *x* and *y*, respectively) or for the new Alcon calculator ($p = .587$ and .020 for *x* and *y*, respectively).

Figure 29 shows double-angle plots of the centroid prediction errors for all calculation methods.

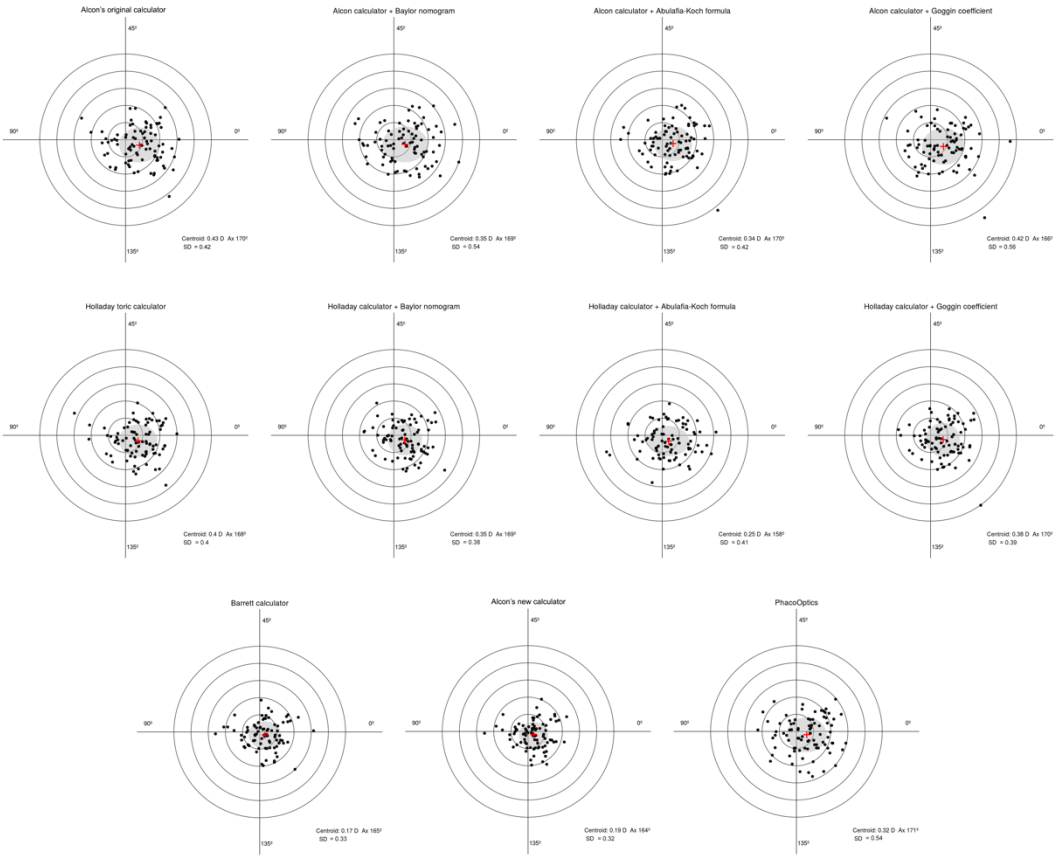

Figure 29 - Double-angle plots showing the centroid prediction errors in residual astigmatism for each calculation method.

Table 13 shows the subgroup analysis results for the MAE and centroid residual astigmatism prediction errors.

Table 13 - Mean absolute and centroid errors in predicted residual astigmatism in eyes with WTR and ATR corneal astigmatism.

Calculator/Nomogram	Eyes with WTR corneal astigmatism (*n* = 41)		Eyes with ATR corneal astigmatism (*n* = 36)	
	Mean (D) ± SD (range)	Centroid (D @ angle) ± SD	Mean (D) ± SD (range)	Centroid (D @ angle) ± SD
Original Alcon calculator	0.77 ± 0.42 (0.02, 1.49)	0.59 ± 0.56 @ 169	0.49 ± 0.26 (0.07, 0.98)	0.39 ± 0.37 @ 172
Original Alcon calculator + Baylor nomogram	0.69 ± 0.41 (0.00, 1.55)	0.44 ± 0.58 @ 169	0.48 ± 0.29 (0.00, 1.07)	0.26 ± 0.48 @ 170
Original Alcon calculator + Abulafia-Koch formula	0.63 ± 0.33 (0.00, 1.23)	0.45 ± 0.48 @ 170	0.50 ± 0.33 (0.06, 1.21)	0.18 ± 0.39 @ 168
Original Alcon calculator + Goggin nomogram	0.75 ± 0.34 (0.09, 1.47)	0.58 ± 0.55 @ 170	0.55 ± 0.31 (0.08, 1.37)	0.22 ± 0.43 @ 167

Holladay toric calculator	0.66 ± 0.37 (0.01, 1.67)	0.44 ± 0.48 @ 163	0.51 ± 0.35 (0.01, 1.14)	0.37 ± 0.40 @ 172
Holladay calculator + Baylor nomogram	0.59 ± 0.34 (0.01, 1.42)	0.41 ± 0.41 @ 167	0.47 ± 0.30 (0.01, 0.98)	0.27 ± 0.36 @ 169
Holladay calculator + Abulafia-Koch formula	0.54 ± 0.25 (0.00, 1.06)	0.30 ± 0.49 @ 156	0.51 ± 0.25 (0.00, 1.07)	0.26 ± 0.38 @ 161
Holladay calculator + Goggin nomogram	0.70 ± 0.38 (0.06, 1.67)	0.48 ± 0.47 @ 166	0.55 ± 0.34 (0.01, 1.17)	0.34 ± 0.40 @ 171
Barrett calculator	0.28 ± 0.28 (0.00, 0.88)	0.21 ± 0.35 @ 164	0.27 ± 0.25 (0.00, 1.20)	0.12 ± 0.34 @ 167
New Alcon calculator	0.33 ± 0.24 (0.00, 0.84)	0.24 ± 0.37 @ 163	0.32 ± 0.25 (0.00, 1.20)	0.16 ± 0.32 @ 168
Ray tracing software	0.60 ± 0.36 (0.01, 1.59)	0.30 ± 0.58 @ 157	0.53 ± 0.42 (0.04, 1.59)	0.41 ± 0.41 @ 178

With-the-Rule Eyes

In WTR eyes, the Barrett calculator yielded the best results and the new Alcon calculator yielded very similar results. Of the other calculators, the lowest MAE and centroid prediction error were yielded by the Holladay calculator with the Abulafia-Koch formula. Although the centroid error was comparable with that of the Barrett calculator (p = .972 and .057 for *x* and *y* respectively), the SD was higher. Application of the Baylor nomogram to the Alcon and Holladay calculators also reduced MAE and centroid prediction errors, although not statistically significantly (all p > .05). The ray tracing software significantly reduced the prediction error of MAE and centroid compared with the original Alcon calculator (*p* = .004 and < .001 for *x* and *y*, respectively), although it performed worse than the Barrett calculator, the new Alcon calculator, and the Holladay calculator with thee Abulafia-Koch formula.

Against-the-rule Eyes

In eyes with ATR corneal astigmatism, all calculators gave lower MAEs and centroid residual astigmatism prediction errors than in eyes with WTR astigmatism, with the exception of the ray tracing software, for which the centroid error was higher. As in WTR eyes, the Barrett calculator yielded the lowest MAE and centroid errors followed by the new Alcon calculator. In these eyes, the application of the Baylor nomogram, the Abulafia-Koch formula, or the Goggin coefficient did not reduce the MAE for the original Alcon calculator (*p* = .345, p = .789, and *p* = .874 respectively), or for the the Holladay calculator (*p* = .085, *p* = .145, and *p* = .954, respectively). However, they did reduce the centroid prediction errors with the Alcon and Holladay calculators in all cases, reaching statistical significance for the vector *x* component with the three nomograms combined with the Holladay calculator with the Baylor nomogram (*p* = .001) with the Abulafia-Koch formula (*p* = .009) and with the Goggin coefficient (*p* = .001), as well as for the vector *y* component with the Baylor nomogram combined with the Alcon calculator (p = .005).

The Holladay calculator alone resulted in a MAE and centroid prediction error similar to that of the Alcon calculator alone (MAE *p* = .164, centroid *p* = .008; *x* and *y p* = .906). The ray tracing software yielded the highest centroid error in these eyes. With regard to the MAE and centroid prediction error, there were no significant differences between the

original Alcon calculator and the ray tracing software (MAE p = .245; x and y and p = .432 and p = .345, respectively).

6.1.4 Discussion

Recent studies support considering the predicted ELP, spherical power of the IOL, and posterior corneal surface to achieve precise results when implanting toric IOLs. The inclusion of the posterior corneal surface in the calculation of these IOLs is now considered relevant, because ignoring it results in overcorrection in eyes with WTR astigmatism and undercorrection in eyes with ATR astigmatism.[52] The current study compared the accuracy of the different calculation methods available to overcome these limitations. We compared the MAE in predicted residual astigmatism for each calculation method and the centroid error in residual astigmatism, which also considers the axis and is thus a more precise outcome measure for analyzing astigmatism.[112]

With regard to nomograms and adjustment models, we compared the Baylor nomogram, the Abulafia-Koch formula, and the Goggin coefficient of adjustment. When applied to the original Alcon calculator, the Baylor nomogram and the Abulafia-Koch formula improved the accuracy of toric IOL calculation, the centroid error in predicted astigmatism (from 0.43 D to 0.35 D and 0.34 D, respectively) and the MAE, although in both cases only the application of the Abulafia-Koch formula reached statistical significance. When the Baylor nomogram and the Abulafia-Koch formula were combined with the Holladay calculator, the results also improved significantly (reductions in centroid prediction error from 0.40 D to 0.35 D and 0.25 D, respectively). The Goggin coefficient of adjustment did not yield better results than the original Alcon calculator or the Holladay toric calculator for centroid prediction error, except in eyes with ATR corneal astigmatism, in which it improved centroid prediction errors with both calculators. The Abulafia-Koch formula calculates corneal astigmatism as a vector, unlike the Baylor and Goggin nomograms, and addresses changes in the magnitude and the axis, which might explain why it yielded better results.[177] The Goggin coefficient results might have been limited by its application only to eyes requiring 2.0 D or less of cylinder power (which in our series represented only 48.8% of the eyes) or the lower number of eyes in our series with ATR corneal astigmatism, in which it seems to perform better.

Several new calculators have recently been developed to incorporate variable ratios for calculating the cylindrical power of toric IOLs and/or total corneal astigmatism. These include the Holladay IOL consultant calculator, which adjusts the cylinder ratio according to the Holladay 2 formula, and the Barrett toric calculator which considers the ELP and the IOL SE power as well as adjusts the cylindrical power and the axis of alignment according to a mathematical model for the posterior corneal surface.[179,278]

The Holladay toric IOL calculator MAE and centroid error were similar to those of the original Alcon calculator, with both calculators suggesting IOL cylindrical powers resulting in residual ATR astigmatism. This result is concordant with a previous study by Abulafia et al.[11]

The Barrett calculator performed best overall and in WTR eyes and ATR eyes. The mean absolute errors in predicted residual astigmatism were lower for the Barrett calculator in all cases. This calculator significantly reduced the MAE compared with the original Alcon calculator, the Holladay calculator, and all the nomogram methods (all $p < .001$). The Barrett toric IOL calculator also resulted in the lowest ATR centroid error of all calculators (0.17 D). This result was not significantly different from that yielded by the Holladay calculator with the Abulafia-Koch formula, which, excluding the new Alcon calculator, showed the second lowest centroid prediction error (0.25 D). These results are similar to those published by Abulafia et al.,[177] in which their formula reduced errors to a level similar to that of the Barrett toric calculator without adjustments.

The new Alcon calculator overcomes some of the shortcomings of its previous calculator and incorporates the Barrett toric calculator.[276] In our study, this new calculator yielded results comparable to those of the Barrett toric calculator, overall and in WTR eyes and ATR eyes.

The results in the current study confirm those in previous studies, suggesting that consideration of total corneal power might be the most important factor in improving results with toric IOLs.[171,273]

Even when considering this factor, all calculators resulted in overcorrection of WTR astigmatism and undercorrection of ATR astigmatism. The Holladay calculator results

might have been limited by the mean AL in the eyes in our series, because it incorporates only the ELP and IOL spherical power in the calculation and not posterior corneal surface, which might be more important in eyes with unusual ELP or IOL power.[170,173]

A different strategy for overcoming problems related to simplifications (eg, conversion of effective power in different planes) is the use of ray tracing for IOL calculation. In our study, the use of ray tracing software (PhacoOptics) resulted in a MAE that was not significantly different from that yielded by the original Alcon calculator. The associated centroid prediction error (0.32 D) was higher than that of the Barrett calculator and the new Alcon calculator. Although the scientific literature on ray tracing approaches for toric IOL calculation is scant, our results are similar to those published by Hoffmann et al.,[160] who used different ray tracing software (Okulix, Tedics Peric & Jöher GbR). Further studies investigating this calculation method are warranted. Our results suggest that, at present, directly measuring the posterior corneal surface for toric IOL power calculation is not superior to predicting its power with theoretical models or regression formulas. One limitation of our study is its retrospective design, although there were no incomplete data and the follow-up period was similar in all cases. The lower number of eyes with ATR and oblique corneal astigmatism is a limitation for subgroup analysis. Although we excluded the influence of SIA by using postoperative K values, the variability of the prediction error remains high for all the calculators. Future studies of this topic are warranted.

6.2 Comparison of methodologies using estimated or measured values of total corneal astigmatism for toric intraocular lens power calculation

6.2.1 Objectives

The purpose of this study was to compare calculation methods that mathematically estimate the power of the posterior corneal surface (Barrett Toric Calculator and Abulafia-Koch formula) with those that consider real measurements of the posterior corneal surface: a software that uses vectorial calculation to determine total corneal astigmatism (Panacea Toric Calculator: http://www.panaceaiolandtoriccalculator.com) and a ray tracing software (PhacoOptics, Aarhus N, Denmark).

6.2.2 Patients and methods

Patient population

This retrospective case series included 107 eyes of 107 patients and was performed at Luz Hospital, Lisbon, Portugal. Patient records were reviewed to identify individuals who underwent cataract surgery with the implantation of a monofocal toric IOL (Acrysof IQ Toric SN6AT3-T9; Alcon Laboratories Inc., Fort Worth, TX) between January 2014 and April 2016. Inclusion and exclusion criteria were the same as in the previous paper (detailed in 6.1.2).

Preoperative assessment

The preoperative assessment for all patients was similar to the one in the previous paper (detailed in 6.1.2).

Surgical Technique

The Surgical Technique used was the similar to the one in the previous paper (detailed in 6.1.2).

Postoperative assessment

At the 3-month follow-up visit, refraction was evaluated by the same examiner using the cross-cylinder method, and Lenstar keratometry and Scheimpflug tomography were repeated. As suggested by Chen and Lam,[279] for Pentacam examinations, three consecutive readings were performed to improve repeatability. For each of the posterior corneal curvature meridians, an average of the magnitude and axis of the three readings was used for calculations performed in the vectorial calculation and the ray tracing software. For the anterior corneal curvature, the keratometry readings from the Lenstar were used in all calculations, to maintain consistency between calculation methods and because some studies recommended caution when using values from the sagittal map of the Pentacam.[260,280,281]

Toric IOL alignment axis was recorded via slit-lamp digital photography after pupillary mydriasis, in accordance with a previously published method.[277] Eyes exhibiting a

misalignment greater than 5 degrees or any visible tilt or decentration were excluded from the final analysis.

Postoperative calculations

Postoperatively, the preoperative calculation was repeated for each eye using the Barrett Toric Calculator, the Abulafia-Koch formula, the vectorial calculation software and the ray tracing software. To also consider the effects of the effective lens position and the spherical equivalent power of the IOL, as the other calculators do, the Abulafia-Koch formula was used in conjunction with Holladay's IOL consultant toric calculator, which was used to calculate the effective cylindrical power of the IOL at the corneal plane.[278] The postoperative keratometry readings, posterior corneal surface curvature, and measured IOL alignment axis were used to isolate any effects of surgically induced astigmatism or IOL misalignment from the errors induced by each calculator/total corneal astigmatism evaluation method.

For each calculation method, prediction error was calculated as the difference between postoperative manifest refraction corrected for the corneal plane and predicted residual astigmatism. All calculations were performed in accordance with the method described by Holladay et al.[112] and detailed by the authors of this report in a previous article.[282]

Briefly, predicted residual astigmatism was calculated as:

Predicted residual astigmatism = Toric IOL cylindrical power (corneal plane) + Corneal astigmatism (derived from measured keratometry – with or without regression formula adjustment – and posterior corneal surface curvature if applicable)

The error in predicted residual astigmatism was calculated as:

Predicted error = Postoperative refraction (corneal plane) – Predicted residual astigmatism (corneal plane)

Vector analysis was used in all calculations. Mean absolute error and centroid error in predicted residual astigmatism were calculated.[112]

Eyes were further divided into three groups according the steep meridian of the preoperative corneal astigmatism: WTR; ATR and oblique.

Statistical analysis

A power sample calculation for a one-way analysis of variance (ANOVA) test with a significance level of 5% and a power of 80% was performed to determine the sample size required for the study considering a SD of 0.33 D (value obtained in the previous study by the calculator with the lowest centroid prediction error) and four groups. According to this calculation, the total sample size required was 80 eyes (20 per group) and the actual power of the study was 81.2%.

An Excel database (Microsoft Corporation, Redmond, WA, USA) was used for data collection and major calculations. Statistical analyses were performed in accordance with the ICH statistical principles for clinical trials E9 guidelines, using SPSS software (version 21.0; IBM Corporation, Armonk, NY) for Mac (Apple Inc., Cupertino, CA). The normality of the distribution of all data sets was verified using the Kolmogorov-Smirnov test. The distribution was normal for all variables. One-way ANOVA was used for comparisons, applying the Bonferroni method for post hoc analysis. Centroid standard deviations were calculated in accordance with the method described by Holladay et al.[112] Results are expressed as mean ± SD, and a *p* value of less than .05 was considered to be statistically significant.

6.2.3 Results

Patient Demographics

Table 14 summarizes patients' demographics and implanted IOLs. Of the investigated eyes, 46 (43.0%) had WTR astigmatism, 51 (47.7%) had ATR astigmatism, and 10 (9.3%) had oblique astigmatism. In the subgroup analysis, only eyes with WTR and ATR astigmatism were included due to the low number of eyes with oblique astigmatism.

Table 14 - Patient demographics

Parameter		Mean ± SD (range)
Eyes (*n*)		107
Patients (*n*)		107
Age (y)		70 ± 11 (43, 90)
Male sex, *n* (%)		33 (30.8)
Right eyes, *n* (%)		69 (64.5)
Axial length (mm)		23.68 ± 1.82 (20.11, 29.14)
Corneal astigmatism (D)		2.21 ± 0.92 (1.00, 4.50)
IOL SE power (D)		21.08 ± 4.81 (8.00, 33.00)
IOL cylinder power (D)		2.88 ± 1.25 (1.00, 6.00)
Implanted IOL	SN6AT3	27 (25.2)
	SN6AT4	26 (24.3)
	SN6AT5	21 (19.6)
	SN6AT6	16 (15.0)
	SN6AT7	5 (4.7)
	SN6AT8	5 (4.7)
	SN6AT9	7 (6.5)

SD = standard deviation; D = diopters; IOL = intraocular lens; SE = spherical equivalent

Errors in Predicted Residual Astigmatism

The mean absolute error in predicted residual astigmatism for each calculator is listed in Table 15. There were significant differences between groups ($p < .001$), with mean absolute error being lower in methods estimating the influence of the posterior corneal surface than in methods considering measured values. The Barrett Toric Calculator yielded the lowest mean absolute error of all calculators (0.34 D). When compared with the other estimation method (ie, Abulafia-Koch formula), the difference was not statistically significant ($p = .139$). When comparing methods using measured values for the calculation, although Panacea yielded a lower mean absolute error than PhacoOptics, the difference did not reach statistical significance ($p = .102$).

Table 15 - Mean Absolute Error on Predicted Residual Astigmatism

Calculator	Mean ± SD (range) Diopters	*p* value*
Barrett toric calculator	0.34 ± 0.23 (0.03, 1.04)	-
Holladay calculator + Abulafia-Koch formula	0.43 ± 0.34 (0.04, 1.49)	.139
Panacea	0.59 ± 0.29 (0.13, 1.35)	< .001
PhacoOptics	0.64 ± 0.34 (0.15, 1.44)	< .001

* Comparison with the Barrett toric calculator; SD = standard deviation; D = diopters

Table 16 summarizes the centroid errors in predicted residual astigmatism. All calculators resulted in ATR prediction errors.

Table 16 - Centroid Error in Predicted Residual Astigmatism

Calculator	Centroid (D @ angle) ± SD	*p* value x component*	*p* value y component*
Barrett toric calculator	0.07 ± 0.26 @ 172	-	-
Holladay calculator + Abulafia-Koch formula	0.13 ± 0.37 @ 174	.211	.321
Panacea	0.25 ± 0.43 @ 173	< .001	< .001
PhacoOptics	0.29 ± 0.49 @ 171	< .001	< .001

* Comparison with the Barrett toric calculator; SD = standard deviation; D = diopters

Again, the lowest centroid prediction error was yielded by methods estimating the power of the posterior corneal surface ($p < .001$ for *x* and *y* vector components). The Barrett Toric calculator resulted in the lowest centroid error of all calculators (0.07 D), although the difference for the Holladay calculator + Abulafia-Koch formula did not reach statistical significance (0.13 D; $p = .211$ and .321 for *x* and *y*, respectively). Panacea yielded a prediction error similar to PhacoOptics (0.25 D vs 0.29; $p = .452$ and .325 for *x* and *y*, respectively), with a slightly lower standard deviation.

The results for mean absolute error and centroid prediction errors were similar for all the types of IOLs implanted (SN6AT3-T9) (results not shown).

Double-angle plots illustrating the centroid prediction errors for the investigated calculation methods are shown in Figure 30.

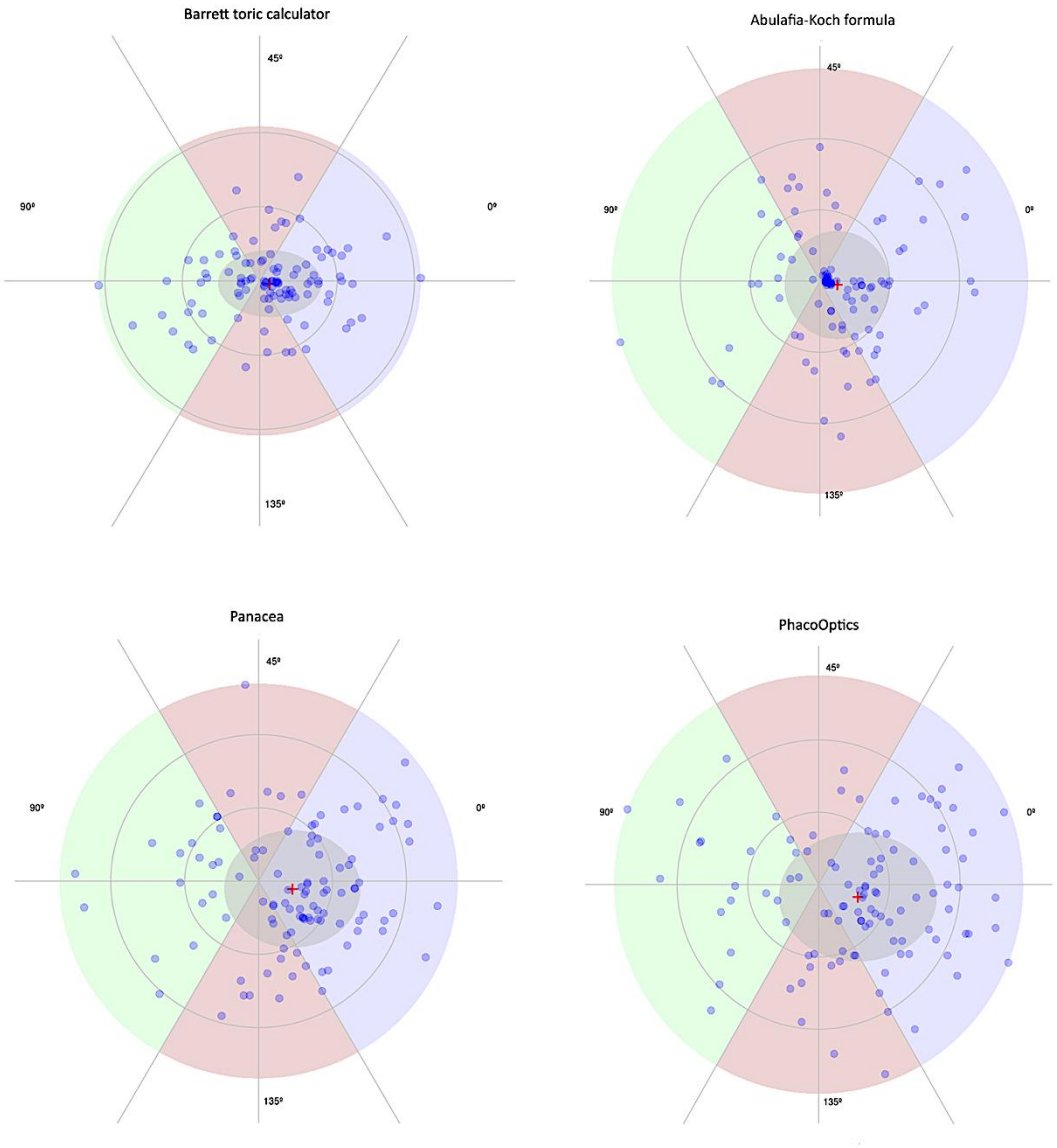

Figure 30 - Double-angle plots of the prediction errors for the investigated calculation methods.

Both the Barrett Toric Calculator and the Holladay calculator + Abulafia-Koch formula resulted in a larger percentage of eyes within 0.25 D, 0.50 D, 0.75 D, and 1.00 D of absolute astigmatic prediction error than either Panacea or PhacoOptics. The

percentage of eyes within these values of absolute prediction error for each calculation method is shown in Figure 31.

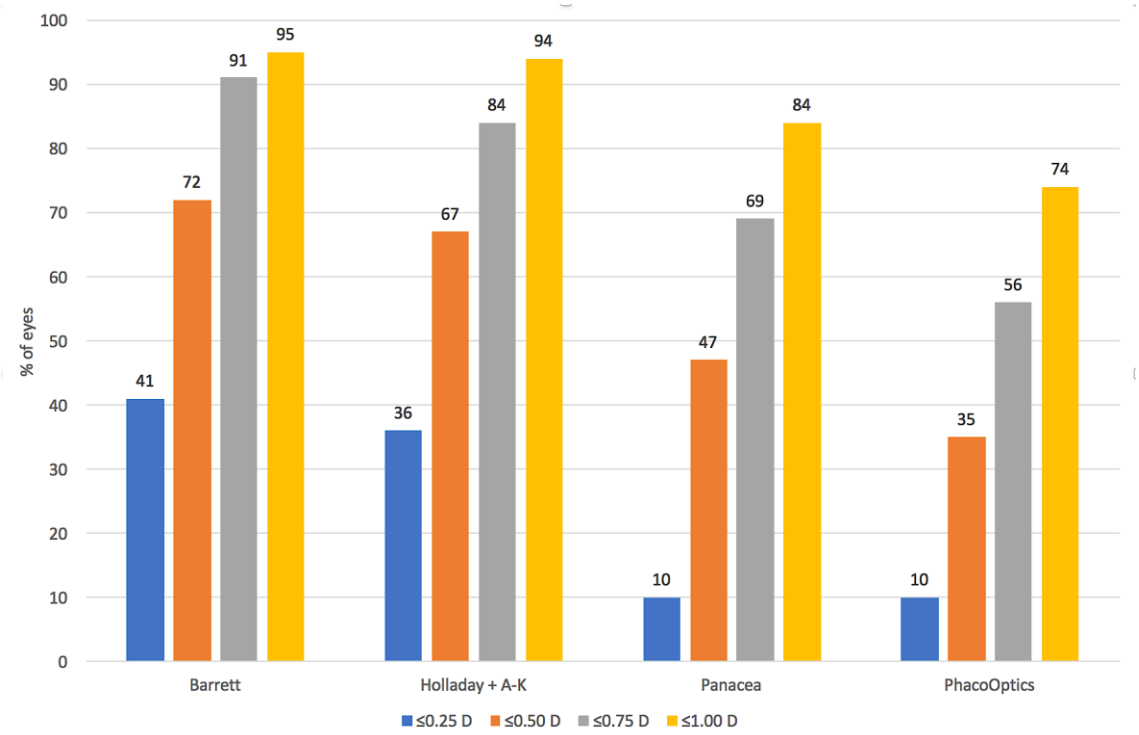

Figure 31 - Percentage of eyes within 0.25, 0.50, 0.75, and 1.00 diopters (D) of absolute astigmatic prediction error with each calculation method.

Subgroup analysis of WTR and ATR eyes

Subgroup analysis results for mean absolute error and centroid residual astigmatism prediction error are presented in Table 17. In WTR eyes, the Barrett calculator had the best results (mean absolute error: 0.31 D; centroid: 0.10 D), and the combination of Holladay calculator with the Abulafia-Koch formula yielded similar results (mean absolute error: 0.42 D; centroid: 0.16 D). Both methods using measured values performed worse ($p < .001$ for mean absolute error *x* and *y* components when compared with both the Barrett Toric Calculator and Abulafia-Koch formula).

Table 17 - Mean absolute and centroid errors in predicted residual astigmatism for eyes with with-the-rule (WTR) and against-the-rule (ATR) corneal astigmatism

Calculator	Eyes with WTR corneal astigmatism (*n* = 46)		Eyes with ATR corneal astigmatism (*n* = 51)	
	Mean ± SD (range) diopters	Centroid (diopters @ angle) ± SD	Mean ± SD (range) diopters	Centroid (diopters @ angle) ± SD
Barrett toric calculator	0.31 ± 0.24 (0.03, 0.89)	0.10 ± 0.28 @ 169	0.30 ± 0.25 (0.03, 1.04)	0.04 ± 0.29 @ 174
Holladay calculator + Abulafia-Koch formula	0.42 ± 0.25 (0.06, 1.49)	0.16 ± 0.39 @ 168	0.40 ± 0.26 (0.04, 1.08)	0.11 ± 0.38 @ 175
Panacea	0.61 ± 0.31 (0.13, 1.35)	0.34 ± 0.44 @ 163	0.51 ± 0.35 (0.15, 1.30)	0.24 ± 0.41 @ 178
PhacoOptics	0.60 ± 0.35 (0.05, 1.44)	0.36 ± 0.52 @ 159	0.54 ± 0.41 (0.15, 1.31)	0.28 ± 0.41 @ 177

WTR = with-the-rule; ATR = against-the-rule; SD = standard deviation; D = diopters

In eyes with preoperative ATR corneal astigmatism, mean absolute errors and centroid astigmatism prediction errors were lower for all calculation methods than in eyes with WTR astigmatism. Again, estimation methods performed significantly better ($p < .001$ in

all cases), although the differences for methods using measured values were lower than in eyes with WTR astigmatism.

6.2.4 Discussion

In the previous study we suggested that, currently, estimating the influence of the posterior corneal surface in total corneal astigmatism may yield better results in toric IOL calculation than measuring it directly.[282] In the current study, we compared methods that estimate total corneal astigmatism and resulted in the lowest prediction error in our previous study with methods considering real measurements of the posterior corneal surface obtained using a Scheimpflug camera. We compared the mean absolute error in predicted residual astigmatism between calculation methods, and the centroid error in residual astigmatism, which, by also considering its axis, is more precise for evaluating astigmatic outcomes of cataract surgery.[11,112]

For the estimation methods, the Barrett Toric Calculator and the Abulafia-Koch formula were assessed. The Barrett Toric Calculator resulted in the lowest mean absolute errors and centroid astigmatism prediction errors both overall and in subgroups of eyes with WTR and ATR astigmatism. It also resulted in the largest proportion of eyes within 0.25 to 1.00 D of prediction error. The combination of the Holladay toric calculator with the Abulafia-Koch formula resulted in a higher mean absolute error and centroid prediction error, although the difference for the Barrett Toric Calculator was not statistically significant. These results are similar to those we reported in a recent study and those published by Abulafia et al.[177], in which their formula reduced errors to a level similar to that of the Barrett Toric Calculator.[282] In a recent prospective study, Gundersen and Potvin confirmed the superior results of the Barrett Toric Calculator when compared with standard calculators.[283]

For methods that permit toric IOL calculation with real measurements of the posterior corneal surface curvature, we used two calculation software programs (Panacea and PhacoOptics) combined with curvature data from the Pentacam. Panacea uses vector summation of anterior and posterior astigmatism to calculate total corneal astigmatism, which may be more precise than other calculation methods based on Gaussian optics or the Pentacam's ray tracing calculation through the total corneal refractive power

map.[111,273] PhacoOptics uses ray tracing calculation. Using a different ray tracing software (Okulix, Tedics, Dortmund, Germany), Hoffmann et al.[160] reported improved results when a combination of anterior and posterior surface measurements was used for toric IOL calculation. Although some studies demonstrated improved results when considering total corneal astigmatism measured using the Pentacam,[160,171,284,285] a study by Zhang et al.[286] using a different Scheimpflug imaging device, did not find a significantly lower prediction error than that obtained using data from an automated keratometer. Aside from the conflicting evidence, no studies have compared the prediction error of toric IOL calculation using methods that estimate the posterior corneal surface power with methods that use real measurements.

In the present study, both methods of calculation using real-world data showed a higher mean absolute error and centroid error in predicted residual astigmatism than methods using estimated data. Although Panacea yielded lower errors than PhacoOptics, the difference was not statistically significant. We used a version of PhacoOptics preinstalled in the optical biometry device. Recently, it was shown that, in the same biometry device, the Olsen formula was more accurate as a standalone than as a preinstalled version.[287] We are not aware of whether this may be the case with PhacoOptics. Different ray tracing approaches for toric IOL calculation should be investigated in future studies.

Nevertheless, using real measurements, the differences for the estimation methods were higher in WTR than in ATR eyes, indicating that the Pentacam may underestimate the posterior corneal surface power in WTR eyes. A study by Reitblat et al. also showed that the Pentacam may underestimate vertical posterior astigmatism and overestimate it in the horizontal meridian.[273] Using the total corneal power from the Galilei, Koch et al. achieved similar results.[52] A different limitation of Scheimpflug cameras that may also explain our results is the repeatability of posterior corneal curvature evaluation, which has been shown to be lower than that of anterior corneal curvature.[288] Although the reason for this is uncertain, some studies suggest that that Pentacam software may have more difficulty finding and extracting the posterior corneal edge because the smaller difference in index of refraction between the cornea and aqueous results in an edge with lower contrast.[289]

Although no other study has performed a direct comparison of prediction methods and methods that use measured values for toric IOL calculation, the percentage of eyes within 0.25 to 1.00 D of absolute prediction error in our study correlate well with those published in the literature for the Barrett Toric Calculator, the Abulafia-Koch formula and calculations using Pentacam measurements.[11,177,273,283]

Although real measurements from the Pentacam in our study yielded higher astigmatic prediction errors than estimation methods, new technologies, such color-LED topography, swept source anterior segment optical coherence tomography, or intraoperative aberrometry, may yield different results. Studies investigating the prediction error of these methods in the calculation of toric IOLs are, therefore, warranted. Apart from its retrospective nature, the use of posterior surface measurements obtained using the Pentacam may be a limitation of our study, given its limited repeatability. The use of vector analysis for total corneal astigmatism or other total corneal astigmatism evaluation methods from the Pentacam, such as True Net Power and Total Corneal Refractive Power, should also be investigated in future studies.

6.3 Summary of conclusions from both studies

Among the different new toric IOL calculation methods, the Barrett toric calculator (and the new Alcon calculator) yielded the lowest astigmatic prediction errors in the whole sample and in subgroups of eyes (WTR/ATR corneal astigmatism). The application of the Abulafia-Koch formula combined with the Holladay toric calculator achieved similar results.

Findings from the consecutive study demonstrated that, at present, directly measuring the posterior corneal surface with a Scheimpflug camera is not superior to predicting its power with mathematical models.

Using the Barrett toric calculator or the Abulafia-Koch formula combined with a strategy to predict the ELP for toric IOL power calculation may improve the clinical results of cataract surgery with these IOLs.

Chapter 7: Enhancing knowledge on surgically induced astigmatism

This chapter is based on the paper:

- "Comparison of Surgically Induced Astigmatism and Morphologic Features Resulting From Femtosecond Laser and Manual Clear Corneal Incisions for Cataract Surgery" published by Ferreira et al. in J Refract Surgery 2018; 34(5):322-329.

7.1 Introduction and objectives

Considering SIA is an integral part of any toric IOL calculation, since the postoperative corneal power is the vectorial combination of the preexisting corneal astigmatism with the one generated by the creation of a CCI.

SIA is highly variable, with a large dispersion of values, even with small incisions and fixed meridians. SIA is further discussed on Chapter 2 – 2.8 (Theroretical introduction).

The femtosecond laser is a new technology for cataract surgery that allows the execution of several surgical steps, including capsulotomy, lens fragmentation, and CCI construction.[290] The femtosecond laser allows the surgeon to choose the location of the incision and its precise size and architecture. Femtosecond laser-created CCIs are highly precise, reproducible, and stable.[291] They are self-sealing due to the near-perfect wound geometry[292] and are potentially subjected to less mechanical trauma during surgery.[290]

Despite the theoretical benefits of femtosecond laser-created CCIs, their superiority in reducing SIA when compared to manual CCIs has not been proven, and most studies show only a reduction in the SD of mean SIA or in the deviation from the intended SIA axis.[296-301] However, these studies are limited by the use of just one femtosecond laser platform across studies, early software versions, fixed incision locations, small sample sizes, and different SIA evaluation methods.

Several factors influencing SIA have been identified. Although the literature on the influence of incision width (showing a smaller SIA in 2.0 to 2.2-mm than in 2.75 to 3.0-mm incisions) and location (smaller SIA with temporal incisions) on SIA during cataract surgery is extensive, the association of SIA with other ocular features is less well known and has not been studied for femtosecond laser-created CCIs.

The objective of this study was to compare SIA in patients who underwent phacoemulsification with CCIs created by femtosecond laser or manually at two different meridians and to determine the correlation of SIA with individual features and incision morphology.

7.2 Materials and methods

Patient population

Preoperative Assessment

All patients had a full preoperative ophthalmologic examination, including uncorrected and corrected distance visual acuity, manifest refraction, slit-lamp biomicroscopy, Goldmann applanation tonometry, and fundoscopy under mydriasis. Corneal astigmatism and curvature were evaluated using the automated keratometry feature of the Lenstar LS 900 (Haag-Streit AG, Koeniz, Switzerland). As recommended by the manufacturer, five scans were performed in each case. Keratometry readings with this system have shown high precision and repeatability.[144]

Surgical Technique

Two experienced surgeons (TBF, JP) performed all surgeries under topical anesthesia using a microcoaxial phacoemulsification technique. Each surgeon located the incision according to his usual preference (temporal for JP [180° in the right eye and 0° in the left eye] or at 120° for TBF [superotemporal in the right eye and superonasal in the left eye]. The sideport incision was performed at a 90 to 110° angle from the main incision to be astigmatically neutral.[293]

In the femtosecond laser group, CCIs were performed with the Catalys Precision Laser System platform (V. cOS 3.0; Johnson & Johnson Vision, Santa Ana, CA). After the liquid optics interface was engaged to the patient's eye, ensuring precise centration, and the built-in AS-OCT was used to identify the ocular surfaces, the same parameters for CCI creation were used in all cases: 0.3 mm limbus offset, 2.4 mm incision width, and 1.7 mm incision length. The incision architecture was triplanar, with an anterior plane depth of 35%, a posterior plane depth of 70%, an anterior side cut angle of 80°, and a posterior side cut angle of 55°. The anterior line density was 10, and the posterior line density was 4, both at a distance of 30%. The horizontal spot spacing was 5 µm, the vertical spot spacing was 10 µm, and the laser pulse energy was 5 µJ. The sideport incision

parameters were similar, with a width and length of 1 mm. The capsulotomy (5 mm, centered on the scanned capsule, incision depth: 600 µm, horizontal spot spacing: 5 µm, vertical spot spacing: 10 µm, pulse energy: 4 µJ) and the lens fragmentation (sextant pattern, 3 segmentation repetitions, horizontal spot spacing: 10 µm, vertical spot spacing: 40 µm, anterior pulse energy: 9 µJ, posterior pulse energy: 10 µJ) were performed in a similar manner in all cases. The femtosecond laser CCIs were gently dissected with a flat spatula, and the anterior chamber was entered.

In the manual CCI group, the main incision was performed with a diamond blade (E0130 Trapezoid Diamond Knife; Bausch & Lomb GmbH/Storz Ophthalmic Instruments, Heidelberg, Germany) that had a 2.4 mm width, a 1.75 mm length (from the tip of the blade to the shoulder). Triplanar construction was targeted. After the blade was buried perpendicularly in the stroma, a tunnel was created parallel to the iris surface until the engraving on the blade was reached, and then, the blade was directed to enter the anterior chamber. The side-port incision was created with a diamond keratome (E0100 M Universal-Diamond Knife, Bausch & Lomb GmbH/Storz Ophthalmic Instruments), single-planar and parallel to the iris surface, with a width of 1 mm and approximately the same 1 mm length.

In both groups, phacoemulsification was performed via a standard technique with combined longitudinal/torsional ultrasound using the Alcon Infinity System (Alcon Laboratories, Inc., Fort Worth, TX). The intraocular lens (IOL) was implanted through the main incision and was either the Tecnis PCB00 preloaded IOL (Johnson & Johnson Vision), the Tecnis Toric IOL (Johnson & Johnson Vision), the Tecnis Symfony IOL (Johnson & Johnson Vision), the Acrysof IQ AU00T0 preloaded IOL (Alcon Laboratories, Inc.), or the Acrysof Panoptix IOL (Alcon Laboratories, Inc.). Both the Tecnis Toric and the Tecnis Symfony IOLs were implanted with the Unfolder Emerald One Series cartridge system (Johnson & Johnson Vision), whereas the Acrysof Panoptix IOL was implanted with the D cartridge of the Monarch III IOL injector (Alcon Laboratories, Inc.). In both groups, after the viscosurgical device was removed, the width of the inner lips of the

main CCI was measured using a calibrated incision gauge. The CCIs were hydrated with balanced salt solution, and watertight closure was confirmed.

Postoperative Assessment

All the outcomes were evaluated by examiners masked for the type of surgery performed (femtosecond laser or manual). Post-operative examinations were performed at 1 day, 1 month, and 3 months postoperatively and included the same tests as those administered preoperatively. At the 3-month visit, Lenstar keratometry was repeated, and corneal imaging AS-OCT (V. 6.0.13.0, Spectralis, Heidelberg Engineering GmbH, Heidelberg, Germany) was performed. The AS-OCT images were captured using 8-mm line scans in 11 Sections (15° x 5°), with EDI and automatic real-time image averaging modes activated. The scanning line was oriented parallel to the middle plane of the CCI. The three best-quality scans were selected for each patient and imported into ImageJ (V.150i, National Institutes of Health, Bethesda, MD; http://imagej.nih.gov/ij) to enable measurements. Contrast adjustment and bi-thresholding were adjusted if necessary to optimize identification of the ocular structures. As shown in Figure 32, the incision length was measured as the linear distance between the most internal and external incision sites. Peripheral corneal thickness was measured at the mid-course of the incision. Distance from the external incision site to the limbus was measured considering the limbus according to previously reported optical properties.[294] All measurements were performed by 2 examiners, and the mean of the 6 measurements (3 scans x 2 examiners) was used for statistical purposes. Incisions were classified as triplanar if three steps, each greater than 0.2 mm in length, could be identified.

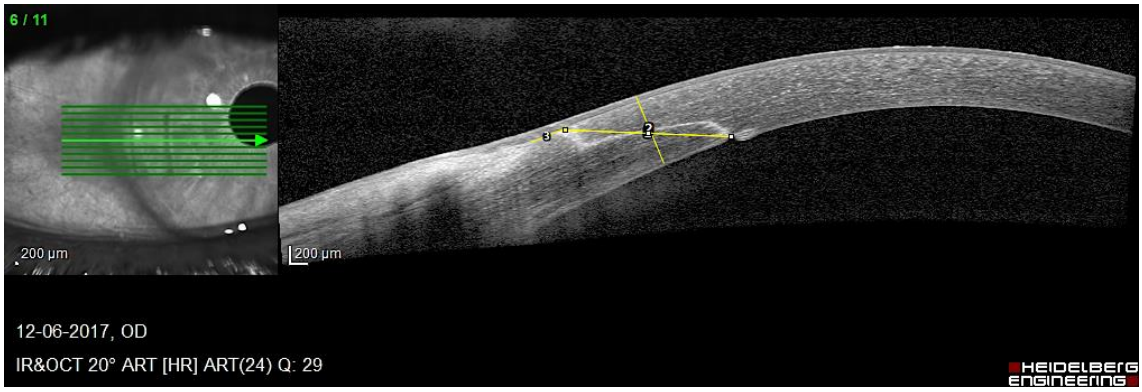

Figure 32 – The three measurements taken after importing the AS-OCT images into ImageJ.

Postoperative Calculations

Eyes in each group were divided according to the incision location (temporal or superior oblique). All SIA calculations were performed by vectorial calculation in accordance with the method described by Alpins.[113-115] In each group, the SIA, the flattening effect (FE) at the meridian of the incision (negative representing a flattening of that meridian and positive representing a steepening), and the torque (positive representing counterclockwise and negative representing clockwise rotation) were calculated. While the FE changes the magnitude of the astigmatism, the torque acts to rotate the preoperative astigmatism with only a small increase in magnitude.[113,115]

The summated vector mean (SVM) was also calculated for each group (femtosecond laser versus manual) and each incision location (temporal and superior oblique). The SVM was calculated by dividing the total vector length of all SIAs by the number of component vectors, thus considering both magnitude and orientation of all SIAs.[114]

The influence of the following preoperative factors on SIA were investigated in each group: age, corneal astigmatism, central corneal pachymetry, axial length, anterior chamber depth, corneal curvature, corneal diameter, and intraocular pressure. The influence of the implanted IOL power and incision characteristics (peripheral pachymetry, final incision width, location in mm anterior to the limbus, and incision length) were also investigated.

Statistical analysis

After the first 50 eyes in each group were included, the sample size required to detect a difference of 0.25 D in mean SIA between groups was determined via a power sample calculation. For mean SIA, a SD of 0.53 D (largest value obtained from the first 50 eyes) was assumed, with a significance level of 5% and a power of 80%. According to this calculation, 142 eyes were required, corresponding to 71 in each group.

Statistical analysis was performed in accordance with ICH statistical principles for clinical trials E9 guidelines. SPSS for Mac (version 21.0; SPSS, Inc, Armonk, NY) was used to perform statistical tests. The normality of the distribution for each data set was checked using the Kolmogorov-Smirnov test. Where parametric analysis was appropriate, a Student's *t* test for independent samples was used for comparisons. For non-parametric analyses, differences were evaluated via the Wilcoxon rank-sum test. A one-way ANOVA test with a Bonferroni correction was applied for multiple comparisons. A Pearson Chi-Square test was used for categorical variables. Pearson or Spearman's coefficients were used to assess correlations depending on the existence or non-existence of normality. The predictability of SIA as a function of multiple factors was evaluated using multiple regression analysis. Results are expressed as mean ± SD, and a *p* value of .05 was considered statistically significant.

7.3 Results

Patient Demographics

The analysis included 300 eyes in the femtosecond laser group and 300 eyes in the manual incision group. Table 18 shows the patient demographics and clinical information.

Table 18 – Patient demographics and Clinical Information

Parameter	**Femtosecond laser group** **Mean ± SD (range)**	**Manual group** **Mean ± SD (range)**	***p* value**
Eyes (*n*)	300	300	-
Patients (*n*)	176	185	-
Age (y)	69 ± 8 (52, 83)	71 ± 8 (49, 87)	.063
Male sex, *n* (%)	52 (29.5)	65 (35.1)	.104
Right eyes, *n* (%)	158 (52.7)	175 (58.3)	.372
UDVA (LogMAR)	0.88 ± 0.72 (2, 0.3)	0.70 ± 0.81 (2, 0.22)	.051
CDVA (LogMAR)	0.34 ± 0.49 (1.92, -0.1)	0.36 ± 0.52 (0.0, 1.92)	.225
Axial length (mm)	23.34 ± 1.51 (21.50, 27.74)	23.50 ± 1.55 (21.12, 30.15)	.098
ACD (mm)	3.11 ± 0.52 (2.31, 5.12)	3.16 ± 0.43 (2.19, 5.22)	.592
K1 (D)	43.52 ± 1.91 (39.10, 46.23)	42.90 ± 1.92 (38.89, 46.75)	.408
K2 (D)	44.38 ± 1.79 (40.08, 47.20)	43.87 ± 1.90 (39.28, 47.94)	.538
Corneal astigmatism (D)	0.90 ± 0.70 (0.01, 3.71)	0.96 ± 0.68 (0.17, 2.89)	.564
CD (mm)	11.83 ± 0.49 (11.00, 12.90)	11.80 ± 0.42 (11.90, 12.60)	.842
Central pachymetry (μm)	538 ± 37.9 (438, 601)	528 ± 36.7 (417, 604)	.181
Intraocular pressure (mmHg)	16.41 ± 4.44 (9, 27)	15.81 ± 3.77 (7, 29)	.099
Temporal	162 (54.0)	169 (56.3)	-

Incision location, *n* (%)	Superior oblique	138 (46.0)	131 (43.7)	-
IOL power (D)		22.84 ± 2.98 (12.00, 27.00)	21.96 ± 3.90 (5.00, 29.00)	.062
Implanted IOL	Tecnis PCB00	72 (24.0)	131 (43.7)	-
	Tecnis ZXR00	112 (37.3)	42 (14.0)	-
	Tecnis ZCT100-525	47 (15.7)	58 (19.3)	-
	Tecnis ZXT100-375	46 (15.3)	24 (8.0)	-
	Acrysof AU00T0	11 (3.7)	35 (11.7)	-
	Acrysof TFNT00	12 (4.0)	10 (3.3)	-

UDVA = uncorrected distance visual acuity, CDVA = corrected distance visual acuity, ACD = anterior chamber depth, K1 = flat keratometry, K2 = steep keratometry, CD = corneal diameter, IOL = intraocular lens

Surgically induced astigmatism, flattening effect, and torque effect

The results of the SIA, FE, and torque calculation results for each group are presented in Table 19.

Table 19 – SIA Vector, Flattening Effect, and Torque in the Femtosecond Laser and Manual Clear Cornea Incision Groups

Parameter Mean ± SD (range)		Femtosecond laser group	Manual group	*p* value
Temporal incision group	SIA magnitude (D)	0.43 ± 0.35 (0.02, 1.61)	0.55 ± 0.46 (0.01, 2.45)	.183
	FE incision (D)	-0.11 ± 0.41 (-1.26, 0.81)	-0.13 ± 0.54 (-2.36, 1.48)	.713
	Torque (D)	0.05 ± 0.40 (-0.96, 1.05)	0.05 ± 0.43 (-1.26, 1.59)	.958
Superior oblique incision group	SIA magnitude (D)	0.62 ± 0.46 (0.18, 1.46)	0.79 ± 0.63 (0.36, 2.05)	.328
	FE incision (D)	-0.21 ± 0.47 (-1.12, 0.48)	-0.34 ± 0.58 (-1.10, 0.26)	.515
	Torque (D)	-0.06 ± 0.59 (-0.85, 0.94)	-0.09 ± 0.69 (-0.89, 0.33)	.946

SIA = surgically induced astigmatism, FE = flattening effect, D = diopters

In the temporal incision group, both SIA magnitude and FE were smaller and showed a lower SD in the femtosecond laser group than in the manual group, although the differences did not reach statistical significance. The torque was similar in both groups.

The superior oblique group results were similar to those obtained from the temporal CCI group, with the femtosecond laser group showing lower values for mean SIA and FE and smaller SDs. Although the differences between the two techniques of CCI construction were larger in the superior oblique incision group than in the temporal incision group, they also did not reach statistical significance. As in the temporal incision group, both torque magnitude and differences in torque between groups were very small. However, the superior oblique group showed a clockwise direction.

SIA was similar in the right and the left eyes (for temporal CCIs: p = .458 for the femtosecond laser group and p = .602 for the manual group; superior oblique CCIs: p = .344 for the femtosecond laser group and p = .231 for the manual group). Induced astigmatism was generally larger in the superior oblique incision group than in the temporal incision group regardless of CCI construction method. However, neither SIA magnitude nor FE nor torque were significantly different between the temporal and superior oblique incision groups (p = .233, .924, and .653, respectively, in the femtosecond laser group and p = .061, .277, and .601, respectively, in the manual group).

The SVM of SIA values for each of the groups are presented in Figure 33. A histogram of corneal astigmatism before and after surgery in the femtosecond laser and manual groups is presented in Figure 34.

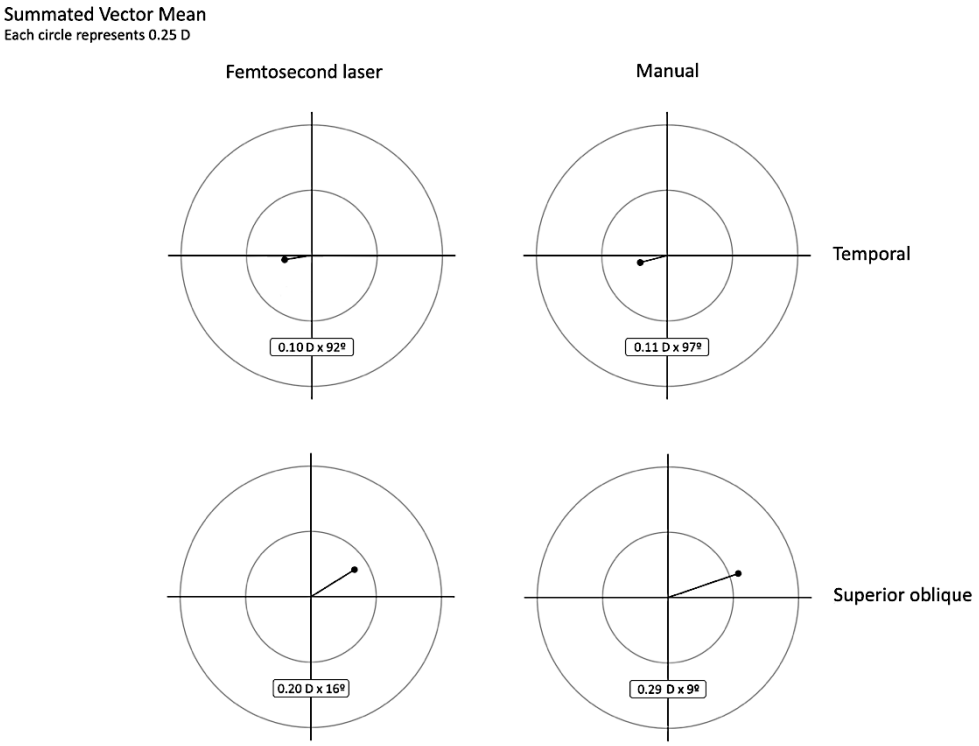

Figure 33 – Summated vector mean values of surgically induced astigmatism in the studied groups. D = diopters

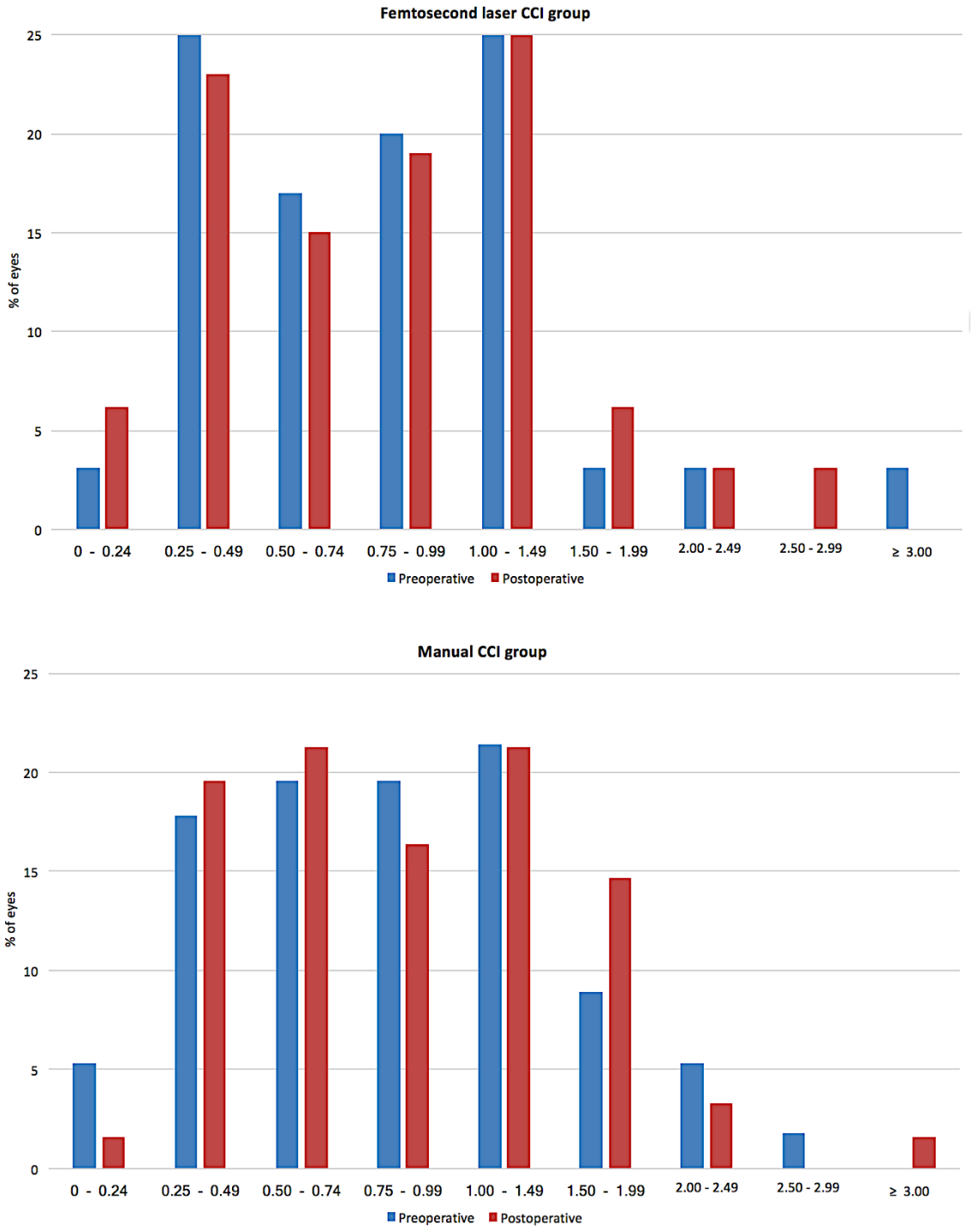

Figure 34 – Histograms of corneal astigmatism before and after surgery in the studied groups. CCI = clear cornea incision.

Correlations with ocular and individual features

Correlations of surgery type with ocular features were analyzed with the temporal and superior oblique incision groups combined, only separated by femtosecond laser versus manual surgery. The results were similar when the temporal and superior oblique incisions were considered separately (results not shown). All significant correlations at 3 months post-surgery are presented in Table 20.

Table 20 – Correlation Between Surgically Induced Astigmatism Magnitude and Individual Parameters

Feature	Femtosecond laser group Correlation coefficient *p* value	Manual group Correlation coefficient *p* value
Preoperative flat K	-.387 .005	-.017 .839
Preoperative steep K	-.222 .050	-.033 .701
Preoperative corneal astigmatism	.521 <.001	.092 .284
Preoperative ACD	-.303 .032	-.094 .275
Preoperative AL	.313 .027	.048 .575
Preoperative CD	-.476 <.001	-.047 .587
Final incision width	.091 .659	.301 .002

K= keratometry, ACD = anterior chamber depth, AL = axial length, CD = corneal diameter

In the manual incision group, no significant correlations between SIA and the investigated features were found, except for the positive correlation between SIA and final incision width. No significant correlations were found with regards to other incision characteristics (peripheral pachymetry, incision length, and distance to the limbus) in both groups. The correlation between SIA and age at time of surgery was positive but not significant in both groups (r = 0.201, p = .187 in the femtosecond laser group; r = 0.141, p = .585 in the manual group). No statistically significant correlation was found between SIA and preoperative intraocular pressure (r = 0.088, p = .651 in the femtosecond laser; r = 0.002, p = .991 in the manual group). No significant correlations were found in either group between any of the investigated features and FE or torque (p > .05 in all cases).

SIA predictability

Given the lack of significant correlations in the manual incision group, multiple regression analysis was only performed for the femtosecond laser group. In this group, a multiple linear regression was calculated to predict SIA magnitude based on preoperative flat keratometry (K1), steep keratometry (K2), corneal astigmatism, anterior chamber depth (ACD), axial length (AL), and corneal diameter (CD). A significant regression equation was found (F(22,198) = 4.371, p = .003), with an R^2 of 0.332. Participants' predicted SIA was equal to: 0.429 - 0.01 (K1) - 0.021 (K2) - 0.114 (ACD) + 0.21 (AL) - 0.38 (CD) + 0.387 (pre-operative corneal astigmatism), where K1, K2, and astigmatism are measured in diopters and the other variables in millimeters. Of the investigated variables, only preoperative astigmatism was a significant predictor of SIA (p = .003).

Incision architecture and reproducibility

The incision characteristics at 3-months post-surgery are reported in Table 21. All incisions were triplanar as intended in the femtosecond laser group, whereas only 28% of the incisions in the manual incision group were triplanar. Thus, in the manual group, only 84 eyes were analyzed on AS-OCT images. The deviation from the intended length

was significantly less in the femtosecond laser group, as was the wound enlargement at the end of surgery ($p < .001$ in both cases). No incision in the femtosecond laser group showed Descemet membrane detachments, whereas 20% of the eyes in the manual group had small detachments that were visible on AS-OCT ($p = .015$).

Table 21 – Clear Corneal Incision Architecture Evaluated by Anterior Segment OCT

CCI parameter **Mean ± SD** **(range)**	**Femtosecond laser group** **(n = 300)**	**Manual group** **(n = 84)**	***p* value**
Length (mm)	1.80 ± 0.09 (1.53, 1.82)	1.29 ± 0.23 (1.20, 2.11)	.056
Deviation from intended length (mm, %)	0.10, 5.9	0.46, 26.3	<.001
Distance to the limbus (mm)	0.43 ± 0.02 (0.40 – 0.51)	0.53 ± 0.06 (0.39 – 0.65)	.005
Thickness at incision site (μm)	746 ± 17 (701 – 779)	762 ± 12 (741 – 786)	.299
Final incision width (mm)	2.48 ± 0.17 (2.45 – 2.55)	2.63 ± 0.14 (2.60 – 2.75)	.364
Wound enlargement (mm, %)	0.08, 0.03	0.23, 9.6	<.001
Triplanar architecture (n, %)	300, 100	84, 28.0	<.001
Epithelial misalignment (n, %)	0, 0	0, 0	-
Endothelial misalignment (n, %)	181, 60.3	83, 98.9	.037
Descemet membrane detachment (n, %)	0, 0	17, 20.2	.015

OCT = optical coherence tomography; CCI = clear corneal incision; SD = standard deviation

7.4 Discussion

In this study, the SIA and morphology of 2.4 mm CCIs created by a femtosecond laser were compared with those manually created in eyes that underwent phacoemulsification. Temporal and superior oblique incisions in both the femtosecond laser and manually-created CCI groups were addressed.

Results revealed that SIA, FE, torque, and the SVM for SIA were lower in the femtosecond laser group for both temporal and superior oblique incisions, although these differences did not reach statistical significance. The femtosecond laser group also showed smaller SDs in all cases, having a lower dispersion of both SIA magnitude and FE. The SVM of the SIA (Figure 33) represents not only the mean magnitude of SIA but also considers the orientation of each vector. As expected, this variable was lower than the mean SIA in all cases. Like the centroid value described by Holladay et al.,[111] this value may be a better representation of the whole sample.[114] As recommended by Alpins et al.[295], the FE at the incision meridian should be used for toric IOL calculation. For temporal incisions, the FE was -0.11 D in the femtosecond laser group and -0.13 D in the manual group. For superior oblique incisions, the FE was -0.21 D in the femtosecond laser group and -0.34 D in the manual group. The accuracy of these values for toric IOL calculation should be investigated in future prospective trials.

Theoretically, femtosecond laser-created CCIs have perfect architecture. However, most studies comparing the SIA of femtosecond versus manually-created incisions show similar results.[186,296,297,298,299,300,301] Results of these published studies comparing SIA in femtosecond laser and manually-created CCIs are presented in Table 22.

Table 22 – Summary of the Published Studies Comparing SIA in Femtosecond Laser and Manual Clear Corneal Incisions for Cataract Surgery.

Study	Astigmatism evaluation method	Femto platform	Incision location	Incision Configuration Femto group	Incision Configuration Manual group	Incision width (mm) Femto group	Incision width (mm) Manual group	Mean SIA (D) Femto group (mean ± SD)	Mean SIA (D) Manual group (mean ± SD)	*p*
Espaillat et al.	N/A	LenSx	Temporal	Tri-planar	Single-planar	2.3 internal, 2.4 external	2.2	0.51 ± 0.46 n=53	0.50 ± 0.35 n=62	.95
Makombo et al.	Autokeratometer	LenSx	Superior	Tri-planar	Tri-planar	2.2	2.2	0.37 ± 0.92 n=20	0.60 ± 0.73 n=28	.318
Diakonis et al.	Placido based topography	LenSx	200° OD 20° OS	Tri-planar	Tri-planar	2.4	2.5	M=0.09; J0=0.11; J45=-0.17 n=36	M=0.09; J0=0.06; J45=-0.07 n=36	>.05

Álvarez-Rementería et al.	Autokeratometer	LenSx	135°	Tri-planar	N/A	2.2 outer; 2.4 inner edge	2.0	0.50 ±0.22 n=25	0.41 ± 0.28 n=25	.225
Nagy Z et al.	Scheimpflug camera	LenSx	Steep meridian	Biplanar	N/A	2.8	2.8	0.47 ± 0.13 n=20	0.41 ± 0.14 n=20	.218
Serrao et al. (in vitro)	Scheimpflug camera	iFS	3 o'clock	Triplanar	Single-planar	2.75	2.75	0.78 ± 0.36 n = 7	0.92 ± 0.46 n = 7	>.05
Mastropasqua et al.	Scheimpflug camera	LenSx	130° (OD only)	Biplanar	Biplanar	2.8	2.75	0.64 ± 0.32 n = 30	0.69 ± 0.50 n = 30	.779
Ferreira et al.	Lenstar keratometry	Catalys	Temporal	Triplanar	Triplanar	2.5	2.4	0.44 ± 0.37 n = 122	0.55 ± 0.43 n = 223	.185
Ferreira et al.	Lenstar keratometry	Catalys	130°	Triplanar	Triplanar	2.5	2.4	0.65 ± 0.48 n = 88	0.97 ± 0.93 n = 137	.495

SIA = surgically induced astigmatism; femto = femtosecond laser; SD = standard deviation; D = diopters; N/A = not available; OD = right eye; OS = left eye. The LenSx is manufactured by Alcon Laboratories, Inc., Forth Wort, TX and the iFS and Catalys are manufactured by Johnson & Johnson Vision, Santa Ana, CA

A direct comparison between this study and other published studies is difficult due to differing methods used to analyze SIA. In the present study, we used the Alpins method for astigmatic analysis, as recommended by the Journal of Cataract and Refractive Surgery and the Journal of Refractive Surgery.[302,303] To the best of our knowledge, our study is the first to report results of SIA using this method of analysis and the first to report results of FE and torque for CCIs in femtosecond laser-assisted cataract surgery. When comparing results in the manual group with studies investigating manual CCIs, results presented in this study revealed to be similar to those previously reported using the Alpins method of analysis.[188,295,304] Also most of the published studies comparing femtosecond and manual CCIs [186,296,297,298,299,300,301] have other limitations, including small sample sizes, fixed incision locations, failure to account for the multitude of factors related to SIA, a lack of incision imaging techniques, and the use of just one laser platform (LenSx, Alcon Laboratories Inc.). In our study, we used the Catalys femtosecond laser platform (Johnson & Johnson Vision). Differences in SIA may exist between the commercially available laser platforms, either because of different incision morphologies or because of different interfaces (liquid versus applanation).

Two different incision locations were analyzed – temporal and superior oblique. SIA was higher in the superior oblique incision group, although this result did not reach statistical significance. This result is in line with previous studies investigating manual incisions.[196,304,295] This difference may be due to the greater distance from the center of the cornea in temporal incisions. In the superior oblique group, similar SIA for superotemporal and superonasal incisions was found, a finding which is both supported[193] and contradicted[295] by other literature.

It is known that SIA depends on factors related to the individual, the surgery type, and the incision characteristics. Correlations between SIA and these factors had not previously been investigated in femtosecond laser-created CCIs. In this study, a positive correlation between SIA and age at time of surgery has been found, which is in accordance with other studies.[65,188] In the manual group, no significant correlations between SIA and any of the investigated variables could be established, except for final incision size ($r = 0.301$, $p = .002$), showing that incision stretching during surgery was a

deciding factor for SIA. For small incision sizes, this finding is in accordance with a study by Chang et al.[188] A positive correlation between SIA and preoperative astigmatism was found in both groups, although this only reached statistical significance in the femtosecond laser group (r = 0.521, $p < .001$). Also in the femtosecond laser group, significant correlations between SIA and several of the studied features were found, including preoperative keratometry (flatter corneas were associated with greater SIA), ACD (deeper anterior chambers associated with lower SIA), axial length (greater AL associated with greater SIA), CD (smaller corneas associated with greater SIA). These findings are in accordance with several studies that investigated manual CCIs.[188,305] Although more associations were possible in the femtosecond group, and a significant multiple regression equation was established, SIA remains a highly unpredictable variable, as shown by the weak positive correlation ($R^2 = .332$) and by the preoperative astigmatism magnitude being the only significant predictor of SIA (p = .003).

The architecture of the incisions using spectral-domain AS-OCT was also compared for both groups. In the manual incision group, tri-planar architecture was only achieved in 28% of the cases, in contrast to 100% of the cases in the femtosecond laser group (p <.001). This result is similar to that reported by Grewal et al.[292] Femtosecond laser-created CCIs showed less deviation from the intended length, more precise location in relation to the limbus, less wound enlargement, lower endothelial misalignment, and fewer Descemet membrane detachments. These results are similar to those reported in previous studies.[291,292,301] Perfect and reproducible wound construction may be important to prevent wound leakage and endophthalmitis.[306] Notably, AS-OCT scans were only carried out 3 months postoperatively in order to avoid corneal edema and to allow the evaluation of the final results with high-quality images.

It needs to be pointed out that the present study has limitations, such as not evaluating SIA at various time points across the follow-up, considering only one incision size, not including corneal biomechanical properties and not considering the influence of the posterior corneal surface on SIA. Thus, further large series evaluating changes at various time points after surgery are warranted.

In summary, we found that comparing femtosecond-created CCIs to manually-created CCIs for both temporal and superior oblique incision locations showed that the femtosecond laser-created CCIs resulted in more reproducible wound architecture and smaller SIA values, although this difference was not statistically significant. Association of SIA with specific individual features remains highly variable. Thus, for each incision meridian, the calculated FE for the specific incision location is recommended for toric IOL calculation.

Chapter 8: General discussion

Cataract surgery is the most frequent surgical procedure in developed countries[1] In recent years, it shifted into a refractive procedure. Preoperative corneal astigmatism is highly prevalent in cataract surgery candidates.[4,5,6] It is recognized that minimizing this astigmatic component at the time of cataract surgery not only increases spectacle independence but also improves visual outcomes.[3,7] So, accurate correction of preexisting astigmatism is mandatory.

Studies show that toric IOLs are the most effective and predictable surgical method for correcting astigmatism.[100] However, with the use of classical toric IOL calculation, only 26 to 35% of the eyes achieve a result within ±0.50 D of residual astigmatism.[11] This result is clearly insufficient, as implantation of aspheric, multifocal or toric IOL designs is ineffective unless minimal postoperative astigmatism is achieved.[13] Moreover, residual astigmatism is one of the main causes of dissatisfaction after multifocal IOL implantation.[137]

Toric IOL implantation is a complex process in which multiple steps must be optimized to minimize errors (Figure 8 – Chapter 2 – 2.4.3.2).

For any IOL power calculation formula knowledge of biometric parameters is essential. The lack of a large study of normative biometric parameters in the Portuguese population encouraged us to investigate such values using optical biometry (Chapter 4). We found a mean AL of 23.87 ± 1.55 mm, a value longer than the ones published in different studies of European populations[5,246,247,248], and closer to the reported in Caucasian populations of the USA[234,243] In the former populations, there is a great similarity in the AL values in different countries; hence, the mean difference in AL we found (about 0.4 mm) is relevant, since a 1 mm error in AL results in a residual postoperative refractive error of 2.35 D in a 23.5 mm eye, 1.75 D in a 30.0 mm eye and 3.75 D in a 20 mm eye, or about 2.0 to 4.0 D in the power of the implanted IOL.[250] The mean ACD in our population (3.25 ± 0.44 mm) was higher than that reported in most studies in Eastern[234,239,242] and in Western populations,[5,234,238,240] and it is comparable with that reported by Hoffer in the USA.[243] The mean keratometry in our study was 43.91 ± 1.71 D. This value is similar to that reported in the Caucasian population in

Europe[246 acima247 acima] and USA.[243,250] We found a mean LT of 4.32 ± 0.49 mm, and a mean CD of 12.02 ± 0.46 mm.

Importantly, in our series, the mean corneal astigmatism was 1.08 ± 0.84 D, with 43.5% of the eyes showing corneal astigmatism ≥ 1 D. These values are higher than those reported in most studies, such as those by Ferrer-Blasco et al.[4] (34.8%) in Spain and by Hoffmann et al. in Germany (36%).[5]

In summary, the obtained AL, ACD, and mean K values were closer to the US population than most published series in different European Caucasian populations, and the disparities found could represent differences greater than 1 D in both refractive error evaluation and IOL power calculation.

Given the high prevalence of astigmatism in our population, it is mandatory to accurately evaluate it. Recent technologies allow the direct measurement of the posterior corneal surface curvature. In this emerging field of research and development, different tomographers for evaluating TCA are available. There is, however, a lack of recognized gold standard.

Between the various technologies of corneal tomography, one of the most widespread is Scheimpflug-based imaging. However, its repeatability for evaluating the posterior corneal surface has been questioned.[288] Color-LED topography (Cassini; i-Optics) is a recent alternative, specifically developed to assess eyes before cataract surgery. Its theoretical principles and advantages are detailed in Chapter 2 – 2.6.3.5. Being a new technology, its precision, repeatability and comparability with other established topographers should be investigated. This was the basis for conducting the studies in Chapter 5 – 5.1 and 5.2.

The goal of the first study (Chapter 5 – 5.1) was to assess the accuracy of corneal astigmatism measured by four techniques: slit-scanning topography (Orbscan IIz), automated keratometry (Lenstar LS900), and color-LED topography (Cassini - anterior corneal surface and TCA), using subjective refraction of pseudophakic eyes as a comparator. We found that, for astigmatism axis, all linear regression analysis models showed a high R^2 (Orbscan < TCA < Lenstar < Cassini), with color-LED topography's TCA

model having the least difference to the unit slope and to a null constant. Regarding astigmatism magnitude, the color-LED topography TCA model showed the highest R^2 (0.808). The regression coefficient was lower for the Lenstar model and was not statistically significant for the Orbscan. This data suggests that evaluating both the anterior and posterior corneal surfaces translates into a more accurate measurement of astigmatism.

Several studies have investigated the comparability and repeatability of different topography devices, including the Cassini, to evaluate corneal power and astigmatism, with contradictory results.[252,253,254,255] None of these studies has compared the Cassini with the Orbscan and the Lenstar. This was the basis for conducting a subsequent study (Chapter 5 – 5.2), where we assessed the comparability and repeatability of these topographic methods. Our agreement analysis for astigmatism magnitude showed that Cassini and Lenstar had the highest mean difference, with agreement between Orbscan and Lenstar showing the highest range of LoA. Comparability was high regarding astigmatism magnitude and axis for all paired devices, except for astigmatism magnitude measured by Cassini compared to Lenstar (ICC=0.798) and Lenstar compared to Orbscan (ICC=0.810). Repeatability was high for all measurement techniques and assessed parameters, with ICC>0.900, except for K2 and J45 measured by Cassini. In conclusion, all measurement techniques showed high comparability regarding K1, K2 and astigmatism axis. However, the wide data spread observed suggests that these devices should not be used interchangeably.

We acknowledge both studies of the color-LED topography device have limitations. Besides the confounders and bias associated with observational studies, and the number of patients needed to achieve a 90% power to assess differences between very similar instruments with small effect differences; the fact that measurements were taken by two technicians, although very experienced and using automatic software; the inherent subjectivity of subjective refraction; and the use of an initial version of the Cassini software was used.

When calculating a toric IOL, studies support considering the predicted ELP, the SE power of the IOL, and the posterior corneal surface to achieve precise results. With this

acknowledgment, new nomograms and mathematical models were developed to account for the effect of the posterior corneal surface when it is not directly measured. It is important to note that many IOL manufacturers still do not include these factors in their toric IOL calculators, despite their recognized importance as factors of error.

We conducted a study (Chapter 6) to compare the original, and still available online, with the recently updated Alcon calculator, incorporating the Barrett toric algorithm. This study showed the advantage of the latter, showing a reduction in the mean prediction error in residual astigmatism of about 50%. This clearly demonstrated the added value of accounting for the ELP, SE power of the IOL and posterior corneal surface when calculation a toric IOL.[272] Given the multitude of new toric calculators available and the absence of studies comparing their results, we saw the necessity to determine the optimal method(s).

In the study on Chapter 6 – 6.1, we compared the prediction error in residual astigmatism of each of the methods listed on table 9 with that of the original Alcon calculator. When applied to the original Alcon calculator, the Baylor nomogram and the Abulafia-Koch formula improved the accuracy of toric IOL calculation, reducing the centroid error in predicted astigmatism (from 0.43 D to 0.35 D and 0.34 D, respectively) and the MAE, although in both cases only the application of the Abulafia-Koch formula reached statistical significance. When the Baylor nomogram and the Abulafia-Koch formula were combined with the Holladay calculator, the results also improved, again showing the advantage of adding ELP to the calculation. The Barrett calculator performed best overall and in subgroups of eyes (WTR and ATR), significantly reducing the MAE compared with the original Alcon calculator, the Holladay calculator, and all the nomogram methods (all $p < .001$). The Barrett toric IOL calculator also resulted in the lowest ATR centroid error of all calculators (0.17 D). This result was not significantly different from that yielded by the Holladay calculator combined with the Abulafia-Koch formula (0.25 D). The ray tracing software yielded a centroid prediction error (0.32 D) similar to that of the original Alcon calculator. These results are in line with those published by Abulafia et al.[177], in which their formula reduced errors to a level similar to that of the Barrett Toric Calculator. In a recent prospective study, Gundersen and Potvin

confirmed the superior results of the Barrett Toric Calculator when compared with standard calculators.[283]

We were somewhat surprised to find that direct measurements of total corneal astigmatism with a Scheimpflug camera had worse results than theoretical models estimating it, so we designed a study (Chapter 6 – 6.2) specifically to compare the calculators that showed the best results in the previous study (6.1) with direct measurements of total corneal power. In this follow-up study, we used the Barrett Toric Calculator and the Abulafia-Koch formula as calculation methods that estimate the power of the posterior corneal surface and a Scheimpflug camera for the direct measurements. Toric IOL cylindrical power calculation was performed through ray tracing and vectorial calculation of total corneal astigmatism (the latter, having previously shown to be the most precise calculation method for toric IOLs when using a Scheimpflug camera).[273] In our study (6.2), both methods of calculation using direct measurements resulted in higher errors in predicted residual astigmatism than methods using estimated data. Although the vectorial calculation software yielded lower errors than the ray tracing calculation, this difference was not statistically significant. Using real measurements, the differences for the estimation methods were higher in WTR than in ATR eyes, indicating that the Pentacam may underestimate the posterior corneal surface power in eyes with WTR astigmatism.[296] Both studies on Chapter 6 have as main limitation their retrospective nature.

Recently, Savini et al. [307] compared the use of keratometric astigmatism, total corneal astigmatism measured with a Scheimpflug camera and a newly developed formula where preoperative corneal astigmatism was optimized by back-calculation from the postoperative refractive astigmatism in toric IOL calculation. Similarly to our studies (Chapter 6), results showed that, compared with direct measurements of TCA, optimization of corneal astigmatism measurements led to more accurate results.[307] Also, the optimization equation showed similar results to the Abulafia-Koch formula and the Barrett toric calculator. In another study, the same group developed a new formula for estimating TCA from anterior corneal data.[308]

Finally, an integral part of any toric IOL calculation is accounting for the SIA, since the postoperative corneal power will be the vectorial combination of the preexisting corneal astigmatism with the one generated by the CCI.[290] Femtosecond laser-created CCIs are highly precise, reproducible, and stable.[291] They are self-sealing due to the near-perfect wound geometry[292]and are potentially subjected to less mechanical trauma during surgery.[290] However, most studies show only a reduction in the SD of mean SIA or in the deviation from the intended SIA axis, although it should be considered that these studies have important limitations.[296-301] The association of SIA with ocular features other than incision size or location is not well known and has not been studied for femtosecond laser-created CCIs.

With the objective of improving knowledge on SIA, we investigated (Chapter 7) SIA in patients who underwent phacoemulsification with CCIs created by femtosecond laser or manually in two different meridians and determined the correlation of SIA with individual features and incision morphology. Temporal and superior oblique 2.4 mm incisions in both groups were addressed. Results revealed that SIA, FE, torque, and the SVM for SIA were lower in the femtosecond laser group for both temporal and superior oblique incisions, although these differences did not reach statistical significance. The femtosecond laser group also showed smaller SDs. As recommended by Alpins et al.[295] , the FE at the incision meridian should be used for toric IOL calculation. In our study, for temporal incisions, the FE was -0.11 D in the femtosecond laser group and -0.13 D in the manual group. For superior oblique incisions, the FE was -0.21 D in the femtosecond laser group and -0.34 D in the manual group. We found a positive correlation between SIA and age at time of surgery, which is in accordance with other studies.[65,188] In the manual group, no significant correlations between SIA and any of the investigated variables could be established, except for final incision size ($r = 0.301$, $p = .002$), showing that incision stretching during surgery was a deciding factor for SIA. A positive correlation between SIA and preoperative astigmatism was found in both groups, although this only reached statistical significance in the femtosecond laser group. Also, in the femtosecond laser group, significant correlations between SIA and several of the studied features were found, including preoperative keratometry (flatter corneas were associated with greater SIA), ACD (deeper anterior chambers associated with lower SIA),

axial length (greater AL associated with greater SIA), and CD (smaller corneas associated with greater SIA). These findings are in accordance with several studies that investigated manual CCIs. [188,305] Although more associations were possible in the femtosecond group, and a significant multiple regression equation was established, SIA remains a highly unpredictable variable, as shown by the weak positive correlation (R^2 = .332) and by preoperative astigmatism magnitude being the only significant predictor of SIA (p = .003).

The architecture of the CCIs was also compared for both groups using AS-OCT. In the manual incision group, triplanar architecture was only achieved in 28% of the cases, in contrast to 100% of the cases in the femtosecond laser group. Femtosecond laser-created CCIs showed less deviation from the intended length, more precise location in relation to the limbus, less wound enlargement, lower endothelial misalignment, and fewer Descemet membrane detachments. These results are similar to those reported in previous studies.[291,292,301] However, this advantage in architecture does not seem to translate in a more predictable SIA. Although this was a prospective randomized trial, its main limitation was investigating SIA at only one time point (3 months) after surgery. Even considering this is enough time for the CCI to stabilize, we admit different results may be obtained at different time points.

Chapter 9: Conclusions

The study results on normative biometric parameters and their relationships in a Portuguese population may be relevant not only in the evaluation of the refractive error but also in IOL calculation for cataract surgery. Interestingly, obtained AL, ACD, and mean K values were closer to the US population than most published series in different European Caucasian populations. The fact that the prevalence of corneal astigmatism in the study was higher than that in most published series may affect the type of IOL to be implanted.

When comparing four measurment techniques (automated keratometry, slit-scanning topography, color-LED topography (anterior corneal and TCA measurements) in cataract surgery candidates, color-LED topography measurements showed higher precision. Also, they showed high repeatability. However, even though the comparability with the other evaluated techniques was high, there was a wide data spread, suggesting these devices should not be used interchangeably. Total corneal measurement with the color-LED topographer seems to be a better technique for astigmatism assessment.

When comparing the new toric IOL calculators, our data showed that the Barrett toric calculator and the application of the Abulafia-Koch formula with the Holladay toric calculator resulted in the lowest astigmatic prediction errors, both overall and in subgroups of eyes (WTR/ATR corneal astigmatism), with small differences between them. Findings from the consecutive study demonstrated that, at present, directly measuring the posterior corneal surface for toric IOL power calculation is not superior to predicting its power with theoretical models or regression formulas. Thus, clinical results of toric IOL implantation may be improved by choosing the Barrett Toric Calculator or the Abulafia-Koch Formula, combined with a strategy to consider ELP as calculation methods.

When comparing femtosecond-created CCIs to manually-created CCIs for temporal and superior oblique incision locations, our results showed that the femtosecond laser-created CCIs resulted in more reproducible wound architecture and smaller SIA values, although the difference for manually-created CCIs was not statistically significant. Association of SIA with specific individual features remains highly variable. Thus, the use

of a centroid or of the calculated FE for the specific incision meridian is recommended for toric IOL calculation.

In conclusion, we would consider it ideal to individualize toric IOL calculation for each particular eye. With this in mind, new technologies such as the color-LED topography we addressed, or other (eg. AS-OCT or intraoperative aberrometry) are promising approaches. Until this becomes possible with high predictability, the use of mathematical models to estimate TCA and a centroid or FE for the specific CCI meridian are the most accurate alternatives when calculating a toric IOL.

Chapter 10: Future directions for research

This thesis leaves the path open for further studies in the near future.

Overall, and keeping in mind research is required to assess the validity and precision of astigmatism measurements obtained with different devices and there is no gold standard to measure astigmatism, the use of several different instruments and the comparison of their results is now the norm. Given its apparent superiority in evaluating TCA, the construction of a formula (and its clinical validation) for estimating TCA from anterior corneal measurements using color-LED topography might be an interesting alternative to generate optimized corneal measurements when these cannot be measure accurately. Such a formula is being created and tested by our study group.

Reflecting the need for better astigmatism measurements, a recent update in the Barrett toric calculator allows the introduction of keratometry values from different instruments and calculates mean or median keratometry values to be used in toric IOL calculation. This "Median K" value seems to improve results of this calculator even more.[309] However, as this update together with new nomograms and formulas to estimate TCA and are being published, there is still a lack of their clinical validation or comparison in prospective trials. Our study group is currently conducting a prospective randomized trial comparing the Barrett toric calculator with direct measurements of TCA by color-LED topography, using its latest software update (v. 2.5).

Although real measurements from the Pentacam in our study (6.2) yielded higher astigmatic prediction errors than estimation methods, new technologies, such color-LED topography, AS-OCT, or intraoperative aberrometry, may yield different results. Studies investigating results of these methods on toric IOL implantation are, therefore, warranted.

SIA remains a highly unpredictable factor in toric IOL power calculation, given its high variability, even in FLACS. We proposed values for using in toric IOL calculation. Accuracy of these values for toric IOL calculation should be investigated in future prospective trials. Also, studies with larger series of patients and other incision meridians are necessary.

List of Figures

Figure 1 - Graphical representation an eye with astigmatism

Figure 2 - A) illustrates the interval of Sturm, the circle of least confusion and the retinal images of a circular spot when astigmatism is induced. (B) astigmatic foci in a myopic with-the-rule astigmat. (C) in a myopic against-the-rule astigmat.

Figure 3 - Correlation between the magnitude of posterior corneal astigmatism and keratometric astigmatism.

Figure 4 - Location of steep meridian on anterior and posterior corneal surfaces.

Figure 5 - Magnitude of astigmatism on the anterior corneal surface and posterior corneal surface grouped according to the orientation of the steep meridian on the anterior cornea.

Figure 6 - Distributions of different kinds of astigmatism by age group.

Figure 7 - Diagram illustrating the surgical techniques for the correction of astigmatism.

Figure 8 - Steps involved in the pre-, intra- and postoperative study for implanting a toric IOL.

Figure 9 - Diagram demonstrating the principle of vector analysis of the change in the astigmatic refraction following surgery.

Figure 10 - Graphic representation of vectors M, J0, J45, and B.

Figure 11- differences between single- and doubled-angle plots for reporting astigmatism data.

Figure 12 - A: Polar astigmatism diagram, B: Double-angle vector diagram (DAVD) C: Polar surgical vector diagram.

Figure 13 - : Polar analysis of vectors. A: Multiple vectors are present on a polar diagram at their actual orientation, as they would appear on an eye. B: vectors on a DAVD.

Figure 14 - The Placido disk.

Figure 15 - Elevation data of a cornea with regular astigmatism with a best-fit-sphere as reference.

Figure 16 - Diagram of forward ray tracing model.

Figure 17 - Histogram of axial length (AL) of the study population.

Figure 18 - Histogram of mean keratometry (K) of the study population.

Figure 19 - Histogram of corneal astigmatism of the study population.

Figure 20 - Histogram of anterior chamber depth (ACD) of the study population.

Figure 21 - Histogram of lens thickness (LT) of the study population.

Figure 22 - Histogram of corneal diameter (CD) of the study population.

Figure 23 - Distribution of corneal astigmatism in the study population.

Figure 24 - Bland-Altman plots for astigmatism axis, J0 and J45.

Figure 25 - Linear regression models for astigmatism axis assessment by Total Cassini, Cassini, Orbscan and Lenstar Methods.

Figure 26 - Linear regression models for astigmatism values assessment by Total Cassini, Cassini, Orbscan and Lenstar Methods in patients with axis difference ≤5 degrees.

Figure 27 - Centroids of the difference between each method of assessment and the subjective value of vectors J0 and J45.

Figure 28 - Bland–Altman plots for astigmatism axis, astigmatism magnitude and Km.

Figure 29 - Double-angle plots illustrating the centroid prediction errors in residual astigmatism

Figure 30 - Double-angle plots of the prediction errors for the investigated calculation methods.

Figure 31 - Percentage of eyes within 0.25 D, 0.50 D, 0.75 D and 1.00 D of absolute astigmatic prediction error with each calculation method.

Figure 32 - Measurements on AS-OCT images (incision length, peripheral corneal thickness and distance to the limbus).

Figure 33 - Summated vector mean values of surgically induced astigmatism in the studied groups.

Figure 34 - Histograms of corneal astigmatism before and after surgery in the studied groups.

List of Tables

Table 1: Demographic data and mean ocular biometric parameters in Portuguese population.

Table 2: Matrix of correlations of ocular biometric parameters in Portuguese population

Table 3: Mean values of biometric parameters published in previous studies.

Table 4: Comparison between astigmatism assessment methods.

Table 5: Comparison between assessment methods for patients with difference in axis equal or less than |10º|.

Table 6: J0 and J45 vectors assessed by Total Cassini, Cassini, Orbscan and Lenstar.

Table 7: Descriptive statistics.

Table 8: Repeatability and comparability.

Table 9 - Toric IOL calculation methods compared in the study.

Table 10 - Patient demographics and clinical information.

Table 11 - Mean absolute error in predicted residual astigmatism.

Table 12 - Centroid error in predicted residual astigmatism.

Table 13 - Mean absolute and centroid errors in predicted residual astigmatism in eyes with WTR and ATR corneal astigmatism.

Table 14 - Patient demographics

Table 15 - Mean Absolute Error on Predicted Residual Astigmatism

Table 16 - Centroid Error in Predicted Residual Astigmatism

Table 17 - Mean Absolute and Centroid Errors in Predicted Residual Astigmatism for Eyes With Corneal Astigmatism

Table 18 – Patient demographics and Clinical Information

Table 19 – SIA Vector, Flattening Effect, and Torque in the Femtosecond Laser and Manual Clear Cornea Incision Groups

Table 20 – Correlation Between Surgically Induced Astigmatism Magnitude and Individual Parameters

Table 21 – Clear Corneal Incision Architecture Evaluated by Anterior Segment OCT

Table 22 – Summary of the Published Studies Comparing SIA in Femtosecond Laser and Manual Clear Corneal Incisions for Cataract Surgery

References

[1] Taylor HR. Cataract: how much surgery do we have to do? Br J Ophthalmol 2000;84:1-2.

[2] Koch DD, Hill W, Abulafia A, Wang L. Pursuing perfection in intraocular lens calculations: I. Logical approach for classifying IOL calculation formulas. J Cataract Refract Surg. 2017 Jun;43(6):717-718.

[3] Lundström M, Dickman M, Henry Y, Manning S, Rosen P, Tassignon MJ, Young D, Stenevi U. Risk factors for refractive error after cataract surgery: Analysis of 282 811 cataract extractions reported to the European Registry of Quality Outcomes for cataract and refractive surgery. J Cataract Refract Surg. 2018 Apr;44(4):447-45.

[4] Ferrer-Blasco T, Montes-Mico R, Peixoto-de-Matos SC, Gonzalez-Meijome JM, Cervino A. Prevalence of corneal astigmatism before cataract surgery. J Cataract Refract Surg. 2009;35(1):70-75.

[5] Hoffmann PC, Hutz WW. Analysis of biometry and prevalence data for corneal astigmatism in 23,239 eyes. J Cataract Refract Surg. 2010;36(9):1479-1485.

[6] Khan MI, Muhtaseb M. Prevalence of corneal astigmatism in patients having routine cataract surgery at a teaching hospital in the United Kingdom. J Cataract Refract Surg. 2011;37(10):1751-1755.

[7] Villegas EA, Alcon E, Artal P. Minimum amount of astigmatism that should be corrected. J Cataract Refract Surg. 2014;40(1):13-19.

[8] Laurendeau C, Lafuma A, Berdeaux G. Modelling lifetime cost consequences of toric compared with standard IOLs in cataract surgery of astigmatic patients in four European countries. J Med Econ. 2009;12(3):230-237.

[9] Melles RB, Holladay JT, Chang WJ. Accuracy of Intraocular Lens Calculation Formulas. Ophthalmology. 2018;125(2):169-178.

[10] Kane JX, Van Heerden A, Atik A, Petsoglou C. Accuracy of 3 new methods for intraocular lens power selection. J Cataract Refract Surg. 2017;43(3):333-339.

[11] Abulafia A, Barrett GD, Kleinmann G, Ofir S, Levy A, Marcovich AL et al. Prediction of refractive outcomes with toric intraocular lens implantation. J Cataract Refract Surg. 2015;41(5):936-44.

[12]Teus MA, Arruabarrena C, Hernández-Verdejo JL, Sales-Sanz A, Sales-Sanz M. Correlation between keratometric and refractive astigmatism in pseudophakic eyes. J Cataract Refract Surg. 2010;36(10):1671-5.

[13] Hayashi K, Hayashi H, Nakao F, Hayashi F. Influence of astigmatism on multifocal and monofocal intraocular lenses. Am J Ophthalmol 2000;130:477-482.

[14] Meyer CH. Anatomie und Physiologie des Auges, Auge und Innere Medizin. Tischendorf FW, Meyer CH, Spraul CW. Schattauer, Stuttgart 2004, ISBN 3-7945-2240-0.

[15] Crisp WH. Edward Jackson's place in the history of refraction. Am J Ophthalmol 1945;28(1):1–12.

[16] Jackson E. Trial set of small lenses, and a modified trial-frame. Trans Am Ophthalmol Soc. 1887;4:595–598.

[17] Jackson E. Symmetrical aberration of the eye. Trans Am Ophthalmol Soc. 1888;5:141.

[18] Jackson E. Value of the ophthalmometer in practical refraction work. Trans Am Ophthalmol Soc. 1894;7:177–180.

[19] DelMonte DW, Kim T. Anatomy and physiology of the cornea. J Cataract Refract Surg. 2011;37:588-598.

[20] Dua HS, Faraj LA, Said DG, Gray T, Lowe J. Human corneal anatomy redefined: a novel pre-Descemet's layer (Dua's layer). Ophthalmology. 2013;120(9):1778-85.

[21] Barishak YR. Embryology of the eye and its adnexae. Dev Ophthalmol. 1992;24:1-142.

[22] Fares U, Otri AM, Al-Aqaba MA, Dua HS. Correlation of central and peripheral corneal thickness in healthy corneas. Cont Lens Anterior Eye. 2012;35:39-45.

[23] Meek KM, Boote C. The organisation of collagen in the corneal stroma. Exp Eye Res. 2004;78:503-12.

[24] Meek KM, Knupp C. Corneal structure and transparency. Prog Retin Eye Res. 2015;49:1-6.

[25] Boote C, Dennis S, Newton RH, Puri H, Meek KM. Collagen fibrils appear more closely packed in the prepupillary cornea: Optical and biomechanical implications. Invest Ophthalmol Vis Sci 2003. 44:2941-8.

[26] Bourne WM, Nelson LR, Hodge DO. Central corneal endothelial cell changes over a ten year period. Invets Ophthalmol Vis Sci. 1997;38:779-82.

[27] Rio-Cristobal A, Martin R. Corneal assessment technologies: Current status. Surv Ophthalmol. 2014;59:599-614.

[28] Sridhar MS. Anatomy of cornea and ocular surface. Indian J Ophthalmol. 2018,66:190-194.

[29] Cerviño A, Hosking SL, Montes-Mico R, Bates K. Clinical ocular wavefront analyzers. J Refract Surg. 2007;23(6):603-16.

[30] Howarth PA, Bradley A. The longitudinal chromatic aberration of the human eye, and its correction. Vision Res. 1986;26(2):361-6.

[31] Lombardo M, Lombardo G. Wave aberration of human eyes and new descriptors of image optical quality and visual performance. J Cataract Refract Surg. 2010;36(2):313-31.

[32] Basic and Clinical Science Course, Section 13: Refractive Surgery (2011-2012. ed.). American Academy of Ophthalmology. 2011–2012. pp. 7–9. ISBN 978-1615251209.

[33] Lawless MA, Hodge C. Wavefront's role in corneal refractive surgery. Clin Exp Ophthalmol. 2005 Apr;33(2):199-209.

[34] Kaimbo DKW (2012). Astigmatism – Definition, Etiology, Classification, Diagnosis and Non-Surgical Treatment, Astigmatism – Optics, Physiology and Management, Dr. Michael Goggin (ed), ISBN:978-953-51-0230-4.

[35] Shankar S, Bobier WR. Corneal and lenticular components of total astigmatism in a preschool sample. Optom Vis Sci. 2004;81(7):536-42.

[36] Vaughn LW, Schepens CL. Progressive lenticular astigmatism associated with nuclear sclerosis and coloboma of the iris, lens, and choroid: case report. Ann Ophthalmol. 1981;13(1):25-27.

[37] Korynta J, Bok J, Cendelin J, Michalova K. Computer modeling of visual impairment caused by intraocular lens misalignment. J Cataract Refract Surg. 1999;25(1):100–105.

[38] Mitchell DE, Freeman RD, Westheimer G. Effect of orientation on the modulation sensitivity for interference fringes on the retina. J Opt Soc Am. 1967;57(2):246-9.

[39] Flüeler UR, Guyton DL. Does a tilted retina cause astigmatism? The ocular imagery and the retinoscopic reflex resulting from a tilted retina. Surv Ophthalmol. 1995;40(1):45-50.

[40] Marcos S, Werner JS, Burns SA, Merigan WH, Artal P, Atchison DA et al. Vision science and adaptive optics, the state of the field. Vision Res. 2017;132:3-33.

[41] Marcos S, Velasco-Ocana M, Dorronsoro C, Sawides L, Hernandez M, Marin G. Impact of astigmatism and high-order aberrations on subjective best focus. Journal of Vision. 2015;15(11)4:1-12.

[42] Yoon G., Pantanelli S., MacRae S. Comparison of Zernike and Fourier wavefront reconstruction algorithms in representing corneal aberration of normal and abnormal eyes. J Refract Surg. 2008;24(6):582-590.

[43] Huang D, Arif M. Spot size and quality of scanning laser correction of higher-order wavefront aberrations. J Cataract Refract Surg. 2002;28:407–16.

[44] Levy Y., Segal O, Avni I, Zadok D. Ocular higher-order aberrations in eyes with supernormal vision. Am J Ophthalmol. 2005;139: 225–228.

[45] Basic and Clinical Science Course, Section 3: Clinical Optics (2011-2012 last major rev. 2010-2012. ed.). American Academy of Ophthalmology. 2011–2012. p. 100. ISBN 978-1615251100.

[46] Bottos KM, Leite MT, Aventura-Isidro M, Bernabe-Ko J, Wongpitoonpiya N, Ong-Camara NH, Purcell TL, Schanzlin DJ. Corneal asphericity and spherical aberration after refractive surgery. J Cataract Refract Surg. 2011;37(6):1109-15.

[47] Karimian F, Feizi S, Doozande A. Higher-order aberrations in myopic eyes. J Ophthalmic Vis Res. 2010;5(1):3-9.

[48] Sakai H, Hirata Y, Usui S. Relationship between residual aberration and light-adapted pupil size. Optom Vis Sci. 2007;84(6):517-21.

[49] de Gracia P, Dorronsoro C, Gambra E, Marin G, Hernández M, Marcos S. Combining coma with astigmatism can improve retinal image over astigmatism alone. Vision Res. 2010;50(19):2008-14.

[50] Ho JD, Tsai CY, Liou SW. Accuracy of corneal astigmatism estimation by neglecting the posterior corneal surface measurement.Am J Ophthalmol. 2009;147(5):788-95.

[51] Savini G, Versaci F, Vestri G, Ducoli P, Næser K. Influence of posterior corneal astigmatism on total corneal astigmatism in eyes with moderate to high astigmatism. J Cataract Refract Surg. 2014;40(10):1645-53.

[52] Koch DD, Ali SF, Weikert MP, et al. Contribution of posterior corneal astigmatism to total corneal astigmatism. J Cataract Refract Surg. 2012;38:2080–7.

[53] Tonn B., et al. Anterior surface based keratometry compared with Scheimpflug tomography-based total corneal astigmatism. Invest Ophthalmol Vis Sci. 2014;56(1):291-298.

[54] LaHood BR, Goggin M. Measurement of Posterior Corneal Astigmatism by the IOLMaster 700. J Refract Surg. 2018;34(5):331-336.

[55] Tianyu Zheng, Zhanghua Chen, Yi Lu. Influence factors of estimation errors for total corneal astigmatism using keratometric astigmatism in patients before cataract surgery. J Cataract Refract Surg. 2016; 42:84–94.

[56] Kamiya K., et al. Assessment of anterior, posterior, and total corneal astigmatism in eyes with keratoconus. Am J Ophthalmol. 2015;5:851-857.e1.

[57] Feizi S, Delfazayebaher S, Javadi MA, Karimian F, Ownagh V, Sadeghpour F. Mean Posterior Corneal Power and Astigmatism in Normal Versus Keratoconic Eyes. J Ophthalmic Vis Res. 2018;13(2):93-100.

[58] Anstice J. Astigmatism—its components and their changes with age. Am J Optom Arch Am Acad Optom. 1971;48:1001–1006.

[59] Gudmundsdottir E, Arnarsson A, Jonasson F. Five-year refractive changes in an adult population: Reykjavik eye study. Ophthalmology. 2005;112: 672–677.

[60] Hayashi K, Hayashi H, Hayashi F. Topographic analysis of the changes in corneal shape due to ageing. Cornea. 1995;14:527–532.

[61] Goto T, Klyce SD, Zheng X, et al. Gender and age-related differences in corneal topography. Cornea. 2001;20:270–276.

[62] Lin LL, Shih YF, Lee YC, Hung PT, Hou PK.. Changes in ocular refraction and its components among medical students-a 5-year longitudinal study. Optom Vis Sci. 1996;73 (7), 495-8.

[63] Ho JD, Liou SW, Tsai RJ, Tsai CY. Effects of aging on anterior and posterior corneal astigmatism. Cornea. 2010;29(6):632-7.

[64] Naeser K, Savini G, Bregnhøj JF. Age-related changes in with-the-rule and oblique corneal astigmatism. Acta Ophthalmol. 2018 Jan 25. doi: 10.1111/aos.13683. [Epub ahead of print]

[65] Hayashi K, Ogawa S, Manabe SI & Hirata A. Influence of patient age at surgery on long-term corneal astigmatic change subsequent to cataract surgery. Am J Ophthalmol 2015;160: 171–178.

[66] Hayashi K, Manabe SI, Hirata A, Yoshimura K. Changes in corneal astigmatism during 20 years after cataract surgery. J Cataract Refract Surg .2017;43: 615–621.

[67]Arzu Taskiran Comez and Yelda Ozkurt (2012). Surgical Correction of Astigmatism During Cataract Surgery, Astigmatism - Optics, Physiology and Management, Dr. Michael Goggin (Ed.), ISBN: 978-953-51-0230-4, InTech, Available from: http://www.intechopen.com/books/astigmatism-optics-physiology-and- management/correction-of-astigmatism-during-cataract-surgery.

[68] Nichamin, L.D. Astigmatism control. Ophthalmol Clin N Am. 2006;19:485–493

[69] Budak, K. Yılmaz G, Aslan BS, Duman S. Limbal relaxing incisions in congenital astigmatism: 6 month follow-up. J Cataract Refract Surg. 2001;27:715–719.

[70] Coloma-González I, González-Herrera M, Mengual-Verdú E, Hueso-Abacens JR Incisiones limbares relajantes y cirugía de la catarata: nuestra experiencia [Limbal relaxing incisions and cataract surgery: our experience]. Arch Soc Esp Oftalmol. 2007;82:551–554.

[71] Hirnschall N, Wiesinger J, Draschl P, Findl O. Factors Influencing Efficacy of Peripheral Corneal Relaxing Incisions during Cataract Surgery. Journal of Ophthalmology. Volume 2015, Article ID 706508, 6 pages.

[72] Qammar A, Mullaney P. Paired opposite clear corneal incisions to correct preexisting astigmatism in cataract patients. J Cataract Refract Surg. 2005;31:1167-70.

[73] Medicute J, Irigoyen C, Ruiz M, Illarramendi I, Ferrer-Blasco T, Montes-Mico R. Toric intraocular lenses versus opposite clear corneal incisions to correct astigmatism in eyes having cataract surgery. J Cataract Refract Surg. 2009;35:451-458.

[74] Kim P, Sutton GL, Rootman DS. Applications of the femtosecond laser on corneal refractive surgery. Curr Opin Opthalmol. 2011;22:238-244.

[75] Dick HB, Schultz T. A Review of Laser-Assisted Versus Traditional Phacoemulsification Cataract Surgery. Ophthalmology and Therapy. 2017;6:7–18.

[76] Wetterstrand O, Holopainen JM, Krootila K. Femtosecond Laser-Assisted Intrastromal Relaxing Incisions After Penetrating Keratoplasty: Effect of Incision Depth. J Refract Surg. 2015;31:474–9.

[77] Chang JSM. Femtosecond laser-assisted astigmatic keratotomy: a review. Eye and Vision. 2018;5:6.

[78] Jin GJC, Merkley KH, Crandall AS, Jones YJ. Laser in situ keratomileusis versus lens based surgery for correcting residual refractive error after cataract surgery. J Cataract Refract Surg. 2008;34:562-569.

[79] Zaldivar R, Davidorf JM, Oscerow S et al. Combined posterior chamber phakic intraocular lens and laser in situ keratomileusis. Bioptics for extreme myopia. J Refract Surg. 1999;15:299-308.

[80] Nejima R, Miyata K, Tanabe T, et al. Corneal barrier function, tear fim stability, and corneal sensation after photorefractive keratectomy and laser in situ keratomileusis. Am J Opthalmol. 2005;139:64-71.

[81] Patel S, Alió J, Walewska A, et al. Patient age, refractive index of the corneal stroma, and outcomes of uneventful laser in situ keratomileusis. J Cataract Refract Surg. 2013;39:386-392.

[82] Chamon W., Alleman N. Refractive Surgery Outcomes and Frequency of Complications. In: Alió JL, Azar DT (eds) Management of Complications in Refractive Surgery. Springer Berlin Heidelberg 2008:1-8.

[83] Shimizu KA, Misawa et al. Toric intraocular lenses: correcting astigmatism while controlling axis shift. J Cataract Refract Surg, 1994;20(5): 523-6.

[84] Lombardo M, Carbone G, Lombardo G, De Santo MP, Barberi R. Analysis of intraocular lens surface adhesiveness by atomic force microscopy. J Cataract Refract Surg. 2009 Jul;35(7):1266-72.

[85] Oshika T, Nagata T, Yshii Y. Adhesion of lens capsule to intraocular lenses of polymethylmethacrylate, silicone, and acrylic foldable materials: an experimental study. Br J Ophthalmol. 1998;82(5): 549-53.

[86] Ahmed, II, G. Rocha, et al.. Visual function and patient experience after bilateral implantation of toric intraocular lenses. J Cataract Refract Surg. 2010;36(4): 609-16.

[87]Alió JL, Agdeppa MC, Pongo VC, El Kady B. Microincision cataract surgery with toric intraocular lens implantation for correcting moderate and high astigmatism: pilot study. J Cataract Refract Surg. 2010 Jan;36(1):44-52.

[88]Holland E, Lane S, Horn JD, Ernest P, Arleo R, Miller KM. The AcrySof Toric intraocular lens in subjects with cataracts and corneal astigmatism: a randomized, subject-masked, parallel-group, 1-year study. Ophthalmology. 2010 Nov;117(11):2104-11.

[89] Patel CK., Ormonde S, et al. Postoperative intraocular lens rotation: a randomized comparison of plate and loop haptic implants.Ophthalmology. 1999;106(11): 2190-5; discussion 2196.

[90] Chang DF. Comparative rotational stability of single-piece open-loop acrylic and plate-haptic silicone toric intraocular lenses. J Cataract Refract Surg. 2008 Nov;34(11):1842-7.

[91] Sheppard AL., Wolffsohn JS, Bhatt U, Hoffmann PC, Scheider A, Hütz WW, Shah S. Clinical outcomes after implantation of a new hydrophobic acrylic toric IOL during routine cataract surgery. J Cataract Refract Surg. 2013;39:41–47.

[92] Pérez-Vives C, Ferrer-Blasco T, Madrid-Costa D, García-Lázaro S, Montés-Micó R. Optical quality of aspheric toric intraocular lenses at different degrees of decentering. Graefes Arch Clin Exp Ophthalmol. 2014;252:969–975

[93] Buckhurst PJ, Wolffsohn JS, Davies LN Naroo. SA Surgical correction of astigmatism during cataract surgery. Clin Exp Optom. 2010;93:409–418.

[94] Mertens E. Evaluation of a new toric IOL optic by means of intraoperative wavefront aberrometry (ORA System): the effect of IOL misalignment on cylinder reduction. Paper presented at: the 2014 European Society of Cataract and Refractive Surgeons meeting; September 13-17, 2014; London.

[95] Denoyer A, Le Lez M-L, Majzoub S, Pisella PJ. Quality of vision after cataract surgery after Tecnis Z9000 intraocular lens implantation; effect of contrast sensitivity and wavefront aberration improvements on the quality of daily vision. J Cataract Refract Surg. 2007; 33: 210–216

[96] Rocha KM, Soriano ES, Chalita MR, Yamada AC, Bottós K, Bottós J, Morimoto L, Nosé W. Wavefront analysis and contrast sensitivity of aspheric and spherical intraocular lenses: a randomized prospective study. Am J Ophthalmol. 2006; 142: 750–756

[97] Altmann GE, Nichamin LD, Lane SS, Pepose JS. Optical performance of 3 intraocular lens designs in the presence of decentration. J Cataract Refract Surg. 2005;31: 574–585

[98] Sandoval HP, Fernández de Castro LE, Vroman DT, Solomon KD. Comparison of visual outcomes, photopic contrast sensitivity, wavefront analysis, and patient satisfaction following cataract extraction and IOL implantation: aspheric vs spherical acrylic lenses. Eye. 2008; 22: 1469–1475.

[99] Pieh S, Fiala W, Malz A, Stork W. In vitro Strehl ratios with spherical, aberration-free, average, and customized spherical aberration-correcting intraocular lenses. Invest Ophthalmol Vis Sci. 2009; 50: 1264–1270.

[100] Kessel L, Andresen J, Tendal B, Erngaard D, Flesner P, Hjortdal J. Toric Intraocular Lenses in the Correction of Astigmatism During Cataract Surgery: A Systematic Review and Meta-analysis. Ophthalmology. 2016;123(2):275-86.

[101] Ouchi M, Kinoshita S. AcrySof IQ toric IOL implantation combined with limbal relaxing incision during cataract surgery for eyes with astigmatism >2.50 D. J Refract Surg. 2011 Sep;27(9):643-7.

[102] Mardia, K.V. Statistics of Directional Data. Academic Press, London; 1972.

[103] Stokes GG (1849). Transactions of 19th meeting of the British Association for the Advancement of Science, published London 1850.

[104] Naylor EJ. Astigmatic difference in refractive errors. Br J Ophthalmol, 1968;52:422–425.

[105] Jaffe NS, Clayman HM. The pathophysiology of corneal astigmatism after cataract extraction. Trans Am Acad Ophthalmol Otolaryngol, 1975;79:615–630.

[106] Thibos LN The new visual optics (editorial). Optom Vis Sci. 1997;74:465–466.

[107] Thibos LN, Horner D. Power vector analysis of the optical outcome of refractive surgery. J Cataract Refract Surg.2001;27(1):80-5.

[108] de Oliveira Freitas G, Ambrósio R, Ruiz Alves M. Vector analysis of astigmatism according to the methods of Alpins and Thibos: a systematic review. e-Oftalmo.CBO: Rev Dig Oftalmol. 2016;2(3):1-6.

[109] Thibos LN, Wheeler W, Horner D. Power vectors: an application of Fourier analysis to the description and statistical analysis of refractive error. Optom Vis Sci. 1997;74(6):367-75.

[110] Holladay JT, Cravy TV, Koch DD. Calculating the surgically induced refractive change following ocular surgery. J Cataract Refract Surg 1992; 18:429–443.

[111] Holladay JT, Dudeja DR, Koch DD. Evaluating and reporting astigmatism for individual and aggregate data. J Cataract Refract Surg 1998; 24:57–65.

[112] Holladay JT, Moran JR, Kezirian GM. Analysis of aggregate surgically induced refractive change, prediction error, and intraocular astigmatism. J Cataract Refract Surg. 2001 Jan;27(1):61-79.

[113] Alpins NA. A new method of analyzing vectors for changes in astigmatism. J Cataract Refract Surg. 1993;19:524-533.

[114] Alpins NA, Goggin M. Practical astigmatism analysis for refractive outcomes in cataract and refractive surgery. Surv Ophthalmol 2004; 49:109-122.

[115] Alpins NA. Vector analysis of astigmatism changes by flattening, steepening, and torque. J Cataract Refract Surg. 1997;23:1503-1514.

[116] Ferreira TB, Ribeiro FJ, Pinheiro J, Ribeiro P, O'Neill JG. Comparison of Surgically Induced Astigmatism and Morphologic Features Resulting From Femtosecond Laser and Manual Clear Corneal Incisions for Cataract Surgery. J Refract Surgery, 2018; 34(5):322-329.

[117] Naeser K, Hjortdal JO. Bivariate analysis of surgically induced regular astigmatism. Mathematical analysis and graphical display.Ophthalmic Physiol Opt. 1999 Jan;19(1):50-61.

[118] Naeser K. Assessment and statistics of surgically induced astigmatism. Acta Ophthalmol. 2008 May;86 Suppl 1:5-28..

[119] Kohnen T, Kook D, Auffarth GU, Derhartunian V. Einsatzmoglichkeiten intraokularer Multifokallinsen und Kriterien der Patientenselektion [Use of multifocal intraocular lenses and criteria for patient selection].Ophthalmologe 2008; 105:527–532

[120] Patient selection and education. In: Chang DF, ed, Mastering Refractive IOLs; The Art and Science. Thorofare, NJ, Slack, 2008; 331–431.

[121] Visser N, Bauer N, Nuijts R. Toric intraocular lenses: Historical overview, patient selection, IOL calculation, surgical techniques, clinical outcomes, and complications. J Cataract Refract Surg 2013; 39:624–637.

[122] Visser N, Gast STJM, Bauer NJC, Nuijts RMMA. Cataract surgery with toric intraocular lens implantation in keratoconus: a case report. Cornea 2011; 30:720–723.

[123] Yu Y, Hua H, Wu M, et al., Evaluation of dry eye after femtosecond laser-assisted cataract surgery, J Cataract Refract Surg, 2015;41:2614–23.

[124] The definition and classification of dry eye disease: Report of the Definition and Classification Subcommittee of the International Dry Eye WorkShop (2007). Ocul Surf 2007;5:75‐92.

[125] Weisenthal RW, Afshari NA, Bouchard CS, Colby KA, Rootman DS,Tu EY, et al. Examination techniques for the external eye and cornea.In: External Disease and Cornea, Basic and Clinical Science Course. Sec. 8. Singapore: American Academy of Ophthalmology; 2013. p. 11‐36.

[126] Binkhorst RD. The accuracy of ultrasonic measurement of the axial length of the eye. Ophthalmic Surg 1981;12:363–365.

[127] Seres A, Németh J, Süveges I. Unexpected ametropia after intraocular lens implantation: the role of different factors of ultrasound biometry and surgery. Doc Ophthalmol Proc Ser 1997; 61:415–420.

[128] Olsen T, Nielsen PJ. Immersion versus contact technique in the measurement of axial length by ultrasound. Acta Ophthalmol 1989; 67:101–102.

[129] Haigis W, Lege B, Miller N, Schneider B. Comparison of immersion ultrasound biometry and partial coherence interferometry for intraocular lens calculation according to Haigis. Graefes Arch Clin Exp Ophthalmol 2000; 238:765–773.

[130] Drexler W, Findl O, Menapace R, et al. Partial coherence interferometry: a novel approach to biometry in cataract surgery [letter]. Am J Ophthalmol 1998; 126: 524 –534.

[131] Kiss B, Findl O, Menapace R et al. Refractive outcome of cataract surgery using partial coherence interferometry and ultrasound biometry. Clinical feasibility study of a commercial prototype II. J Cataract Refract Surg 2002; 28:230–234.

[132] Németh J, Fekete O, Pesztenlehrer N. Optical and ultrasound measurement of axial length and anterior chamber depth for intraocular lens power calculation. J Cataract Refract Surg 2003; 29:85–88.

[133] Nagpal KM, Desai C, Trivedi RH, et al. Is pseudophakic astigmatism a desirable goal? Indian J Ophthalmol 2000;48:213-6.

[134] Nanavaty MA, Vasavada AR, Patel AS, et al. Analysis of patients with good uncorrected distance and near vision after monofocal intraocular lens implantation. J Cataract Refract Surg 2006;32:1091-7.

[135] Singh A, Pesala V, Garg P, Bharadwaj SR. Relation between uncorrected astigmatism and visual acuity in pseudophakia. Optom Vis Sci 2013;90:378-84

[136] Zheleznyak L, Kim MJ, MacRae S, Yoon G. Impact of corneal aberrations on through-focus image quality of presbyopia-correcting intraocular lenses using an adaptive optics bench system. J Cataract Refract Surg 2012;38:1724-33.

[137] de Vries NE, Webers CAB, Touwslager WRH, et al. Dissatisfaction after implantation of multifocal intraocular lenses. J Cataract Refract Surg 2011;37:859-65.

[138] Nemeth J, Erdelyi B, Csakany B. Corneal topography changes after a 15 second pause in blinking. ~~J Cataract~~ Refract Surg 2001;27:589-92.

[139] Dursun D, Monroy D, Knighton R, et al. The effects of experimental tear film removal on corneal surface regularity and barrier function. Ophthalmology 2000;107:1754-60.

[140] Dursun D, Piniella AM, Pflugfelder SC. Pseudokeratoconus caused by rosacea. Cornea 2001;20:668-9

[141] Gutmark R, Guyton DL. Origins of the Keratometer and its Evolving Role in Ophthalmology. Survey of Ophthalmology 2010;55(5):481-497.

[142] Elliott, M., Callender, M.G., and Elliott, D.B. Accuracy of Javal's rule in determining spectacle astigmatism. Optom Vis Sci. 1994; 71: 23–26

[143] Lenstar LS 900® Biometer Instruction Manual, Section 4.3.2. Haag-Streit AG, Koeniz, Switzerland.

[144] Laursen JV, Jeppesen P, Olsen T. Precision of 5 different keratometry devices. Int Ophthalmol 2016; 36:17-20

[145] Huerva V, Ascaso FJ, Soldevila J, Lavilla L. Comparison of anterior segment measurements with optical low-coherence reflectometry and rotating dual Scheimpflug analysis. J Cataract Refract Surg 2014; 40:1170-1176.

[146] Potvin R, Gundersen KG, Masket S, Osher RH, Snyder ME, Vann R, Solomon KD, Hill WE. Prospective multicenter study of toric IOL outcomes when dual zone automated keratometry is used for astigmatism planning. J Refract Surg 2013; 29:804-809.

[147] Ferreira TB, Hoffer KJ, Ribeiro F, Ribeiro P, O'Neill JG. Ocular biometric measurements in cataract surgery candidates in Portugal. PLoS ONE 12(10):e0184837

[148] Ferreira TB, Ribeiro FJ. A novel color-LED corneal topographer to assess astigmatism in pseudophakic eyes. Clinical Ophthalmology 2016;10:1521-1529.

[149] Ferreira TB, Ribeiro FJ. Comparability and repeatability of different methods of corneal astigmatism assessment. Clinical Ophthalmology 2018;12:29-34.

[150] Ferreira TB, Ribeiro P, Ribeiro FJ, O'Neill JG. Comparison of astigmatic prediction errors associated with new calculation methods for toric intraocular lenses. J Cataract Refract Surg 2017;43:340-347.

[151] Ferreira TB, Ribeiro P, Ribeiro FJ, O'Neill JG. Comparação do erro de predição do astigmatismo residual entre dois calculadores de uma lente intraocular tórica. Oftalmologia 2017;41(4):55-62.

[152] Ferreira TB, Ribeiro P, Ribeiro FJ, O'Neill JG. Comparison of Methodologies Using Estimated or Measured Values of Total Corneal Astigmatism for Toric Intraocular Lens Power Calculation. J Refract Surg 2017;33:794-800.

[153] Martin R. Cornea and anterior eye assessment with placido-disc keratoscopy, slit scanning evaluation topography and Scheimpflug imaging topography. Indian J Ophthalmol 2018;66:360-6.

[154] Cavas-Martínez F, De la Cruz Sánchez E, Nieto Martínez J, Fernández Cañavate FJ, Fernández-Pacheco DG. Corneal topography in keratoconus: state of the art. Eye Vis (Lond). 2016 Feb 22;3:5.

[155] Belin MW. Khachikian SS. An introduction to understanding elevation-based topography: how elevation data are displayed – a review. Clinical & Experimental Ophthalmology 2009;37:14-29.

[156] Pastoura E. Posterior corneal astigmatism and its importance in selection of toric intraocular lens. EC Ophthalmology. 2017;4.5: 608-612.

[157] Kohnen T. Posterior corneal astigmatism. J Cataract Refract Surg. 2013 Dec;39(12):1795.

[158] Fityo S, Buhren J, Shajari M, Kohnen T. Keratometry versus total corneal refractive power: Analysis of measurement repeatability with 5 different devices in normal eyes with low astigmatism. Journal of cataract and refractive surgery. Apr 2016;42(4):569-576.

[159] Frings A, Hold V, Steinwender G, El-Shabrawi Y, Ardjomand N. Use of true net power in intraocular lens power calculations in eyes with prior myopic laser refractive surgery. Int Ophthalmol. 2014 Oct;34(5):1091-6.

[160] Hoffmann PC, Wahl J, Hütz WW, Preußer PR. A ray tracing approach to calculate toric intraocular lenses. J Refract Surg 2013;29:402-408.

[161] Grewal DS, Grewal SPS. Clinical applications of Scheimpflug imaging in cataract surgery. Saudi Journal of Ophthalmology. 2012;26(1):25-32.

[162] Snellenburg JJ, Braaf B, Hermans EA, van der Heijde RG, Sicam VA. Forward ray tracing for image projection prediction and surface reconstruction in the evaluation of corneal topography systems. Opt Express. 2010 Aug 30;18(18):19324-38.

[163] Kanellopoulos AJ, Asimellis G. Forme Fruste Keratoconus Imaging and Validation via Novel Multi-Spot Reflection Topography. Case reports in ophthalmology. 2013;4(3):199-209.

[164] Kanelloupoulos J, Asimelles G. Cassini : Providing True Axis and Magnitude of Astigmatism. J Cataract Surgery 2014, pp. 54–57.

[165] Klijn S, Reus NJ, Sicam VA. Evaluation of keratometry with a novel color LED corneal topographer. J Refract Surg 2015;31:249-256.

[166] Savini G, Schiano-Lomoriello D, Hoffer KJ. Repeatability of automatic measurements by a new anterior segment optical coherence tomographer combined with Placido topography and agreement with 2 Scheimpflug cameras. J Cataract Refract Surg. 2018 Apr;44(4):471-478.

[167] Tang, M., Chen, A., Li, Y., Huang, D. Corneal power measurement with Fourier-domain optical coherence tomography. J Cataract Refract Surg. 2010;36:2115–2122

[168] http://acrysoftoriccalculator.com (acessed July 12th 2018).

[169] Savini G, Hoffer KJ, Ducoli P. A new slant on toric intraocular lens power calculation. J Refract Surg. 2013 May;29(5):348-54.

[170] Savini G, Hoffer KJ, Carbonelli M, Ducoli P, Barboni P. Influence of axial length and corneal power on the astigmatic power of toric intraocular lenses. J Cataract Refract Surg 2013; 39:1900-1903

[171] Savini G, Naeser K. An analysis of the factors influencing the residual refractive astigmatism after cataract surgery with toric intraocular lenses. Invest Ophthalmol Vis Sci 2015; 56:827-835.

[172] Fam HB, Lim KL. Meridional analysis for calculating the expected spherocylindrical refraction in eyes with toric intraocular lenses. J Cataract Refract Surg 2007; 33:2072-2076

[173] Goggin M, Moore S, Easterman A. Outcome of toric intraocular lens implantation after adjusting for anterior chamber depth and intraocular lens sphere equivalent power effects. Arch Ophthalmol 2011; 129:998–1003; correction, 1494.

[174] Ninomiya Y, Minami K, Miyata K et al. Toric intraocular lenses in eyes with with-the-rule, against-the-rule, and oblique astigmatism: One-year results. J Cataract Refract Surg 2016; 42:1431-1440

[175] Koch DD, Jenkins RB, Weikert MP et al. Correction astigmatism with toric intraocular lenses: effect of posterior corneal astigmatism. J Cataract Refract Surg. 2013 Dec;39(12):1803-9.

[176] Goggin M, Zamora-Alejo K, Esterman A, van Zyl L. Adjustment of anterior corneal astigamtism values to incorporate the likely effect of posterior corneal curvature for toric intraocular lens calculation. J Refract Surg 2015;31: 98-102.

[177] Abulafia A, Koch DD, Wang L, Hill WE, Assia EI, Franchina M, Barrett GD. New regression formula for toric intraocular lens calculations. J Cataract Refract Surg 2016;42:663-671.

[178] https://www.apacrs.org/toric_calculator20/Toric%20Calculator.aspx, accessed June 29 2018.

[179] Barrett GD. An improved universal theoretical formula for intraocular lens power prediction. J Cataract Refract Surgery 1993;19:713-720.

[180] http://acrysoftoriccalculator.com (acessed July 12th 2018).

[181] Preussner PR. Ray Tracing for IOL Power Calculations. Cataract and Refractive Surgery Today Europe. May 2012:46-48.

[182] Olsen T, Funding M. Ray tracing analysis of intraocular lens power in situ. J Cataract Refract Surg. 2012 Apr;38(4):641-7.

[183] Tejedor J, Perez-Rodriguez JA. Astigmatic change induced by 2.8-mm corneal incisions for cataract surgery. Invest Ophthalmol Vis Sci. 2009;50:989-994.

[184] Tadros A, Habib M, Tejwani D et al.. Opposite clear corneal incisions on the steep meridian in phaco-emulsification: early effects on the cornea. J Cataract Refract Surg. 2004;30:414-417.

[185] Wilczynski M, Supady E, Piotr L et al. Comparison of surgically induced astigmatism after coaxial phacoemulsification through 1.8 mm microincision and bimanual phacoemulsification through 1.7 mm microincision. J Cataract Refract Surg. 2009 Sep;35(9):1563-9.

[186] Nagy ZZ, Dunai A, Kránitz K et al. Evaluation of femtosecond laser-assisted and manual clear corneal incisions and their effect on surgically induced astigmatism and higher-order aberrations. J Refract Surg. 2014 Aug;30(8):522-5.

[187] Klamann MK, Gonnermann J, Maier AK, Torun N, Bertelmann E. Smaller incision size leads to higher predictability in micro¬coaxial cataract surgery. Eur J Ophthalmol. 2013;23:202-207.

[188] Chang SW, Su TY, Chen YL. Influence of ocular features and incision width on surgically induced astigmatism after cataract surgery. J Refract Surg. 2015 Feb;31(2):82-88.

[189] Denoyer A, Ricaud X, Van Went C et al. Influence of corneal biomechanical properties on surgically induced astigmatism in cataract surgery. J Cataract Refract Surg. 2013 Aug;39(8):1204-10.

[190] Morcillo-Laiz R, Zato MA, Muñoz-Negrete FJ et al. Surgically induced astigmatism after biaxial phacoemulsification compared to coaxial phacoemulsification. Eye (Lond). 2009 Apr;23(4):835-9.

[191] van Rij G, Waring GO 3rd. Changes in corneal curvature induced by sutures and incisions. Am J Ophthalmol. 1984 Dec 15;98(6):773-83.

[192] Kwon HJ, Nam SM, Stulting RD et al. Comparison of surgically induced astigmatism following iris-claw PIOL insertion with scleral, limbal, or corneal incisions. J Refract Surg. 2014 May;30(5):330-5.

[193] Ermiş SS, Inan UU, Oztürk F. Surgically induced astigmatism after superotemporal and superonasal clear corneal incisions in phacoemulsification. J Cataract Refract Surg. 2004 Jun;30(6):1316-9.

[194] Kohnen S, Neuber R, Kohnen T. Effect of temporal and nasal unsutured limbal tunnel incisions on induced astigmatism after phacoemulsification. J Cataract Refract Surg. 2002 May;28(5):821-5.

[195] Barequet IS, Yu E, Vitale S et al. Astigmatism outcomes of horizontal temporal versus nasal clear corneal incision cataract surgery. J Cataract Refract Surg. 2004 Feb;30(2):418-23.

[196] Borasio E, Mehta JS, Maurino V. Surgically induced astigmatism after phacoemulsification in eyes with mild to moderate corneal astigmatism: temporal versus on-axis clear corneal incisions. J Cataract Refract Surg. 2006 Apr;32(4):565-72.

[197] Shimizu KA, Misawa et al. Toric intraocular lenses: correcting astigmatism while controlling axis shift. J Cataract Refract Surg. 1994; 20(5): 523-6.

[198] Smith EM Jr, Talamo JH, Assil KK, Petashnick DE (1994) Comparison of astigmatic axis in the seated and supine positions. J Refract Corneal Surg 10: 615-620.

[199] Smith EM Jr, Talamo JH (1995) Cyclotorsion in the seated and supine patient. J Cataract Refract Surg 21: 402-403.

[200] Swami AU, Steinert RF, Osborne WE, White AA (2002) Rotational malposition during laser in situ keratomileusis. Am J Ophthalmol 133: 561-562.

[201] Visser N, Berendschot TT, Bauer NJ, Jurich J, Kersting O, Nuijts RM. Accuracy of Toric Intraocular Lens Implantation in Cataract and Refractive surgery. J Cataract Refract Surg. 2011 Aug;37(8):1394-402.

[202] Popp N, Hirnschall N, Maedel S, Findl O. Evaluation of 4 corneal astigmatic marking methods. J Cataract Refract Surg. 2012 Dec;38(12):2094-9.

[203] Kent C. Toric IOLs: Nailing the alignment. Review of Ophthalmology 1/22/2013.

[204] Ferreira TB, Pinheiro J, Santos J, Relha C, Eirô N, Ribeiro FJ. Reprodutibilidade de um novo marcador corneano de alinhamento pendular. 58º Congresso Português de Oftalmologia, Vilamoura, 2015.

[205] Elhofi AH, Helaly HA. Comparison Between Digital and Manual Marking for Toric Intraocular Lenses: A Randomized Trial. Abdulrahman. K, ed. Medicine. 2015;94(38):e1618..

[206] Hura AS, Osher RH. Comparing the zeiss callisto eye and the alcon verion image guided system toric lens alignment technologies. J Refract Surg. 2017;33:482–7.

[207] Webers VSC, Bauer NJC, Visser N, Berendschot TTJM, van den Biggelaar FJHM2, Nuijts RMMA2

Image-guided system versus manual marking for toric intraocular lens alignment in cataract surgery.

J Cataract Refract Surg. 2017 Jun;43(6):781-788.

[208] Wiley WF, Bafna S. Intra-operative aberrometry guided cataract surgery. International Ophthalmology Clinics. 2011;51(2):119-129.

[209] Hill W. Intraoperative aberrometer evolves with new standard for accuracy. Ophthalmology Times.
http://ophthalmologytimes.modernmedicine.com/ophthalmologytimes/news/intraoperative-aberrometer-evolves-new-standard-accuracy. Accessed February 28, 2016.

[210] Woodcock MG, Lehmann R, Cionni RJ, Breen M, Scott MC. Intraoperative aberrometry versus standard preoperative biometry and a toric IOL calculator for bilateral toric IOL implantation with a femtosecond laser: One-month results. J Cataract Refract Surg. 2016;42:817–25.

[211] Yesilirmak N, Palioura S, Culbertson W, Yoo SH, Donaldson K. Intraoperative wavefront aberrometry for toric intraocular lens placement in eyes with a history of refractive surgery. J Refract Surg. 2016;32:69–70.

[212] Solomon JD, Ladas J. Toric outcomes: Computer-assisted registration versus intraoperative aberrometry. J Cataract Refract Surg. 2017;43:498–504.

[213] Guarnieri A, Moreno-Montañes J, Sabater AL et al. Final incision size after cataract surgery with toric intraocular lens implantation using 2 techniques. J Cataract Refract Surg 2013; 39:1675–1681.

[214] Chang DF. Pearls for implanting the Staar toric IOL. Brit J Ophthalmol. 2001;85:supplement. Available at http://bjo.bmj.com/cgi/content/full/85/1/DC1. Accessed March 22, 2018.

[215] Chang DF. Comparative rotational stability of single-piece open loop acrylic and plate-haptic silicone toric intraocular lenses. J Cataract Refract Surg 2008; 34:1842–1847.

[216] Bauer NJ, De Vries NE, Webers CA, Hendrikse F, Nuijts RM. Astigmatism management in cataract surgery with the AcrySof toric intraocular lens. J Cataract Refract Surg 2008; 34:1483–1488.

[217] Shah GD, Praveen MR, Vasavada AR, Vasavada VA, Rampal G, Shastry LR. Rotational stability of a toric intraocular lens: influence of axial length and alignment in the capsular bag. J Cataract Refract Surg 2012; 38:54–59

[218] Patel CK, Ormonde S, Rosen PH, Bron AJ. Postoperative intraocularlens rotation: a randomized comparison of plate and loophaptic implants. Ophthalmology 1999; 106:2190–2195; discussionby DJ Apple, 2196

[219] Aristodemou P, Knox Cartwright NE, Sparrow JM, Johnston RL. Intraocular lens formula constant optimization and partial coherence interferometry biometry: refractive outcomes in 8108 eyes after cataract surgery. J Cataract Refract Surg 2011; 37:50–62

[220] Preussner PR, Wahl J, Weitzel D, Berthold S, Kriechbaum K, Findl O. Predicting postoperative intraocular lens position and refraction. J Cataract Refract Surg 2004; 30:2077–2083

[221] International Organization for Standardization. Ophthalmic Implants – Intraocular Lenses – Part 2: Optical Properties and

Test Methods. Geneva, Switzerland, ISO, 2003; 1999 (ISO 11979–2); technical corrigendum 1

[222] Marcos S. Special circumstances: effect of IOL tilt on astigmatism. In: Hoffer KJ, ed, IOL Power. Thorofare, NJ, Slack, 2011; 223–230.

[223] Vinas M, Sawides L, de Gracia P, Marcos S. Perceptual adaptation to the correction of natural astigmatism. PLoS One 2012; 7:e46361. Available at: http://www.plosone.org/article/fetchObject.action?uriZinfo%3Adoi%2F10.1371%2Fjournal.pone.0046361&representationZPDF. Accessed June 7, 2018.

[224] Chang DF. Repositioning technique and rate for toric intraocular lenses. J Cataract Refract Surgery 2009; 35:1315–1316.

[225] Alpins N, Ong JK, Stamatelatos G. Refractive surprise after toric intraocular lens implantation: graph analysis. J Cataract Refract Surg. 2014 Feb;40(2):283-94.

[226] https://www.astigmatismfix.com; Berdahl & Hardten Toric IOL Calculator. Accessed May 2, 2018.

[227] https://www.apacrs.org/barrett_rx105/. Accessed May 2, 2018.

[228] Ferreira TB, Ribeiro P, Ribeiro FJ, O'Neill JG. Distribuição e determinantes de parâmetros biométricos oculares em candidatos a cirurgia de catarata em Portugal. Oftalmologia 2017;41(4):17-26.

[229] Wong TY, Foster PJ, Ng TP, Tielsch JM, Johnson GJ, Seah SK. Variations in ocular biometry in an adult Chinese population in Singapore: the Tanjong Pagar Survey. Invest Ophthalmol Vis Sci. 2001;42:73–80.

[230] Shufelt C, Fraser-Bell S, Ying-Lai M, Torres M, Varma R. Refractive error, ocular biometry, and lens opalescence in an adult population: the Los Angeles Latino Eye Study. Invest Ophthalmol Vis Sci. 2005;46:4450–4460.

[231] Grosvenor T. Reduction in axial length with age: an emmetropizing mechanism for the adult eye? Am J Optom Physiol Opt. 1987;64:657–663.

[232] Ip JM, Huynh SC, Kifley A, Rose KA, Morgan IG, Varma R et at. Variation of the contribution from axial length and other oculometric parameters to refraction by age and ethnicity. Invest Ophthalmol Vis Sci. 2007;48:4846–4853

[233] Saw SM, Chua WH, Hong CY, Wu HM, Chia KS, Stone RA et al. Height and its relationship to refraction and biometry parameters in Singapore Chinese children. Invest Ophthalmol Vis Sci. 2002;43:1408–1413

[234] Lee KE, Klein BK, Klein R, Quandt Z, Wong TY. Age, Stature, and Education Associations with Ocular Dimensions in an Older White Population. Arch Ophthalmol. 2009;127:88–93.

[235] Santodomingo-Rubido J, Mallen EA, Gilmartin B, Wolffsohn JS. A new non-contact optical device for ocular biometry. Br J Ophthalmol. 2002;86:458–462.

[236] Lege BA, Haigis W. Laser interference biometry versus ultrasound biometry in certain clinical conditions. Graefes Arch Clin Exp Ophthalmol. 2004;242:8–12

[237] Hoffer KJ, Shammas HJ, Savini G. Comparison of 2 laser instruments for measuring axial length. J Cataract Refract Surg. 2010;36(4):644-648, Erratum 2010;36(6):1066.

[238] Olsen T, Arnarsson A, Sasaki H, Sasaki K, Jonasson F. On the ocular refractive components: the Reykjavik Eye Study. Acta Ophthalmol Scand. 2007;85:361–366.

[239] Lim LS, Saw SM, Jeganathan SE, Tay WT, Aung T, Tong L et al. Distribution and determinants of ocular biometric parameters in an Asian population: the Singapore Malay Eye Study. Invest Ophthalmol Vis Sci. 2010;51:103–109.

[240] Fotedar R, Wang JJ, Burlutsky G et al. Distribution of axial length and ocular biometry measured using partial coherence laser interferometry (IOLMaster) in an older white population. Ophthalmology. 2010;117:417–423

[241] Saw SM, Chua WH, Hong CY, Wu HM, Chia KS, Stone RA et al. Height and its relationship to refraction and biometry parameters in Singapore Chinese children. Invest Ophthalmol Vis Sci. 2002;43:1408–1413

[242] Cao X, Hou X, Bao Y. The ocular biometry of adult cataract patients on lifeline express hospital eye train in rural China. J Ophthalmol. 2015 5;2015:171564.

[243] Hoffer KJ. Biometry of 7,500 cataractous eyes. Am J Ophthalmol. 1980;90:360-368 Erratum: 1980;90(6):890.

[244] Jivrajka R, Shammas MC, Boenzi T, Swearingen M, Shammas HJ. Variability of axial length, anterior chamber depth, and lens thickness in the cataractous eye. J Cataract Refract Surg. 2008;34:289–294.

[245] Lee KE, Klein BK, Klein R, Quandt Z, Wong TY. Age, Stature, and Education Associations with Ocular Dimensions in an Older White Population. Arch Ophthalmol. 2009;127:88–93.

[246] Knox Cartwright NE, Johnston RL, Jaycock PD, Tole DM, Sparrow JM. The Cataract National Dataset electronic multicentre audit of 55,567 operations: when should IOLMaster biometric measurements be rechecked? Eye (Lond). 2010;24:894–900.

[247] Siahmed K, Muraine M, Brasseur G. Optic biometry in intraocular lense calculation for cataract surgery. Comparison with usual methods. J Fr Ophtalmol. 2001;24:922–926.

[248] Olsen T. Improved accuracy of intraocular lens power calculation with the Zeiss IOLMaster. Acta Ophthalmol Scand. 2007;85:84–87.

[249] Hoffer KJ, Shammas HJ, Savini G. Comparison of 2 laser instruments for measuring axial length. J Cataract Refract Surg. 2010;36(4):644-648, Erratum 2010;36(6):1066.

[250] Ribeiro F, Castanheira-Dinis A, Dias JM. Refractive error assessment: influence of different optical elements and current limits of biometric techniques. J Refract Surg. 2013;29:206–212.

[251] Tejedor J, Guirao A. Agreement between refractive and corneal astigmatism in pseudophakic eyes. Cornea. 2013 Jun;32(6):783-90

[252] Ventura BV, Al-Mohtaseb Z, Wang L, Koch DD, Weikert MP. Repeatability and comparability of corneal power and corneal astigmatism obtained from a point-source color light-emitting diode topographer, a Placido-based corneal topographer, and a low-coherence reflectometer. Journal of cataract and refractive surgery. Oct 2015;41(10):2242-2250.

[253] Ventura BV, Wang L, Ali SF, Koch DD, Weikert MP. Comparison of corneal power, astigmatism, and wavefront aberration measurements obtained by a point-source color light-emitting diode–based topographer, a Placido-disk topographer, and a combined Placido and dual Scheimpflug device. Journal of cataract and refractive surgery. 2015;41:1658-1671.

[254] Klijn S, Reus NJ, Sicam VA. Evaluation of keratometry with a novel Color-LED corneal topographer. Journal of refractive surgery (Thorofare, N.J. : 1995). Apr 2015;31(4):249-256.

[255] Hidalgo IR, Rozema JJ, Dhubhghaill SN, Zakaria N, Koppen C, Tassignon MJ. Repeatability and inter-device agreement for three different methods of keratometry: Placido, Scheimpflug, and color LED corneal topography. Journal of refractive surgery (Thorofare, N.J. : 1995). Mar 2015;31(3):176-181.

[256] Kanellopoulos AJ, Asimellis G. Distribution and Repeatability of Corneal Astigmatism Measurements (Magnitude and Axis) Evaluated With Color Light Emitting Diode Reflection Topography. Cornea. Aug 2015;34(8):937-944.

[257] Hashemi H, Yekta AA, Ostadimoghaddam H, Norouzirad R, Khabazkhoob M. Comparison of Keratometric Values Using Javal Keratometer, Oculus Pentacam, and Orbscan II. Iranian J Ophthalmol. 2014;26(1):3-10.

[258] Wang Q, Savini G, Hoffer KJ, et al. A comprehensive assessment of the precision and agreement of anterior corneal power measurements obtained using 8 different devices. PloS One. 2012;7(9):e45607.

[259] Fam HB, Lim KL. Validity of the keratometric index: large population-based study. J Cataract Refract Surg. 2007;33(4):686-691.

[260] Goggin M, Patel I, Billing K, Esterman A. Variation in surgically induced astigmatism estimation due to test-to-test variations in keratometry. J Cataract Refract Surg. 2010;36(10):1792-1793.

[261] Savini G, Barboni P, Carbonelli M, Hoffer KJ. Agreement between Pentacam and videokeratography in corneal power assessment. J Refract Surg. 2009;25(6):534-538.

[262] Savini G, Carbonelli M, Sbreglia A, Barboni P, Deluigi G, Hoffer KJ. Comparison of anterior segment measurements by 3 Scheimpflug tomographers and 1 Placido corneal topographer. J Cataract Refract Surg. 2011;37(9):1679-1685.

[263] Kanellopoulos AJ, Asimellis G. Color light-emitting diode reflection topography: validation of keratometric repeatability in a large sample of wide cylindrical-range corneas. Clin Ophthalmol. 2015;9:245-252.

[264] Seitz B, Torres F, Langenbucher A, Behrens A, Suarez E. Posterior corneal curvature changes after myopic laser in situ keratomileusis. Ophthalmology. 2001;108(4):666-672; discussion 673.

[265] Giessler S, Duncker GI. Orbscan pachymetry after LASIK is not reliable. J Refract Surg. 2001;17(3):385-387.

[266] Cairns G, Ormonde SE, Gray T, et al. Assessing the accuracy of Orbscan II post-LASIK: apparent keratectasia is paradoxically associated with anterior chamber depth reduction in successful procedures. Clin Experiment Ophthalmol. 2005;33(2):147-152.

[267] Ciolino JB, Belin MW. Changes in the posterior cornea after laser in situ keratomileusis and photorefractive keratectomy. J Cataract Refract Surg. 2006;32(9):1426-1431.

[268] Freitas Gde O, Ambrosio R, Jr., Ramos I, et al. Astigmatic Vector Analysis of Posterior Corneal Surface: A Comparison Among Healthy, Forme Fruste, and Overt Keratoconic Corneas. American journal of ophthalmology. Jul 2016;167:65-71.

[269] McAlinden C, Khadka J, Pesudovs K. Statistical methods for conducting agreement (comparison of clinical tests) and precision (repeatability or reproducibility) studies in optometry and ophthalmology. Ophthalmic & physiological optics : the journal of the British College of Ophthalmic Opticians (Optometrists). Jul 2011;31(4):330-338.

[270] Visser N, Berendschot TT, Verbakel F, de Brabander J, Nuijts RM. Comparability and repeatability of corneal astigmatism measurements using different measurement technologies. Journal of cataract and refractive surgery. Oct 2012;38(10):1764-1770.

[271] Hua Y, Xu Z, Qiu W, Wu Q. Precision (Repeatability and Reproducibility) and Agreement of Corneal Power Measurements Obtained by Topcon KR-1W and iTrace. PloS one. 2016;11(1):e0147086.

[272] http://www.acrysoftoriccalculator.com, accessed July 04, 2018

[273] Reitblat O, Levy A, Kleinmann G, Abulafia A, Assia E. Effect of posterior corneal astigmatism on power calculation and alignment of toric intraocular lenses: Comparison of methodologies. J Cataract Refract Surg 2016; 42:217–225

[274] Hoffer KJ. The Hoffer Q formula: a comparison of theoretic and regression formulas. J Cataract Refract Surg 1993; 19:700-712.

[275] Retzlaff JA, Sanders DR, Kraff MC. Development of the SRK/T intraocular lens implant power calculation formula. J Cataract Refract Surg 1990; 16:333-340.

[276] Alcon Laboratories, Inc. The new ALCON® online toric IOL calculator incorporating the Barrett toric algorithm. Available at: https://www.acrysoftoriccalculator.com/features.htm. Accessed January 28, 2017.

[277] Shah GD, Praveen MR, Vasavada AR, Rampal NV, Vasavada VA, Asnani PK, Pandita D. Software-based assessment of postoperative rotation of toric intraocular lens. J Cataract Refract Surg 2009; 35:413-418

[278] Holladay JT. Holladay IOL Consultant Computer Program. Houston, TX, Holladay IOL Consultant, 1996

[279] Chen D, Lam AKC. Intrasession and intersession repeatability of the Pentacam system on posterior corneal assessment in the normal human eye. J Cataract Refract Surg 2007; 33:448-454

[280] McAlinden C, Khadka J, Pesudovs K. A comprehensive evaluation of the precision (repeatability and reproducibility) of the Oculus Pentacam HR. Invest Ophthalmol Vis Sci 2011;52:7731-7737

[281] Huang J, Pesudovs K, Wen D, Chen S, Wright T, Wang X, Li Y, Wang Q. Comparison of anterior segment measurements with rotating Scheimpflug photography and partial coherence reflectometry. J Cataract Refract Surg 2011; 37:341-348

[282] Ferreira TB, Ribeiro P, Ribeiro FJ, O'Neill JG. Comparison of the astigmatic prediction errors associated with new calculation methods for toric intraocular lenses. J Cataract Refract Surg 2017; 43:340-347.

[283] Gundersen KG, Potvin R. Clinical outcomes with toric intraocular lenses planned using an optical low coherence reflectometry ocular biometer with a new toric calculator. Clin Ophthalmol 2016; 10:2141-2147

[284] Davison JA, Potvin R. Refractive cylinder outcomes after calculating toric intraocular lens cylinder power using total corneal refractive power. Clin Ophthalmol 2015:9 1511-1517

[285] Zhang B, Ma JX, Liu DY, Guo CR, Du YH, Guo XJ, Cui YX. Effects of posterior corneal astigmatism on the accuracy of AcrySof toric intraocular lens astigmatism correction. Int J Ophthalmol 2016; 9:1276-1282

[286] Zhang L, Sy ME, Mai H, Yu F, Hamilton DR. Effect of posterior corneal astigmatism on refractive outcomes after toric intraocular lens implantation. J Cataract Refract Surg 2015; 41:84-89

[287] Cooke DL, Cooke TL. Comparison of 9 intraocular lens power calculation formulas. J Cataract Refract Surg 2017;42:1157-1164

[288] Aramberri J, Araiz L, Garcia A, et al. Dual versus single Scheimpflug camera for anterior segment analysis: precision and agreement. J Cataract Refract Surg 2012; 38:1934-1949

[289] Shankar H, Taranath D, Santhirathelagan CT, Pesudovs K. Anterior segment biometry with the Pentacam: Comprehensive assessment of repeatability of automated measurements. J Cataract Refract Surg 2008;34:103-113.

[290] Nagy ZZ. New technology update: femtosecond laser in cataract surgery. Clin Ophthalmol. 2014;8:1157-1167.

[291] Masket S, Sarayba M, Ignacio T, Fram N. Femtosecond laser-assisted cataract incisions: Architectural stability and reproducibility. J Cataract Refract Surg. 2010;36(6):1048-1049.

[292] Grewal DS, Basti S. Comparison of morphologic features of clear corneal incisions created with a femtosecond laser or a keratome. J Cataract Refract Surg. 2014;40(4):521-530.

[293] Theodoulidou S, Asproudis I, Kalogeropoulos C et al. The role of sideport incision in astigmatism change after cataract surgery. Clinical Ophthalmology. 2015:9 1421–1428.

[294] Bizheva K, Hutchings N, Sorbara L, Moayed AA, Simpson T. In vivo volumetric imaging of the human corneo-scleral limbus with spectral domain OCT. Biomed Opt Express. 2011;2:1794- 1702.

[295] Alpins N, Ong JKY, Stamatelatos G. Asymmetric Corneal Flattening Effect After Small Incision Cataract Surgery. J Refract Surg. 2016;32(9):598-603.

[296] Espaillat A, Pérez O, Potvin R. Clinical outcomes using standard phacoemulsification and femtosecond laser-assisted surgery with toric intraocular lenses. Clin Ophthalmol. 2016;10:555-563.

[297] Makombo PM, Shao Y, Yang Q. Surgically induced astigmatism using femtosecond laser clear corneal incision for cataract surgery compared to conventional phacoemulsification. IJSER. 2016;7(6):175-180.

[298] Diakonis VF, Yesilirmak N, Cabot F, et al. Comparison of surgically induced astigmatism between femtosecond laser and manual clear corneal incisions for cataract surgery. J Cataract Refract Surg. 2015;41(10):2075-2080.

[299] Álvarez-Rementería L, Blázquez V, Contreras I. Surgical induced astigmatism in femtosecond laser assisted cataract surgery. J Emmetropia. 2012;3:61-65.

[300] Serrao S, Lombardo G, Ducoli P, Rosati M, Lombardo M. Evaluation of femtosecond laser clear corneal incision: an experimental study. J Refract Surg. 2013;29(6):418-424.

[301] Mastropasqua L, Toto L, Mastropasqua A, et al. Femtosecond Laser Versus Manual Clear Corneal Incision in Cataract Surgery. J Refract Surg. 2014;30(1):27-33.

[302] Reinstein DZ, Archer TJ, Srinivasan S et al. Standard for reporting refractive outcomes of intraocular lens-based refractive surgery. J Cataract Refract Surg. 2017;43(4):435-439.

[303] Reinstein DZ, Archer TJ, Randleman JB. JRS standard for reporting astigmatism outcomes of refractive surgery [editorial]. J Refract Surg 2014; 30:654659; erratum 2015; 31:129.

[304] Borasio E, Mehta JS, Maurino V. Torque and flattening effects of clear corneal temporal and on-axis incisions for phacoemulsification. J Cataract Refract Surg. 2006;32(12):2030-2038.

[305] Theodoulidou S, Asproudis I, Kalogeropoulos C et al. Corneal Diameter as a Factor Influencing Corneal Astigmatism After Cataract Surgery. Cornea. 2016;35:132–136.

[306] Miller JJ, Scott IU, Flynn HW Jr et al. Acute-onset endophthalmitis after cataract surgery (2000-2004): incidence, clinical settings, and visual acuity outcomes after treatment. Am J Ophthalmol. 2005; 139:983–987.

[307] Savini G, Naeser K, Schiano-Lomoriello D, Ducoli P. Optimized keratometry and total corneal astigmatism for toric intraocular lens calculation. J Cataract Refract Surg 2017; 43:1140–1148

[308] Næser K, Savini G, Bregnhøj JF. Estimating Total Corneal Astigmatism From Anterior Corneal Data. Cornea 2017;00:1–6

[309] Barret G, Lipsky L. Integrated K to Improve Toric IOL Prediction. ASCRS 2018